Late Glacial to Holocene
Paleoenvironmental Evolution of the Black Sea

Dissertation
zur Erlangung des Doktorgrades

vorgelegt am Fachbereich Geowissenschaften
der Universität Bremen von

André Bahr

Bremen, Oktober 2005

Gutachter:

Herr Prof. Dr. Gerold Wefer

Herr Prof. Dr. Gerhard Bohrmann

Table of contents

ABSTRACT

Due to its almost isolated setting, the Black Sea is particularly sensitive to paleoenvironmental changes and therefore presents an unique archive for paleoclimate studies. While previous investigations focused predominantly on the marine stage of the Black Sea covering the last ca. 7500 years, this thesis aims to shed light on the poorly known glacial and early Holocene evolution of the lacustrine phase of the Black Sea and the paleoclimatic variations recorded in its sediments. For this purpose a transect of 7 gravity cores from the outer shelf down to the lower slope of the NW Black Sea was examined in a multi-proxy approach, including non-destructive XRF and colour-scanning, bulk grain size determinations, and Mg/Ca, Sr/Ca, $\delta^{18}O$ and $\delta^{13}C$ measurements on ostracod and bivalve shells. In addition to the cores from the NW Black Sea, which record primarily climatic changes in southeastern and central Europe, two gravity cores from the southern part of the western Black Sea were used to reconstruct climatic variations in western Anatolia.

The results from the NW Black Sea cores show that the Black Sea underwent significant hydrological changes during its lake stage. While the Last Glacial Maximum was characterised by a stable hydrologic budget, late glacial meltwater pulses derived from the Scandinavian Ice Sheet caused the deposition of characteristic reddish-brown clay layers. The strongly depleted isotopic signature of the meltwater led to a temporary drop in the $\delta^{18}O$ values of the Black Sea. A sudden shift in the hydrochemical properties of the Black Sea is marking the transition from the cold Oldest Dryas to the warm Bølling-Allerød period. The favourable conditions during this period initiated the precipitation of authigenic calcite through enhanced phytoplankton activity that increased the Sr and Mg concentration in the water column as reflected in an abrupt rise of the Mg/Ca and Sr/Ca ratios. The Mg/Ca record shows, that a 1-2°C cooling of the Black Sea deep waters took place during the Younger Dryas, which was also manifested by an interruption of the authigenic calcite precipitation, that resumed later during the early Holocene. $\delta^{18}O$ values became heavier since 15 kyr calBP but this increase occurred in a more gradual manner than in the trace element record and largely reflects the influence of enriched $\delta^{18}O$ of meteoric precipitation.

With the onset of the Bølling the previously homogenous water column of the Black Sea started to show signs of stratification, most clearly reflected in the oxygen isotope record: $\delta^{18}O$ values from the deepest core, located in ca. 1977 m depth that are heavier relative to the shallower cores from 1562 to 168 m water depth. The two shallowest cores from 168 and 465 m water depth are showing lighter $\delta^{18}O$ values than the deeper cores and suggest an increased

influence of the Danube freshwater-plume as well as rising temperatures in the upper water column during a period of low Black Sea level.

The inflow of saline Mediterranean water via the Sea of Marmara and the strait of Bosphorus finally terminated the lacustrine stage of the Black Sea. The start of this inflow is clearly depicted in a steep increase of the Mg/Ca and Sr/Ca ratios since around 9.3 kyr BP and an accompanying homogenisation of the water column expressed in merging of $\delta^{18}O$ values from different depths. The homogenisation of the water column indicates that the inflow might have happened rather vigorously, but the age model is not detailed enough to determine if the flooding happened catastrophically in just a few decades or more gradual.

Since the cores used in this study are under the direct influence of major rivers – the Danube in the northern, the Sakarya in the southern research areas – the reconstruction of fluctuations in the river discharge gives valuable information about the climatic variations in the hinterland, in this case central and southeastern Europe on one side and Anatolia on the other. The data demonstrates that the North Atlantic exerts a persistent influence on the areas surrounding the Black Sea on long time scales and under considerably different climatic conditions. This is evident for the last 7500 years in the Sakarya River sediment discharge that shows multicentennial scale variations linked to NAO-like geographic patterns when compared to a paleoclimate record from the northernmost Red Sea. But this is also valid for the Younger Dryas and Allerød where variations in the run-off of the Danube includes dominant interannual to decadal-scale periods (7.6 and 65 years) that are known from the present-day North Atlantic climate regime. And finally, similarities between the XRF data and the Greenland ice core record between 18 – 15.5 kyr BP suggest that the meltwater delivery during this period was also driven by Arctic or North Atlantic climatic fluctuations.

ZUSAMMENFASSUNG

Auf Grund der beinahe vollständig isolierten Lage des Schwarzen Meeres reagiert es sehr empfindlich auf Schwankungen in den Paläo-Umweltbedingungen und stellt daher ein einmaliges Archiv für Paläoklimastudien dar. Während sich vorhergehende Arbeiten vorwiegend mit dem marinen Stadium der letzten 7500 Jahren im Schwarzen Meer beschäftigt haben, konzentriert sich die vorliegende Arbeit auf die bislang wenig bekannte glaziale und früh-Holozäne Geschichte des damals lakustrinen Schwarzen Meeres und die in seinen Sedimenten dokumentierten Klimaschwankungen. Hierzu wurde ein Profil aus 7 Schwerelotkernen, das vom äußeren Schelf bis zum unteren Schelfhang des NW Schwarzen Meeres reicht, untersucht. In einem Multi-Proxy-Ansatz wurden u.a. RFA- und Farbscannerdaten, Korngrößenmessungen, sowie Mg/Ca-, Sr/Ca-, $\delta^{18}O$- und $\delta^{13}C$-Bestimmungen an Ostrakoden- und Muschelschalen integriert. Zusätzlich zu den Kernen vom nordwestlichen Schwarzen Meer, die im wesentlichen Klimaschwankungen Südost- und Zentral-Europas aufzeichnen, wurden zwei Schwerelote vom südlichen Teil des westlichen Schwarzen Meeres verwendet, um Klimavariationen in Westanatolien zu rekonstruieren.

Die Ergebnisse aus dem NW Schwarzen Meer zeigen, dass das Schwarze Meer signifikante hydrologische und hydrochemische Schwankungen während seines See-Stadiums erfahren hat. Während das Letzte Glaziale Maximum durch ein stabiles hydrologisches Budget gekennzeichnet war, verursachten Schmelzwasserströme, die vom Skandinavischen Eisschild ausgingen, die Ablagerung charakteristischer rötlicher Tonlagen. Die stark abgereicherte Isotopensignatur des Schmelzwassers führte dabei zu einem vorübergehenden Rückgang der $\delta^{18}O$-Werte des Schwarzen Meeres. Ein plötzlicher Wechsel in den hydrochemischen Eigenschaften des Schwarzen Meeres markiert den Übergang von der kalten Ältesten Dryas in die warme Phase des Bølling/Allerød. Die günstigen klimatischen Bedingungen während dieser Periode führten zu vermehrtem Phytoplanktonwachstum, was die Fällung von authigenem Kalzit im Oberflächenwasser nach sich zog. Dies führte wiederum zur Anreicherung von Mg und Sr in der Wassersäule und damit zu einem abrupten Anstieg im Mg/Ca- und Sr/Ca-Verhältnis. Das Mg/Ca-Verhältnis zeigt während der Jüngeren Dryas zusätzlich eine Abkühlung von 1-2°C im tieferen Schwarzen Meer an. Diese Abkühlung geht eine Unterbrechung der Kalzitfällung einher, die sich allerdings im frühen Holozän wieder fortsetzt. Die $\delta^{18}O$-Werte zeigen ebenfalls einen Anstieg seit ca. 15 kyr BP. Allerdings geschieht dieser Anstieg eher allmählich und nicht abrupt wie bei den Spurenelement-

Verhältnissen. Der $\delta^{18}O$-Anstieg spiegelt im Wesentlichen den Einfluss einer angereicherten Sauerstoffisotopenzusammensetzung des atmosphärischen Niederschlages wieder.

Mit dem Beginn der Bølling Warmphase zeigt die vorher eher homogene Wassersäule des Schwarzen Meeres erste Anzeichen einer Stratifizierung. Dies ist deutlich in den Sauerstoffisotopendaten zu beobachten: $\delta^{18}O$-Werte aus dem am tiefsten gelegenen Schwerelotkern (1977 m Wassertiefe) sind schwerer im Vergleich zu denen aus 1562 bis 168 m Wassertiefe. Die flachsten Kerne mit 168 und 465 m Wassertiefe zeigen dagegen $\delta^{18}O$-Werte, die leichter sind als in den tieferen Kernen, was mit dem größer werdenden Einfluss des Süßwassereinflusses der Donau und ansteigenden Temperaturen in der oberen Wassersäule während einer Periode niedrigen Seespiegels erklärt wird.

Der Einstrom salzigen Mittelmeerwassers über das Marmara Meer und den Bosporus in das Schwarze Meer beendet die lakustrine Phase des Schwarzen Meeres. Der Beginn des Einstromes ist klar ersichtlich aus dem steilen Anstieg der Mg/Ca- und Sr/Ca-Verhältnisse um ca. 9,3 kyr BP und der gleichzeitigen Homogenisierung der Wassersäule, die sich in einer Angleichung der $\delta^{18}O$-Werte aus verschiedenen Tiefen äußert. Die Homogenisierung der Wassersäule lässt vermuten, dass der Einstrom recht intensiv gewesen sein muss, allerdings erlaubt es die zeitliche Auflösung des Altersmodells nicht festzustellen, ob die Flutung des Schwarzen Meeres innerhalb weniger Jahrzehnte oder einem viel längeren Zeitraum geschah.

Da die untersuchten Kerne unter dem direkten Einfluss großer Flüsse liegen (der Donau im nördlichen, dem Sakarya im südlichen Arbeitsgebiet) besteht die Möglichkeit, über die Rekonstruktion des Sedimenteintrags und der Wasserführung dieser Flüsse wertvolle Informationen über Klimaschwankungen im Hinterland zu erhalten, in diesem Fall also Zentral- und SO-Europa auf der einen und Anatolien auf der anderen Seite. Die gewonnenen Daten demonstrieren, dass der Nordatlantik einen andauernden Einfluss auf das Klimageschehen im westlichen Schwarzen Meer und den angrenzen Gebieten ausübt, und dies auf langen Zeitskalen und unter unterschiedlichsten klimatischen Gegebenheiten. Das zeigt sich im Falle des Sakarya Flusses während der letzten 7500 Jahre in Form von mehreren Jahrhunderten umfassenden Schwankungen, die, wenn man sie mit einem Paläoklima-Datensatz aus dem nördlichsten Roten Meer vergleicht, eine NAO-ähnliche geographische Verteilung zeigen. Auch während der Jüngeren Dryas und dem Allerød zeigen Variationen des Donau-Abflusses interannuelle und dekadische Schwankungen mit dominanten Perioden von 7,6 und 65 Jahren, die ebenso im heutigen nordatlantischen Klimasystem nachgewiesen werden können. Weiterhin wurden Ähnlichkeiten zwischen den Daten aus dem Schwarzen Meer und dem GRIP-Eiskern aus Grönland für den Zeitraum zwischen 18 und 15,5 kyr BP

festgestellt. Dies ist ein Hinweis darauf, dass das Auftreten der Schmelzwasserpulse zu jener Zeit durch Arktische und Nordatlantische Klimaschwankungen gesteuert wurde.

INTRODUCTION

The Black Sea originated during Cretaceous times as a back-arc basin and experienced since then a complex history of changing compressional and extensional tectonic regimes [*Nikishin et al.*, 2003]. Now it is almost completely isolated from the global ocean, only the narrow Bosphorus strait (0.5-3.5 km broad and at its shallowest point -36 m deep [*Myers et al.*, 2003]) allows an exchange of water between the Mediterranean and Black Sea basins via the Sea of Marmara (Fig. 1).

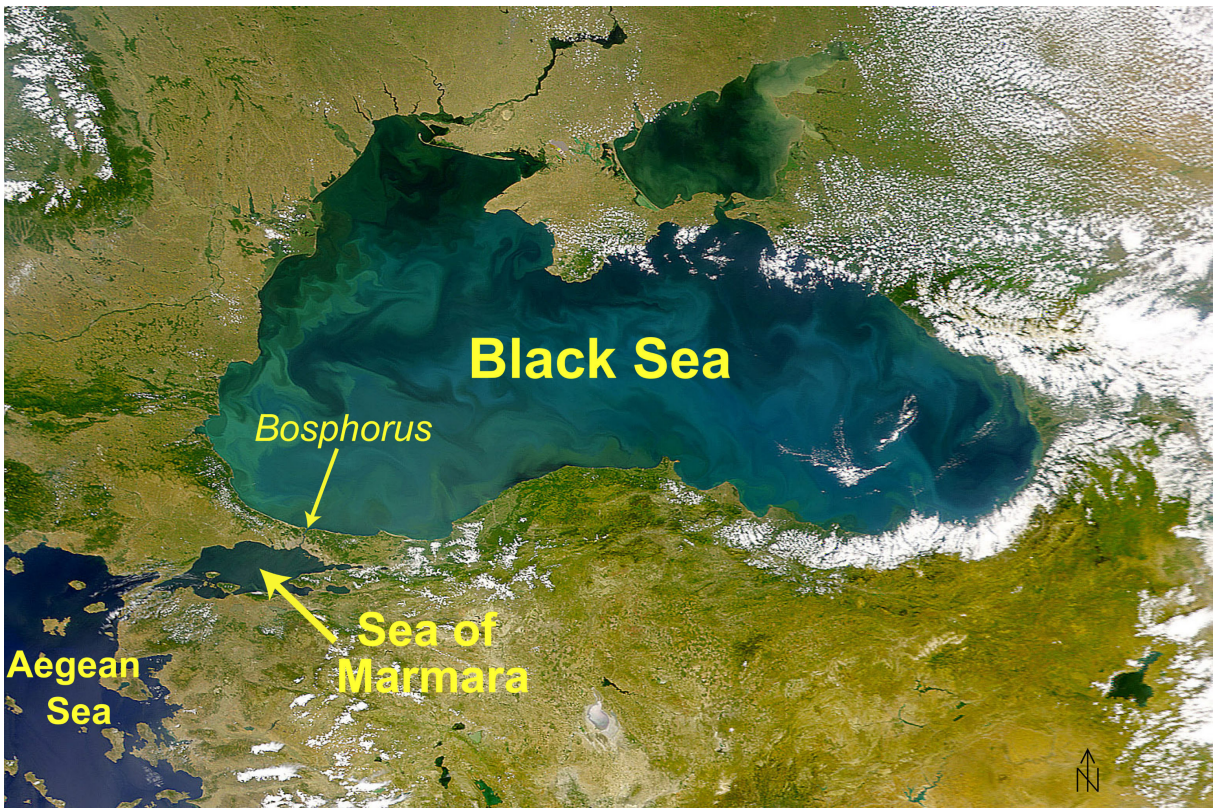

Fig. 1 Satellite image of the Black Sea and its connection to the Aegean part of the Mediterranean Sea via the Sea of Marmara and the Bosphorus strait. Note the meandering currents and filaments distributing algal blooms over the basin (picture from: NASA, Visible Earth).

The connection via the Bosphorus was interrupted during glacial times, when the eustatic sea level fell below the Bosphorus spill point. During these times the Black Sea turned into a freshwater lake, although the "Black Lake" might not have been a freshwater reservoir *sensu strictu*, but had a salinity of 5‰ or more [*Mudie et al.*, 2002b]. Today the water balance of the Black Sea is positive, i.e. more freshwater is entering the Black Sea than leaving via evaporation, but it has been argued that this balance had been negative during the

Bølling/Allerød and Early Holocene [*Ryan et al.*, 1997, 2003; *Major et al.*, 2002]. Consequently the Black Sea level would have dropped to a low lake level when the water balance was very negative. It has been proposed by *Ryan et al.* [1997, 2003] that before the global sea level was high enough to breach the Bosphorus sill, the Black Sea had a lake level as low as – 155 m [*Ballard et al.*, 2000] and was then filled by the entering Mediterranean water in only a few years (Fig. 2). This theory became known as "Noah's Flood Theory" because the authors tried to combine their geologic data with archaeological evidence and inferred that the rapid infill of the Black Sea and the subsequent displacement of people settling near the Black Sea shore was the origin for the catastrophic flooding myths known in the Near East [*Ryan and Pitman*, 1999]. Other authors were sceptic about the proposed rate of the Black Sea inundation and preferred a connection lasting over 1000 or 2000 years [*Lane-Serff et al.*, 1997; *Myers et al.*, 2003] or even suggested that the Black Sea was spilling out into the Sea of Marmara at that time [*Aksu et al.*, 1999; *Hiscott et al.*, 2002] (Fig. 2).

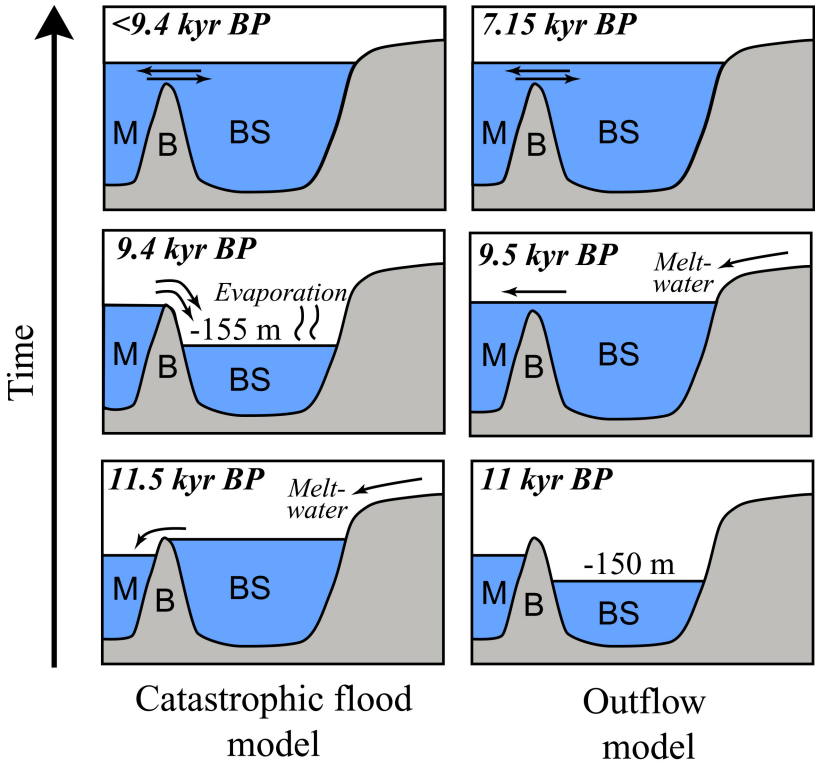

Fig. 2 Snapshots of Black Sea evolution during the past 11.5 kyrs according to the catastrophic flood model [*Ballard et al.*, 2000; *Ryan et al.*, 2003] and the outflow model [*Aksu et al.*, 1999].
M – Sea of Marmara;
B – Bosphorus;
BS – Black Sea.

An alternative view was discussed by *Major et al.* [2002] based on an idea of *Kvasov* [1968] who suggested that the Bosphorus was not sediment-filled like today and therefore had a deeper sill depth of ca. -80 m. This would allow Mediterranean water to enter the Black Sea as early as 14.5 kyrs ago. It has also been argued that the Bosphorus has been indeed around 7 m shallower than today because a delayed flooding of the Black Sea around 8.7 kyr BP would

fit salinity estimates from the Sea of Marmara and Aegean Sea [*Sperling et al.*, 2003]; the Bosphorus would then have been eroded to the present depth during the progress of the flood.

1. Motivation and aims of research

Today the Black Sea is the world's largest permanent anoxic basin [*Murray et al.*, 1989] and attracts as such numerous scientists studying its peculiar hydrology, geochemistry and biology. For geologists it furthermore presents an unique opportunity to compare the mechanisms governing a modern day anoxic basin with times of the geologic past when anoxia was common in the oceans and let to the widespread deposition of black shales. Concerning the recent evolution of the Black Sea, research has focused especially on the marine period of the Black Sea and on the question when and how the reconnection of the Black Sea with the global ocean happened, i.e. if it occurred as a catastrophic flood [*Ryan et al.*, 1997] or more like a slow inflow of Mediterranean water into the "Black Lake" [*Aksu et al.*, 2002; *Hiscott et al.*, 2002]. But so far little is known about the hydrological and hydrochemical properties of the Black Sea during its lake stage in the last glacial and deglacial period. To decipher the glacial to Early Holocene evolution of the Black Sea a set of sedimentological (colour and XRF-scanning, grain size) and geochemical ($\delta^{18}O$, $\delta^{13}C$, Sr/Ca, Mg/Ca) proxy data have been obtained on gravity cores from a lower shelf to slope transect in the NW Black Sea. The main questions they should help answering could be summarized as follows:

- Were there any major changes in the Black Sea water chemistry before 7500 yr BP?
- What was the impact of meltwater pulses coming from the Scandinavian Ice Sheet after the Last Glacial Maximum [*Mangerud et al.*, 2004] on the Black Sea hydrology?
- Was the Black Sea a homogenous water body or did it experience a period of stratification during its lake stage?
- How did the Black Sea react to the abrupt climatic changes during the deglacial period?
- When, how, and especially how fast did the reconnection of the Black Sea with the Mediterranean Sea occur?

The data from the NW Black Sea does not only give valuable information about the evolution of the Black Sea itself but provide an excellent opportunity for high-resolution paleoenvironmental reconstructions. The different sedimentation rates of the studied cores make it possible to examine climatic fluctuations during certain time slices on interannual time scales as well as long-term changes from the Last Glacial Maximum to the Early Holocene. The focus lies hereby on the variability of the freshwater and sediment input by the Danube as an indicator for changes in the precipitation amount in central Europe. Recent studies have shown that the run-off of the Danube is closely linked to the North Atlantic Oscillation. It would therefore be tempting to see if a comparable climatic signal from the North Atlantic region is also detectable in our records from the pre-marine Black Sea. The results obtained could be compared with those from cores of a second research area, located in the southern part of the western Black Sea, which provides an exceptional high-resolution record of fluctuations in Anatolian river discharge during the last ca. 7500 years. In general, the questions raised in this part of the thesis could be summarised as follows:

- Are climatic changes on interannual to cenntennial timescales detectable in the sedimentary record?
- Is it possible to identify the imprint of climatic modes like the North Atlantic Oscillation in the record?
- If this is the case, how did the observed climatic oscillations express themselves on longer time scales and during climatically different periods like the Holocene, Younger Dryas or Bølling/Allerød?

Thus, the scope of this thesis is to provide and combine records of terrestrial origin (e.g., river run-off) with those of the lacustrine/marine realm to improve our knowledge about the evolution of the Black Sea and its surrounding areas.

2. Study area

2.1 Climatology

The western Black Sea is affected by the influence of three climate regimes. The southern part, inlcuding the Pontide Mountains along the Black Sea coast and the central Anatolian plain, are characterised by a typical Mediterranean-type winter-rainfall climate regime [*Algan*

et al., 1999], which is strongly coupled to the North Atlantic Oscillation (NAO) on interannual to decadal time scales [*D'Arrigo and Cullen*, 2001; *Turkes and Erlat*, 2003]. This area is covered by a deciduous broadleaf forest with >600 mm of year-round precipitation [*Mudie et al.*, 2002a].

Further to the north, the headwaters of the Danube are characterised by a temperate mixed forest growing under the humid conditions in the mid-latitudes of SE Europe with an annual precipitation of >1000 mm. The eastern Danube lowlands and the areas surrounding the northern Black Sea are savannah grasslands with a distinct continental climate with <600 mm of annual precipitation falling mostly in the summer [*Mudie et al.*, 2002a].

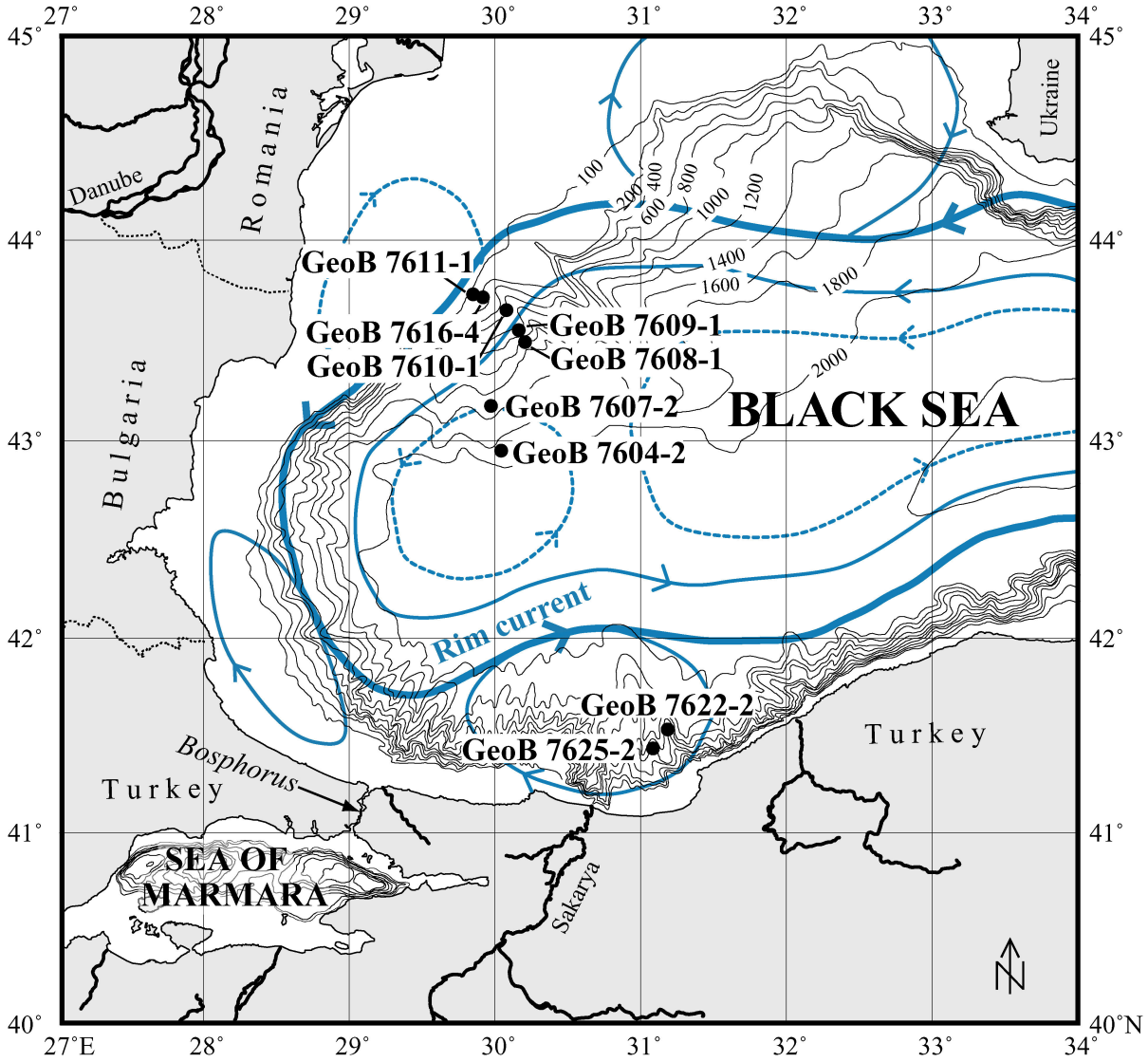

Fig. 3 Location of gravity cores sampled during RV Meteor cruise M51-4. Indicated are also the positions of the Black Sea Rim Current (thick blue line) and associated quasi permanent (thin blue lines) and recurrent (dashed blue lines) eddies (after *Öszoy and Ünlüata* [1997]).

2.2 Oceanography

The general circulation of the Black Sea basin is characterised by a basin-scale, cyclonic boundary current, termed as "Black Sea Rim Current" [*Oguz et al.*, 1992, 1993], with a number of anticyclonic eddies along its periphery and some semi-permanent gyres (Fig. 3) [*Öszoy and Ünlüata*, 1997]. Important for the transport of material into the basin interior are highly variable filaments and meandering currents that originate from the Rim Current [*Öszoy and Ünlüata*, 1997]; these features are particularly important for the spreading of algal blooms from the coast into the entire basin (Fig. 1) [*Cokacar et al.*, 2004].

Another important aspect of Black Sea hydrography is the exchange of water between the Black Sea and the Sea of Marmara via the Bosphorus. This takes place in a two-layer flow with dense, saline Mediterranean water entering the Black Sea in a lower flow and less saline Black Sea water leaving the basin through the upper flow (Fig. 4). The density contrast between the Mediterranean-derived water masses and those diluted by precipitation and river input manifests itself in a two layer stratification of the Black Sea: a stable pycnocline between 100 and 200 m water depth separates relatively saline (22.5‰) deep water of Mediterranean origin from less saline (18‰) water in the upper water column that is influenced by river run-off and precipitation [*Öszoy and Ünlüata*, 1997] (Fig. 4). The persistence of the stratification and the high productivity in the surface waters leads to permanent anoxic condition below ca. 160 m, with significant short-term shifts of the anoxic/oxic interface [*Murray et al.*, 1989].

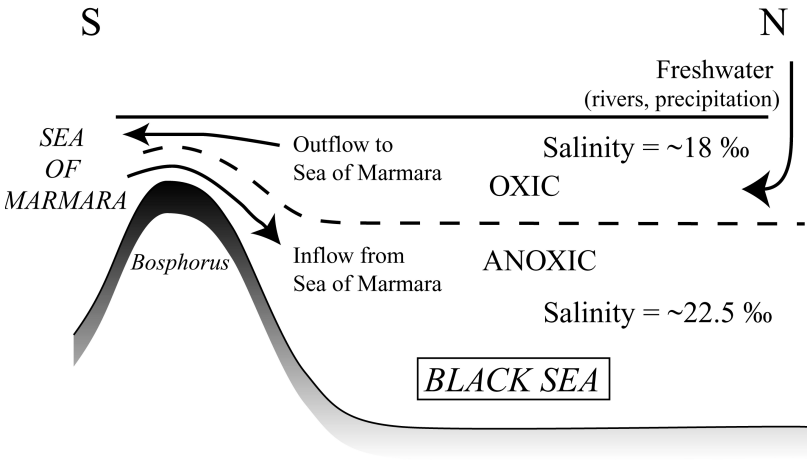

Fig. 4 Schematic cross-section through the Black Sea water column and the water exchange with the Sea of Marmara through the Bosphorus.

The shelf in the NW Black Sea is extremely broad and very flat and comprises 94% of the total shelf area in the Black Sea [*Panin and Jipa*, 2002]. Although the Danube transports vast amounts of sediments into the Black Sea, on average 51.7 million tons per year [*Bondar et al.*,

1991], and its influence on the seabed morphology is evident in the pre-Holocene Delta fans that form the very gentle shape of the slope, the NW Black Sea shelf itself is only covered by a very thin, sometimes even absent, Holocene sediment cover. This is caused by the strong Rim Current (Fig. 3) which reaches velocities of more than 50 cm/s [*Oguz and Besiktepe*, 1999] and transports most of the sediments delivered by the Danube towards the southwestern Black Sea.

The Danube is by far the biggest river reaching the Black Sea - the amount of freshwater delivered by the Danube (190.7 km³/yr, multi-annual mean before damming the river [*Panin and Jipa*, 2002]) makes up more than 50% of the total river run-off entering the basin. The run-off is highly variable on seasonal and interannual timescales; the combined seasonal and interannual variations in the Danube's flow account for a ratio of ca. 3 between the minimum and maximum over a period of several years [*Sur et al.*, 1994] and seems to be largely governed by the NAO [*Stanev and Peneva*, 2001; *Rimbu et al.*, 2002, 2004]. Like the cores in the NW Black, that are subject to the fluctuations in the Danube's discharge, the cores from the SW Black Sea will record changes in the sediment supply of the Sakarya River, which drains part of the Anatolian plain and the Pontide Mountains, areas that are also under the influence of the NAO [*D'Arrigo and Cullen*, 2001; *Turkes and Erlat*, 2003].

2.3 Sedimentary history

Pleistocene sediments from the Black Sea basin show generally a succession of alternating brackish-marine and freshwater deposits, that could be linked to the global sea level curve [*Winguth et al.*, 2000]. High eustatic sea level allowed the flooding of the Bosphorus strait and thus the development of brackish-marine conditions in the Black Sea, while a low sea level led to the disconnection from the global ocean and the Black Sea turned into a freshwater (or slightly brackish) lake [*Zubakov*, 1988]. This is also evident for the late Pleistocene basinal sediments from the Black Sea. They are classically divided into three units [*Ross and Degens*, 1974] (Fig. 5): Unit III, the oldest unit, comprises late Pleistocene to Early Holocene homogenous clay (partly mm to cm-scale laminated) deposited under lacustrine conditions; at ca. 7500 yr, some time after the start of reconnection with the Mediterranean Sea, the development of a stable two-layer stratification and permanent anoxia caused the deposition of finely laminated sapropelic mud (Unit II). At around 2700 yr BP the coccolithophoride *Emiliania huxleyi* invaded the Black Sea and their annual spring-summer blooms [*Cokacar et al.*, 2004] led to the deposition of Unit I, a microlaminated coccolith ooze

with an alternation of light coccolith layers and dark laminae consisting mostly of terrigenous material and organic matter [*Pilskaln and Pike*, 2001]. The first occurrence of *E. huxleyi* is commonly linked to the establishment of a salinity level higher than 11‰, the threshold for survival of this coccolithophoride [*Tekiroglu et al.*, 2001]. It has also been proposed that *E. huxleyi* was transported to the Black Sea in the bilgewater of antique ships [*Ryan and Pitman*, 1999] or that changed nutrient recycling and a shoaling chemocline depth has been responsible for its first occurrence [*Sinninghe Damsté et al.*, 1993]. Although sediment trap studies [*Hay et al.*, 1990] and sedimentological analyses [*Hay et al.*, 1991] suggest that the laminations observed in Unit I and II sediments from the Black Sea abyssal plain represent annual varves, radiocarbon dating on organic matter [*Jones and Gagnon*, 1994] implies that varve counting underestimates the age of the marine deposits by about 20-30%. A reason might be that coccolithophoride blooms do not occur every year, or exceptional productivity events might lead to a destruction of individual lamina by large fecal pellets [*Pilskaln and Pike*, 2001].

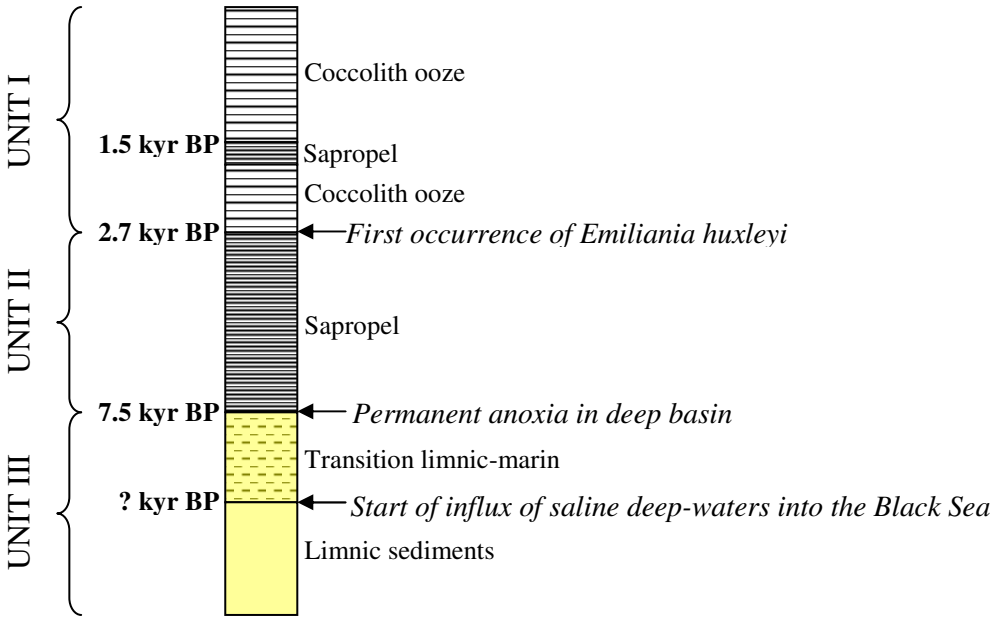

Fig. 5 Stratigraphy of late Glacial to Holocene sediments in the Black Sea (after *Jones and Gagnon* [1994])

In the cores from the NW Black Sea slope the marine Units I and II are both fully developed and have a constant thickness of ca. 45 cm [*Jørgensen*, 2003]. The cores in the southern research area are located on a topographically elevated rise, ca. 65 and 50 km northeast of the Sakarya river mouth. The very narrow shelf in this part of the Black Sea leads to a direct bypass of fluvial sediments to the slope and basin of the Black Sea. This study site is therefore characterised by a very high Holocene sedimentation rate – Unit I and II have a combined

thickness of up to 6 m in the respective cores. Much of this high sedimentation rate is due to the intercalation of cm to mm-scale homogeneous clay layers, interpreted to represent periodical deposits of riverine suspension load; turbidites can be excluded from the elevated topographical position of the core sites [*Jørgensen*, 2003].

3. Material and Methods

The work presented in this thesis is based on gravity cores retrieved during the *RV Meteor* cruise M 51-4 in December 2001 on a transect from the lower shelf to the lowermost slope of the NW Black Sea (7 cores), and from the upper slope in the southwestern Black Sea (2 gravity cores) (Fig. 3).

Because they are of central importance for this thesis two methods used for paleoenvironmental reconstructions, the stable oxygen isotopes and the trace element ratios (Sr/Ca and Mg/Ca), will be discussed in more detail. The other methods used will be presented in a shorter form.

3.1 Stable oxygen isotopes

Stable oxygen isotope ratios are conventionally expressed in the delta notation as relative deviation from the isotopic ratio of a standard:

$$\delta^{18}O\,(in‰) = \frac{^{18}O/^{16}O_{sample} - ^{18}O/^{16}O_{standard}}{^{18}O/^{16}O_{standard}} \cdot 1000$$

The $\delta^{18}O$ of inorganically precipitated calcite is controlled by the temperature and $\delta^{18}O$ of the ambient water:

$$\delta^{18}O_{calcite}=(2.6229 \cdot 10^{6} \cdot (273.15+T)^{-2}+0.97002 \cdot \delta^{18}O_{water}-31.7648)$$ [*Rösler and Lange*, 1976],

where $\delta^{18}O_{calcite}$ is given in ‰ relative to the PDB standard; $\delta^{18}O_{water}$ in ‰ relative to SMOW and the temperature T in °C.

The different masses between the two stable isotopes of oxygen, ^{16}O and ^{18}O, lead to kinetically different reaction rates and thus to fractionation. The oxygen isotope composition in meteoric waters, the ultimate source of water for the Black Sea when disconnected from the

global ocean, is almost entirely a product of fractionation during evaporation and condensation and shows a close relation to geographic factors such as temperature, latitude, and elevation [*Epstein and Mayeda*, 1953; *Craig*, 1961; *Dansgaard*, 1964]. In general there is a decreasing trend in $\delta^{18}O$ of atmospheric precipitation with decreasing temperatures, increasing latitude, and increasing continentality [*Lister*, 1988]. While precipitation might be the dominant component for the stable oxygen isotopic composition of a river, contribution by groundwater and meltwater from snow or glaciers should not be neglected. An example for the importance of meltwater contribution is the formation of large ice-dammed lakes and the southward routing of rivers originally flowing towards the arctic ocean and Baltic Sea during the maximum advance of the Scandinavian Ice Sheet between ca. 17 – 18 kyr BP [*Mangerud et al.*, 2004]. This enhanced the contribution of rivers from the northeastern drainage area of the Black Sea (Dnestr, Dnepr, Don and the Caspian Sea – Manych Depression – Sea of Asov drainage corridor) after the Last Glacial maximum (LGM) until the drainage of meltwater was finally redirected towards the east into the Baltic basin at about 15 – 16 kyr BP [*Mangerud et al.*, 2004]. The highly depleted nature of glacial meltwater should have a significant impact on the $\delta^{18}O$ of the Black Sea.

River water and the lake water itself are permanently subject to fractionation processes through evaporation. Evaporation leads to isotopic enrichment of the remaining water because of the preferential loss of the light isotope ^{16}O during vaporisation. The exact isotopic composition of the water left after evaporation depends on several factors, the most important of them being the relative humidity, temperature, advection of air, and wind stress on the lake surface [*Gat et al.*, 1994]. Hence, the glacial/deglacial isotopic composition of the Black Sea is a complex mixture of factors controlling the $\delta^{18}O$ of its water body. Judging from the present day water fluxes, the most important contribution comes from the total run-off (350 km³ per year) that is more than the precipitation falling on the surface of the Black Sea (230 km³ per year). The annual evaporation from the lake surface accounts for 280 km³ [*Swart*, 1991]. It is evident that changes in the isotopic composition of the run-off will have a major impact on the isotopic composition of the Black Sea. As mentioned previously, more than half of the river run-off entering the present Black Sea is contributed by the Danube with an annual mean $\delta^{18}O$ = -10.5‰ [*Rank et al.*, 1999]. This is close to the isotopic signature of the total run-off (ca. -10‰ [*Swart*, 1991]), which therefore reflects a dominant central European contribution. If during past times the contribution of the Danube was less important, the average $\delta^{18}O$ of the total run-off and therefore the $\delta^{18}O$ of the Black Sea water would have changed. Higher run-off from the northern drainage area, for example, would have lowered

the $\delta^{18}O$ of the Black Sea, because of the generally more isotopic depleted precipitation in the northern catchment areas [*IAEA*, 2001].

The difference in the isotopic composition of Black Sea water between cold and warm periods depends to a large part on the low $\delta^{18}O$ in atmospheric precipitation during the glacial and Younger Dryas. Studies on deep lakes from southern Germany have shown that the difference in meteoric precipitation between the LGM and Bølling/Allerød were as big as 3.5‰ [*von Grafenstein et al.*, 1999a]. This must have had its impact on the $\delta^{18}O$ of the water transported by rivers, as well as on the on-lake atmospheric precipitation. The pace in which a lake is adjusting to a new steady state in its isotopic composition is expressed in the residence time T = V / I (V= volume of lake; I = input). The higher the residence time, the longer it takes the system to adjust to a new isotopic steady state. In the case of the very large water body of the Black Sea (V=537,000 km³) and an inflow (precipitation and run-off) of 580 km³ per year the residence time would be in the order of 900 years. This has to be taken into account when discussing short-term changes or events like single meltwater pulses.

A final exercise might illustrate the importance of the changes in the isotopic composition of the ambient water on the $\delta^{18}O$ of an ostracod valve when comparing it to the influence of the water temperature. For calcite precipitating in isotopic equilibrium a 0.23‰ decrease in $\delta^{18}O$ could be observed for a 1°C rise in temperature [*Holmes and Chivas*, 2002]. However, this temperature effect could easily be masked by changes in the $\delta^{18}O$ of the water; for comparison: a +3.5‰ shift in the $\delta^{18}O$ of the water, produced only by a change in the isotopic composition of the meteoric precipitation between Glacial and Holocene, would equal a calculated temperature decrease (!) of ca. 15.3°C. It is therefore apparent that an understanding of the processes governing the $\delta^{18}O$ composition of the Black Sea is vital for interpreting the $\delta^{18}O$ record obtained on ostracod shells.

Ostracods are mainly benthic crustaceans with calcitic shells, ubiquitous in terrestrial and marine aquatic environments. Their shells are widely used in reconstructing paleoenvironmental conditions in lacustrine and (less often) in marine environments. The physical and chemical mechanisms underlying the precipitation of such low-Mg calcite valves are similar to those governing the authigenic precipitation of inorganic carbonates from the water column. But since the building of a shell is a physiological process additional vital effects have to be considered. The vital offset found in ostracod valves with respect to a inorganic calcite precipitated in isotopic equilibrium is always positive and tends to be more-or-less constant within individual genera and closely related genera [*Holmes and Chivas*,

2002]. The vital offset that must be applied for the two species used for the stable oxygen isotope studies in the Black Sea, *Candona schweyeri* and *C. angulata*, should be near to +2.2‰ as determined for the genus *Candona* [*von Grafenstein et al.*, 1999b].

3.2 Mg/Ca and Sr/Ca ratios

Since the initial study about the relationship between trace-element content (Sr and Mg) in ostracod shells and host water in 1983 [*Chivas et al.*, 1983] extensive laboratory and field work has been done on this subject. These efforts showed that the Mg and Sr-content of ostracod shells is positively correlated to the Mg and Sr-content of the water in which the ostracod calcify. Mg additionally shows a temperature dependence. The partitioning of trace elements into ostracod shells has been described using the partition coefficient

$$D(M)_T = (M/Ca)_{water} / (M/Ca)_{shell}$$

where M = Mg or Sr, T = temperature, M/Ca is given in molar ratios.

It is tempting to use the partition coefficient as a tool for reconstruction the host water trace element ratio. However, there are some pitfalls that make this calculation problematic, especially for the Mg/Ca ratio. The trace element uptake into the ostracod shell is not constant during the growth of an ostracod. Not fully calcified juvenile ostracod valves tend to have anomalously high amounts of Mg and extremely variable Sr-contents [*Holmes and Chivas*, 2002] and should be avoided. Although the partition coefficient is thought to be similar for species belonging to the same genus or closely related genera [*Holmes and Chivas*, 2002], it turned out that different experiments yielded different partition coefficients for the same genus or even on species level, depending on the Mg/Ca of the host water. Calcification under conditions with very low Mg/Ca ratio (Mg/Ca_{water} <2 [*Wansard et al.*, 1999] or <1 [*Wansard et al.*, 1998]) leads to an exponential increase of D(Mg) [*Wansard et al.*, 1998] (Fig. 6). The reason for this excessive uptake of Mg is unclear; it might result from adsorption of Mg [*Wansard et al.*, 1998] or could be related to a critical amount of Mg that the ostracod has to incorporate into their low-Mg calcite shell [*Holmes and Chivas*, 2002]. In a similar way D(Mg) drops when the ostracod is forced to precipitate low-Mg calcite although the Mg/Ca ratio in the water is very high (Mg/Ca > 30) [*Xia et al.*, 1997; *De Deckker et al.*, 1999].
The relation between Sr/Ca in the ostracod shell and the host water seems to be simpler and was described as the linear function for the genus *Candona*:

$$Sr/Ca_{candona} = 0.332\ Sr/Ca_{water}$$ [*Wansard et al.*, 1999].

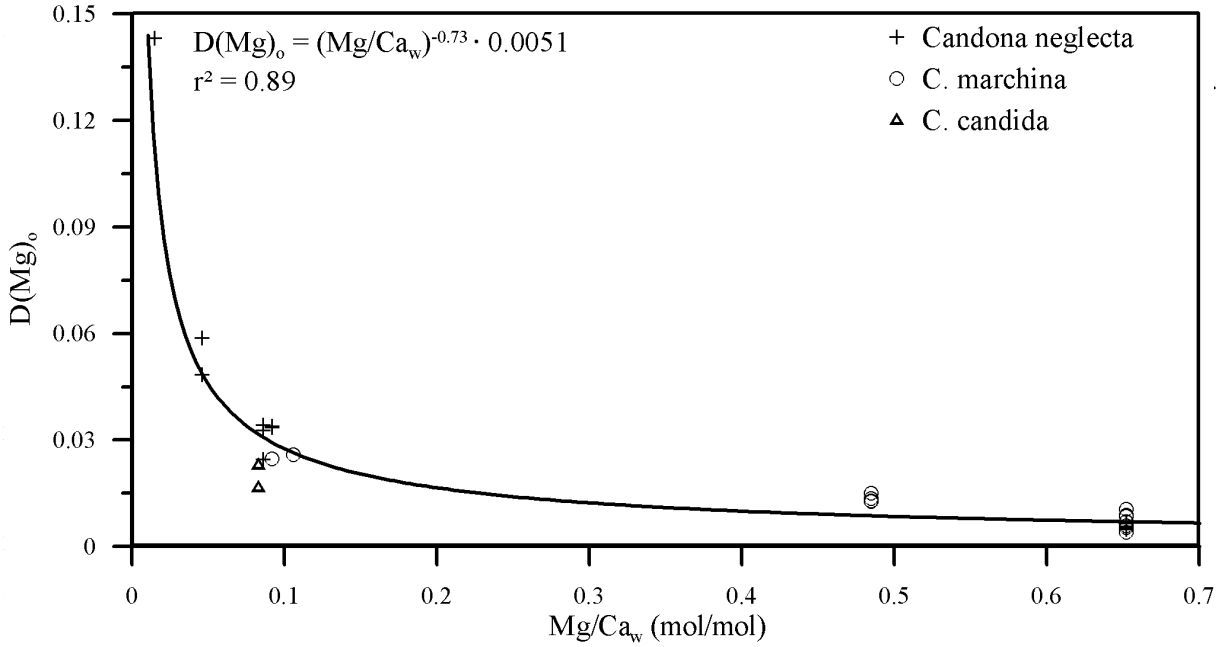

Fig. 6 Relation between the partition coefficient $D(Mg)_o$ of the ostracods *Candona neglecta, C. marchina* and *C. candida* to the host water Mg/Ca_w ratio (after *Wansard et al.* [1998]). The best fit of the data ($r^2 = 0.89$) yielded an exponential curve.

Major factors influencing the trace element composition of lake water are the precipitation of authigenic minerals, the change of the precipitated mineral phase, and modifications in the trace element composition of the sources feeding a lake. If for example low-Mg calcite precipitates, Sr and Mg will be enriched relative to Ca in the water column because low-Mg calcite is depleted in Mg and Sr relative to Ca. If, on the other hand, aragonite precipitates, the Sr/Ca ratio in the water column will drop because of the preferential uptake of Sr into aragonite. Thus a change from authigenic low-Mg calcite to aragonite will be identified in the ostracod Sr/Ca ratio. Since authigenic mineral precipitation is often dependent on the degree of evaporation and the following oversaturation with certain mineral phases Sr/Ca is sometimes misinterpreted to represent salinity changes. This might be true in some cases, e.g. in certain Australian lakes (e.g., Lake Keilambete) where the Sr/Ca of the water corresponds to salinity because of a simple solute evolutionary pathway [*Chivas et al.*, 1985, 1986, 1993], but often Sr/Ca and salinity do not have a systematic relation [*Chivas et al.*, 1993; *Haskell et al.*, 1996] and it is absolutely necessary to understand the hydrology and authigenic mineral precipitation in the lake water before calculating salinity changes from Sr/Ca [*Holmes and Chivas*, 2002].

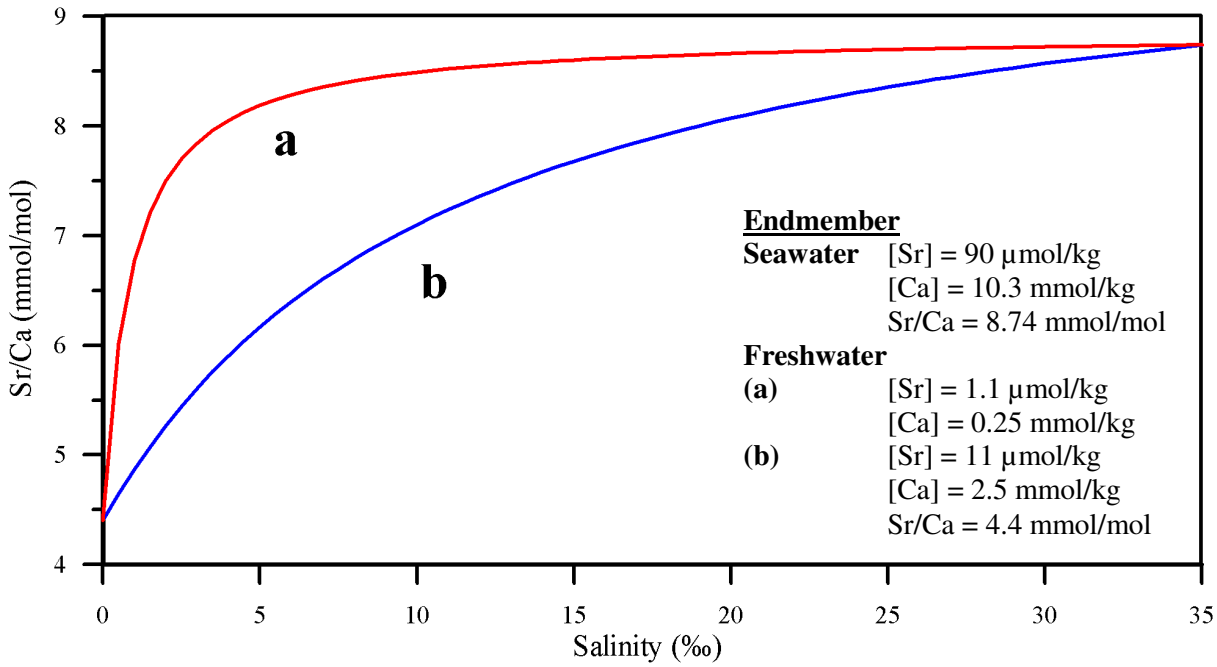

Fig. 7 Mixing lines between the two hypothetic endmembers freshwater (0‰ salinity) and seawater (35‰ salinity) for Sr/Ca. In (**a**) the freshwater endmember contains low, in (**b**) high Sr and Ca concentrations; the Sr/Ca ratio is the same in (a) and (b) (modified after *Anadón et al.* [2002]).

Another subject where the geochemical analysis of ostracods is promising, are reconstructions in environments with changing marine and terrestrial (freshwater) influence like in the Black Sea. Sr/Ca and Mg/Ca ratios are considerably higher in seawater than in freshwater (Sr/Ca in seawater = 8.74 mmol/mol; Sr/Ca in mean river water = 2.73 mmol/mol; Mg/Ca in seawater = 5.16 mol/mol; Mg/Ca in mean river water = 0.45 mol/mol [*Anadón et al.*, 2002]); if marine water intrudes a freshwater reservoir Sr/Ca and Mg/Ca will therefore increase following an (idealized) hyperbolic "two end-member model" mixing line [*Anadón et al.*, 2002]. It is important to note that the time a system needs to attain a steady Mg/Ca or Sr/Ca ratio when seawater enters a freshwater lake, is dependent on the initial concentration of Mg, Sr and Ca. The lower the initial concentration the quicker a steady state will be reached (Fig. 7). This also illustrates that quantifications of past salinities using Sr/Ca measurements in such a scenario are impossible without knowing the initial Sr and Ca element concentrations.

If any changes in the water chemistry can be excluded, Mg/Ca is usable for temperature reconstructions. In our study we use adult ostracods of the species *Candona schweyeri* for trace element analysis. It might therefore be tempting to apply the temperature calibration obtained for the species *Candona rawsoni*:

$$T\ (°C) = (Mg/Ca_{ostracod} - 0.004) / (Mg/Ca_{water} \cdot 0.0000968)$$ [*Engstrom and Nelson*, 1991].

It is nonetheless doubtful if this relation could be adopted for the species *Candona schweyeri* because it is not sure if the taxonomic classification of *C. rawsoni* as belonging to the genus *Candona* is correct [*Holmes and Chivas*, 2002] and, even if this is the case, it is not clear if the temperature relation is the same for the whole genus. Additionally, the prerequisite of a constant Mg/Ca_{water} ratio is not given for the pre-marine Black Sea as discussed in Manuscript 3.

Nevertheless, Sr/Ca and Mg/Ca measurements on ostracod valves are useful tools, which provide valuable informations on changes in the Black Sea solute chemistry and the onset of the reconnection with the Mediterranean Sea.

3.3 Other methods

For the reconstruction of the changes in sediment composition non-destructive X-ray fluorescence (XRF)-scanning on split cores [*Jansen et al.*, 1998; *Röhl and Abrams*, 2000] was performed yielding semiquantitiative concentrations of K, Ca, Ti, Fe, Mn, Cu and Sr. Previous studies (e.g., [*Arz et al.*, 1998, 1999]) have shown that element ratios as Ti/Ca or Fe/Ca are useful parameters to distinguish if biogenic components (rich in Ca, as part of $CaCO_3$) or terrigenous material (rich in elements like Ti or Fe) are the dominant fractions in the examined sediments. Thus periods with high fluvial input or high biologic productivity can be depicted using this technique. In addition, bulk grain size determinations were performed through wet sieving, giving an indication of the sand content of the sediment. The combination of XRF element ratios and grain size gives further insight into the mineralogy of the bulk sediment. High sand content accompanied by low Ti, Fe and Ca concentrations, for example, would point to a quartz-rich source. Due to its high spatial resolution, the XRF data is also valuable for correlating different cores. This was done for the gravity cores from the continental slope transect from the NW Black Sea. The core correlation was also further refined by routinely obtained colour reflectance data.

As part of a preliminary study, the concentration of alkenones (unsaturated methyl and ethyl-ketones) in core tops, distributed around a wide area in the western Black Sea was measured. Alkenones are mainly produced by haptophytic microalgae as for example the coccolithophoride *Emiliania huxleyi*, which is abundant in the Black Sea [*Hay et al.*, 1990]. It is known that the ratio of di- to tri- and tetraunsaturated alkenones is dependent on the sea-surface temperature, where the concentration of the diunsaturated component increases

relative to the more unsaturated components with increasing temperatures [*Marlowe*, 1984; *Brassel et al.*, 1986]. The ratio of di-, tri- and tetraunsaturated C_{37} alkenons ($C_{37:2}$, $C_{37:3}$ and $C_{37:4}$) is usually expressed as the alkenone unsaturation index U^{K}_{37} [*Brassel et al.*, 1986] $U^{K}_{37} = \frac{[C_{37:2}]-[C_{37:4}]}{[C_{37:2}]+[C_{37:3}]+[C_{37:4}]}$, which can be simplified to $U^{K'}_{37} = \frac{[C_{37:2}]}{[C_{37:2}]+[C_{37:3}]}$ if tetraunsaturated components are absent. Temperatures (in °C) can then be calculated using the equation $U^{K}_{37} = 0.033T + 0.043$ [*Prahl and Wakeham*, 1987] or, more commonly, $U^{K'}_{37} = 0.034T + 0.039$ [*Prahl et al.*, 1988]. The comparison of the alkenone-derived temperatures from core tops with the long-term annual mean sea-surface temperature (SST) distribution in the western Black Sea will show if this proxy is also applicable in the Black Sea.

4. Outline of manuscripts

The main part of this thesis is divided into four manuscripts, published or submitted to peer-reviewed international journals and one additional preliminary study.

The first manuscript *"Late glacial to Holocene climate and sedimentation history in the NW Black Sea"* (A. Bahr, F. Lamy, H. Arz, H. Kuhlmann, G. Wefer, 2005, Marine Geology 214, 309-322) is the basis on which the second and third manuscript are founded. It outlines the stratigraphic framework of the gravity cores from the NW Black Sea shelf and slope and draws attention to the major paleoenvironmental changes the glacial to early Holocene Black Sea has experienced.

While the first manuscript makes primarily use of sedimentological proxies (XRF and colour-scanning, bulk grainsize) the second manuscript *"Late glacial to Holocene paleoenvironmental evolution of the Black Sea, reconstructed with stable oxygen isotope records obtained on ostracod shells"* (A. Bahr, H.W. Arz, F. Lamy, G. Wefer, submitted to Earth and Planetary Science Letters) focuses on the hydrological evolution of the Black Sea from 30 to 7.5 kyr BP by means of $\delta^{18}O$ measurements on ostracod and bivalve shells. Another aspect of this publication is the high-resolution reconstruction of Danube river discharge variations during the deglacial period and their link to the North Atlantic climate system.

The third manuscript *"Abrupt changes during the deglacial and early Holocene in the Black Sea recorded with trace element (Sr, Mg, Ca), stable oxygen isotope and strontium isotope records*" (A. Bahr, F. Lamy, H.W. Arz, G. Wefer, to be submitted to Geochemistry,

Geophysics, Geosystems) focuses on Mg/Ca and Sr/Ca data measured on ostracods. In combination with all available proxies presented in the two other previous publications it represents the most complete suite of sedimentological and geochemical proxies available for the pre-marine Black Sea. The wealth of data is used to reconstruct the past hydrochemical changes of the Black Sea and to constrain the timing and nature of the reconnection with the Mediterranean Sea. It also gives information about the temperature-variability in the deep Black Sea over the past 30 000 years.

The fourth manuscript *"Multicentennial-scale hydrological changes in the Black Sea and northern Red Sea during the Holocene and the Arctic/North Atlantic Oscillation"* (F. Lamy, H.W. Arz, G.C. Bond, A. Bahr, J. Pätzold, Paleoceanography, in press) uses proxy-data from gravity cores located in the SW Black Sea and northernmost Red Sea to infer hydroclimatic changes in these areas over the past ca. 7500 years and their link to the Arctic Oscillation/North Atlantic Oscillation on multicentennial time scales.

The fifth manuscript *"A preliminary study on alkenons from the western Black Sea – is there a potential for SST reconstructions?"* (A. Bahr, H.W. Arz, F. Lamy, preliminary study) explores the possibility of sea-surfaces temperature reconstruction with the alkenone method for the last 2700 years in the Black Sea using core-top samples from the western Black Sea.

5. References

Aksu, A. E., P. J. Mudie, M. A. Kaminski, T. Abrajano and D. Yasar (2002), Persisent Holocene outflow from the Black Sea to the Eastern Mediterranean contradicts Noah's Flood hypothesis, *GSA Today*, 4-10.

Aksu, A. E., R. N. Hiscott and D. Yasar (1999), Oscillating Quaternary water levels of the Marmara Sea and vigorous outflow into the Aegean Sea from the Marmara-Black Sea drainage corridor, *Marine Geology*, *153*, 275-302.

Algan, O., C. Gazioglu, M. N. Cagatay, Z. Yücel and B. Gönencgil (1999), Sediment and water influxes into the Black Sea by Anatolien rivers, *Zeitschrift für Geomorphologie*, *43*, 61-79.

Anadón, P., E. Gliozzi and I. Mazzini (2002), Paleoenvironmental reconstruction of marginal marine environments from combined paleoecological and geochemical analyses on ostracods. In: J. A. Holmes (Editor), *Ostracoda: Applications in Quaternary Research*. AGU, Washington, pp. 227-247.

Arz, H. W., J. Patzold and G. Wefer (1998), Correlated millennial-scale changes in surface hydrography and terrigenous sediment yield inferred from last-glacial marine deposits off northeastern Brazil, *Quaternary Research*, *50*(2), 157-166.

Arz, H. W., J. Pätzold and G. Wefer (1999), Climatic changes during the last glaciation recorded in sediment cores from the northeastern Brazil Continental Margin, *Geo-Marine Letters*, *19*(19), 209-218.

Ballard, R. D., D. F. Coleman and G. Rosenberg (2000), Further evidence of abrupt Holocene drowning of the Black Sea shelf, *Marine Geology*, *170*, 253-261.

Bearman, G. (1995), *Open University*, *Oceanchemistry and Deep-sea sediments*, 238 pp., Pergamon, Oxford, New York, Beijing, Frankfurt, Sao Paulo, Sydney, Tokyo, Toronto.

Bondar, C., I. Stare, D. Cernea and E. Harabagiu (1991), Water flow and sediment transport of the Danube at its outlet into the Black Sea, *Meteorology and Hydrology*, *21*, 21-25.

Brassel, S. C., G. Eglinton, I. T. Marlowe, U. Pflaumann and J. M. Sarnthein (1986), Molecular stratigraphy: A new tool for climatic assessment, *Nature*, *320*, 129-133.

Chivas, A. R., P. De Deckker and J. M. G. Shelley (1983), Magnesium, strontium and barium partitioning in nonmarine ostracod shells and their use in paleoenvironmental reconstructions - a preliminary study. In: R. F. Maddocks (Editor), *Applications of Ostracoda*. Univ. Houston Geosci., Houston, pp. 238-249.

Chivas, A. R., P. De Deckker and J. M. G. Shelly (1985), Strontium content of ostracods indicates lacustrine palaeosalinity, *Nature*, *316*, 251.

Chivas, A. R., P. De Deckker and J. M. G. Shelly (1986), Magnesium content of non-marine ostracod shells: a new palaeosalinometer and palaeothermometer, *Palaeogeography, Palaeoclimatology, Palaeoecology*, *54*, 43-61.

Chivas, A. R., P. De Deckker, J. A. Cali, A. Chapman, E. Kiss and J. M. G. Shelley (1993), Coupled stable-isotope and trace-element measurements of lacustrine carbonates as paleoclimate indicators. In: P. K. Swart, K. C. Lohmann, J. McKenzie and S. Savin (Editors), *Climate change in continental isotopic records*. Geophysical Monograph, American Geophysical Union, Washington, D.C., pp. 113-121.

Cokacar, T., T. Oguz and N. Kubilay (2004), Satellite-detected early summer coccolithophore blooms and their interannual variability in the Black Sea, *Deep-Sea Research I*, *51*, 1017-1031.

Craig, H. (1961), Isotope variations in meteoric waters, *Science*, *133*, 1702-1703.

Curtis, J. H. and D. A. Hodell (1993), An isotopic and trace element study of ostracods from Lake Miragoane, Haiti: A 10,500 year record of paleosalinity and paleotemperature changes in the Caribbean. In: P. K. Swart (Editor), *Climate Change in Continental Isotopic records*. American Geophysical Union, Washington D.C., pp. 135-152.

Dansgaard, W. (1964), Stable isotopes in precipitation, *Tellus*, *16*, 436-468.

D'Arrigo, R. and H. M. Cullen (2001), A 350-Year (AD 1628-1980) reconstruction of Turkish precipitation, *Dendrochronologia*, *19*(2), 169-177.

De Deckker, P., A. R. Chivas and J. M. G. Shelly (1999), Uptake of Mg and Sr in the euryhaline ostracode Cyprideis determined from in vitro experiments, *Palaeogeography, Palaeoclimatology, Palaeoecology*, *148*, 105-116.

Engstrom, D. R. and S. Nelson (1991), Paleosalinity from trace metals in fossil ostracodes compared with observational records at Devils Lake, North Dakota, *Palaeogeography, Palaeoclimatology, Palaeoecology*, *83*, 295-312.

Epstein, S. and T. Mayeda (1953), Variations in ^{18}O content of waters from natural sources, *Geochimica et Cosmochimica Acta*, *27*, 213-224.

Gat, J. R., C. J. Bowser and C. Kendall (1994), The contribultion of evaporation from the Great Lakes to the continental atmosphere: estimate based on stable isotope data, *Geophysical Research Letters*, *21*(7), 557-560.

Haskell, B. J., D. R. Engstrom and S. C. Fritz (1996), Late Quaternary paleohydrology in the North American Great Plains inferred from the geochemistry of endogenic carbonate and fossil ostracodes from Devils Lake, North Dakota, USA, *Palaeogeography, Palaeoclimatology, Palaeoecology*, *124*(3-4), 179-193.

Hay, B. J., S. Honjo, S. Kempe, V. Ittekkot, E. T. Degens, T. Konuk and E. Izdar (1990), Interannual variability in particle flux in the southwestern Black Sea, *Deep-Sea Research A*, *37*(6), 911-928.

Hay, B. J., M. A. Arthur, W. A. Dean, E. D. Neff and S. Honjo (1991), Sediment deposition in the Late Holocene abyssal Black Sea with climatic and chronological implications, *Deep Sea Research*, *38*, S1211-S1235.

Hiscott, R. N., A. E. Aksu, D. Yasar, M. A. Kaminski, P. J. Mudie, V. E. Kostylev, J. C. MacDonald, F. I. Isler and A. R. Lord (2002), Deltas south of the Bosphorus Strait record persistent Black Sea outflow to the Marmara Sea since ~10 ka, *Marine Geology*, *190*, 95-118.

Holmes, J. A. and A. R. Chivas (2002), Ostracod shell chemistry - overview. In: J. A. Holmes (Editor), *Ostracoda: Application in Quaternary Research*. AGU, Washington, pp. 185-204.

IAEA, 2001. GNIP Maps and Animations. International Atomic Energy Agency, Vienna.

Jansen, J. H. F., S. J. Van der Gaast, B. Koster and A. J. Vaars (1998), CORTEX, a shipboard XRF-scanner for element analyses in split sediment cores, *Marine Geology*, *151*, 143-153.

Jones, G. A. and A. R. Gagnon (1994), Radiocarbon chronology of Black Sea sediments, *Deep-Sea Research I*, *41*(3), 531-557.

Jørgensen, B. B. (2003), Cruise 51, Leg 4, Istanbul - Istanbul, *METEOR-Berichte 03-1,* 1-57.

Kvasov, D. (Editor) (1968), *Paleohydrology of Eastern Europe in late Quaternary Time*. Yezhegodnkkh Chetniyakh Pamyati L.S. Berga Doklady. Izd. Nauka, Leningrad, 65-81 pp.

Lane-Serff, G. F., E. J. Rohling, H. L. Bryden and H. Charnock (1997), Postglacial connection of the Black Sea to the Mediterranean and its relation to the timing of sapropel formation, *Palaeogeography*, *12*(2), 169-174.

Lister, G. S. (1988) Stable isotopes from lacustrine ostracoda as tracers for continental palaeoenvironments. In: P. De Deckker, J.-P. Colin and J.-P. Peypouquet (Editors), *Ostracoda in the Earth Sciences*. Elsevier, Amsterdam, Oxford, New York, Tokyo, pp. 202-218.

Major, C., W. Ryan, G. Lericolais and I. Hajdas (2002), Constraints on Black Sea outflow to the Sea of Marmara during the last glacial-interglacial transition, *Marine Geology*, *190*, 19-34.

Mangerud, J., M. Jakobsson, H. Alexanderson, V. Astakhov, G. K. C. Clarke, M. Henriksen, C. Hjort, G. Krinner, J.-P. Lunkka and P. Moller (2004), Ice-dammed lakes and rerouting of the drainage of northern Eurasia during the Last Glaciation, *Quaternary Science Reviews*, *23*(11-13), 1313-1332.

Marlowe, I. T., 1984. Lipids as palaeoclimatic indicators. PhD thesis, University of Bristol.

Mudie, P. J., A. Rochon and A. E. Aksu (2002a), Pollen stratigraphy of Late Quaternary cores from Marmara Sea: land-sea correlation and paleoclimatic history, *Marine Geology*, *190*, 233-260.

Mudie, P. J., A. Rochon, A. E. Aksu and H. Gillespie (2002b), Dinoflagellate cysts, freshwater algae and fungal spores as salinity indicators in Late Quaternary cores from Marmara and Black seas, *Marine Geology*, *190*, 203-231.

Murray, J. W., H. W. Jannasch, S. Honjo, F. Anderson, W. S. Reeburgh, Z. Top, E. Friederich, L. A. Codispoti and E. Izdar (1989), Unexpected changes in the oxic/anoxic interface in the Black Sea, *Nature*, *338*, 411-413.

Myers, P. G., C. Wielki, S. B. Goldstein and E. J. Rohling (2003), Hydraulic calculations of postglacial connections between the Mediterranean and the Black Sea, *Marine Geology*, *201*, 253-267.

Nikishin, A. M., M. V. Korotaev, A. V. Ershov and M.-F. Brunet (2003), The Black Sea basin: tectonic history and Neogene-Quaternary rapid subsidence modelling, *Sedimentary Geology*, *156*(1-4), 149-168.

Oguz, T., P. E. LaViolette and Ü. Ünlüata (1992), The upper layer circulation of the Black Sea: its variability as inferred from hydrographic and satellite observations, *Journal of Geophysical Research*, *97*, 12569-12584.

Oguz, T., V. S. Latun, M. A. Latif, V. V. Vladimirov, H. I. Sur, A. A. Markov, E. Öszoy, B. B. Kotovshchikov, V. V. Eremeev and Ü. Ünlüata (1993), Circulation in the surface and intermediate layers of the Black Sea, *Deep Sea Research*, *41*, 603-628.

Oguz, T. and S. Besiktepe (1999), Observations on the Rim Current structure, CIW formation and transport in the western Black Sea, *Deep-Sea Research I*, *46*(10), 1733-1754.

Öszoy, E. and Ü. Ünlüata (1997), Oceanography of the Black Sea: A review of some recent results, *Earth-Science Reviews*, *42*, 231-272.

Panin, N. and D. Jipa (2002), Danube River sediment input and its interaction with the northwestern Black Sea, *Estuarine, Coastal and Shelf Science*, *54*, 551-562.

Pilskaln, C. H. and J. Pike (2001), Formation of Holocene sedimentary laminae in the Black Sea and the role of the benthic flocculent layer, *Paleoceanography*, *16*(1), 1-19.

Prahl, F. G. and S. G. Wakeham (1987), Calibration of unsaturation patterns in long-chain ketone compositions for palaeotemperature assessment, *Nature*, *330*, 367-369.

Prahl, F. G., L. A. Muehlhausen and D. L. Zahnle (1988), Further evaluation of long-chain alkenones as indicators of paleoceanographic conditions, *Geochimica et Cosmochimica Acta*, *52*, 2303-2310.

Rank, D., E. Öszoy and I. Salihoglu (1999), Oxygen-18, deuterium and tritium in the Black Sea and the Sea of Marmara, *Journal of Environmental Radioactivity*, *43*, 231-245.

Rimbu, N., C. Boronean, C. Buta and M. Dima (2002), Decadal variability of the Danube River flow in the lower basin and its relation with the North Atlantic Oscillation, *International Journal of Climatology*, *22*, 1169-1179.

Rimbu, N., M. Dima, G. Lohmann and S. Stefan (2004), Impacts of the North Atlantic Oscillation and the El Nino-Southern Oscillation on Danube river flow variability, *Geophysical Research Letters*, *31*, L23203.

Röhl, U. and L. J. Abrams (2000), High-resolution, downhole, and nondestructive core measurements from site 999 and 1001 in the Caribbean Sea: application to the late Paleocene thermal maximum. In: R. M. Leckies, H. Sigurdsson, G. D. Acton and G. Draper (Editors), *Proc. ODP Sci. Res.*, College Station, TX, pp. 191-203.

Rösler, H. J. and H. Lange (1976), *Geochemische Tabellen*, 674 pp., Ferdinand Enke Verlag, Stuttgart.

Ross, D. and E. T. Degens (1974), Recent Sediments of Black Sea. In: E. T. Degens and D. Ross (Editors), *The Black Sea - Geology, Chemistry and Biology*. AAPG, Tulsa, pp. 183-199.

Ryan, W. B. F., W. C. Pitman III, C. Major, K. Shimkus, V. Moskalenko, G. A. Jones, P. Dimitrov, N. Görür, M. Sakinc and H. Yüce (1997), An abrupt drowning of the Black Sea shelf, *Marine Geology*, *138*, 119-126.

Ryan, W. B. F. and W. C. Pitman (1999), *Noah's flood: the new scientific discoveries about the event that changed history.*, 319 pp., Simon & Schuster, New York.

Ryan, W. B. F., C. O. Major, G. Lericolais and S. L. Goldstein (2003), Catastrophic flooding of the Black Sea, *Annual Review of Earth and Planetary Science*, *31*, 525-554.

Sinninghe Damsté, J. S., S. G. Wakeham, M. E. L. Kohnen, J. M. Hayes and J. W. de Leeuw (1993), A 6,000-year sedimentary molecular record of chemocline excursions in the Black Sea, *Nature*, *362*, 827-829.

Sperling, M., G. Schmiedel, C. Hemleben, K. C. Emeis, H. Erlenkeuser and P. M. Grootes (2003), Black Sea impact on the formation of eastern Mediterranean sapropel S1? Evidence from the Marmara Sea, *Palaeogeography, Palaeoclimatology, Palaeoecology*, *190*, 9-21.

Stanev, E. V. and E. L. Peneva (2001), Regional sea level response to global climatic change: Black Sea examples, *Global and Planetary Change*, *32*(1), 33-47.

Sur, H. I., E. Öszoy and Ü. Ünlüata (1994), Boundary current instabilities, upwelling, shelf mixing and eutrophication processes in the Black Sea, *Progress in Oceanography*, *33*, 249-302.

Swart, P. K. (1991), Factors affecting the oxygen isotopic composition of the Black Sea. In: E. Izdar and J. W. Murray (Editors), *Black Sea Oceanography*. Kluwer, Dordrecht, Boston, London, pp. 75-88.

Tekiroglu, e., V. Ediger, S. Yemenicioglu, S. Kapur and E. Akca (2001), The experimental analysis on the Late Quaternary deposits of the Black Sea, *Oceanologica Acta*, *24*(1), 51-67.

Turkes, M. and E. Erlat (2003), Precipitation changes and variability in Turkey linked to the North Atlantic Oscillation during the period 1930-2000, *International Journal of Climatology*, *23*, 1771-1796.

von Grafenstein, U., H. Erlenkeuser, A. Brauer, J. Jouzel and S. Johnsen (1999a), A Mid-European decadal isotope-climate record from 15,500 to 5000 Years B.P., *Science*, *284*, 1654-1657.

von Grafenstein, U., H. Erlenkeuser and P. Trimborn (1999b), Oxygen and carbon isotopes in modern fresh-water ostracod valves: assessing vital offsets and autecological affects of interest for palaeoclimate studies, *Palaeogeography, Palaeoclimatology, Palaeoecology*, *148*, 133-152.

Wansard, G., P. De Deckker and R. Julia (1998), Variability in ostracod partition coefficients D(Sr) and D(Mg): Implications for lacustrine palaeoenvironmental reconstructions, *Chemical Geology*, *146*(1-2), 39-54.

Wansard, G., J. P. Roca and F. Mezquita (1999), Experimental determination of strontium and magnesium partitioning in calcite of the freshwater ostracod Herpetocypris intermedia, *Arch. Hydrobiol.*, *145*, 237-253.

Winguth, C., H. K. Wong, N. Panin, C. Dinu, P. Georgescu, G. Ungureanu, V. V. Krugliakov and V. Podshuveit (2000), Upper Quaternary water level history and sedimentation in the northwestern Black Sea, *Marine Geology*, *167*, 127-146.

Xia, J., D. R. Engstrom and E. Ito (1997), Geochemistry of ostracode calcite: Part 2. The effects of water chemistry and seasonal temperature variation on Candona rawsoni, *Geochimica et Cosmochimica Acta*, *61*(2), 383-391.

Zubakov, V. A. (1988), Climatostratigraphic scheme of the Black Sea Pleistocene and its correlation with the oxygen-isotope scale and glacial events, *Quaternary Research*, *29*, 1-24.

MANUSCRIPT 1

Late glacial to Holocene climate and sedimentation history in the NW Black Sea

André Bahr[a], Frank Lamy[b], Helge Arz[b], Holger Kuhlmann[a], Gerold Wefer[a]

[a] Universität Bremen, Fachbereich 5 – Geowissenschaften, Postfach 33 04 40, D-28334, Bremen, Germany

[b] GeoForschungsZentrum Potsdam, Telegrafenberg, 14473 Potsdam

(*Marine Geology*, 2005, v. 214, 309-322)

Abstract

Gravity cores from the continental slope in the northwestern Black Sea were studied using high-resolution stable isotope, grain size and XRF-scanning data. The measurements provide a 30 000 yrs AMS ^{14}C-dated record of variations in the hydrological regime of the Black Sea and give insight into changing paleoenvironments in the surrounding areas. Stable climatic conditions during the Last Glacial Maximum were followed by a series of meltwater pulses most likely originating from the Scandinavian ice sheet between 18 000 and 15 500 yr BP[1]. This meltwater input rose the level of the Caspian Sea to a point that Caspian water could spill into the Black Sea via the Manych-depression north of the Caucasian mountains. High-frequency oscillations in the XRF-data during this period suggest a probable link to the arctic climate regime. Later, during the Bølling/Allerød and the early Holocene, prevailing high temperatures led to authigenic calcite precipitation through increased phytoplankton activity, interrupted by the Younger Dryas and the "8200 yr BP cold event" with dominant clastic sedimentation.

Keywords

Black Sea, paleoclimate, paleohydrology, late glacial, Holocene, Caspian Sea

[1] All dates are calibrated to calendar years B.P. (yr BP).

1. Introduction

The Black Sea as an almost isolated marginal sea reacts particularly sensitive to paleoenvironmental changes. Black Sea sediments therefore provide an excellent opportunity for high-resolution studies of past climatic and hydrological changes in the catchment. Whereas previous studies centered mainly around the analysis of marine Holocene deposits (e.g., [*Ross and Degens*, 1974; *Hay et al*., 1991; *Jones and Gagnon*, 1994; *Pilskaln and Pike*, 2001]) and the establishment of the Black Sea-Sea of Marmara-Mediterranean drainage corridor (e.g., [*Ryan et al*., 1997; *Aksu et al*., 1999; *Cagatay et al*., 2000; *Myers et al*., 2003]), first detailed sedimentological and geochemical analyses of the late glacial to Holocene limnic sediments were published only recently [*Major et al.,* 2002; *Ryan et al*., 2003].

A main concern of any work on the limnic sediments is to create a reliable stratigraphy, because the unknown reservoir effect during the lake stage of the Black Sea hampers precise radiocarbon dating. In their study of gravity cores from the northwestern Black Sea, *Major et al.* [2002] assumed a reservoir age of 0 yrs. To further reinforce this stratigraphy they correlated two distinct horizons from the Black Sea with similar ones in the Caspian Sea: a series of reddish-brown clays deposited from about 15.8 to 17.7 kyr BP and, second, a diatom-rich layer from the deep basin floor with ages of 10.6 to 10.7 kyr BP [*Ryan et al*., 2003], which was correlated with the "*Stephanodiscus* horizon" in the Caspian Sea [*Zhakovshchikova*, 1968]. Both horizons were attributed to an outflow of Caspian waters through the Manych-depression into the Black Sea during periods of massive meltwater pulses from the Fennoscandian and Siberian ice shields in the late glacial [*Kroonenberg et al.,* 1997; *Grosswald and Hughes*, 2002].

To decipher the evolution of the Black Sea, the timing and development of the connection via the Sea of Marmara with the Mediterranean Sea has to be known. Some researchers propose a continuous Black Sea outflow during the last glacial and Holocene [*Ross and Degens*, 1974; *Lane-Serff et al.*, 1997] while other authors postulate an evaporative drawdown of the Black Sea level through the Last Glacial Maximum (LGM) down to -110 m [*Aksu et al*., 2002a] or -150 m [*Winguth et al*., 2000], well below the present Bosphorus sill depth (-32 m). It has been pointed out by several authors that the depth of the Bosphorus sill plays a central role for the onset of the Black Sea-Marmara connection [*Major et al.,* 2002; *Myers et al.*, 2003; *Sperling et al*., 2003]. A deep Bosphorus (-80 m) would allow intrusion of Mediterranean water as early as ca. 14 kyr BP [*Major et al.*, 2002], whereas a shallow sill depth of ca. -35 m is consistent with the so-called "Noah's Flood hypothesis", in which *Ryan et al*. [1997]

proposed a catastrophic inundation of the Black Sea following the breeching of the Bosphorus by Mediterranean water at around 9400 yr BP [*Ryan et al.,* 2003]. *Sperling et al.* [2003] argue that a sill at least 7 m higher than today would fit best to the salinity evolution of the Sea of Marmara and the Aegean Sea at around 8700 yr BP. An opposing view offered *Aksu et al.* [2002b], who assumed that a positive water balance led the Black Sea level to rise above the Bosphorus sill depth at around 11.4 to 12.8 kyr BP and allowed water from the Black Sea into the Sea of Marmara.

The aim of this study is to refine the understanding of the late glacial to Holocene evolution of the Black Sea and its surrounding areas. For this purpose we conducted a high-resolution multi-proxy study on gravity cores from the northwestern Black Sea continental slope. These data allow a detailed reconstruction of climatic and hydrologic changes in the western Black Sea basin during the last 30 000 yrs.

2. Study area

The studied gravity cores are located in the northwestern Black Sea, south of the Danube delta, on a lower shelf to slope transect from 118 m to 1977 m water depth (Tab. 1; Fig. 1). The area is characterised by the very broad northwestern Black Sea shelf, which comprises almost 94% of the total shelf area in the Black Sea [*Panin and Jipa*, 2002]. The continental slope is very gentle and shaped by the morphology of the pre-Holocene Danube fan, reaching far out towards the centre of the western Black Sea basin.

Table 1
Location and length of the sampled cores.

Core name	Latitude N	Longitude E	Water depth	Core length
GeoB 7604-2	42°56.2'	30°01.9'	1977 m	592 cm
GeoB 7607-2	43°09.7'	29°57.7'	1562 m	636 cm
GeoB 7608-1	43°29.2'	30°11.8'	1202 m	685 cm
GeoB 7609-1	43°32.8'	30°09.2'	941 m	655 cm
GeoB 7610-1	43°38.9'	30°04.1'	465 m	880 cm
GeoB 7611-1	43°41.8'	30°00.1'	118 m	634 cm
GeoB 7616-4	43°41.0'	30°02.5'	168 m	916 cm

Riverine input to the northwestern Black Sea continental margin derives mainly from the Danube, the second largest river in Europe with a drainage basin of over 817 000 km² [*Panin and Jipa*, 2002]. Although the Danube delivers by far the largest amount of water and sediment load of all rivers to the Black Sea (multiannual mean discharge of water before

damming the river: 190.7 $km^3 \cdot yr^{-1}$; mean sediment discharge: 51.70 $Mt \cdot yr^{-1}$ [*Bondar et al.,* 1991; *Panin and Jipa*, 2002]), the outer shelf in the study area is known to be sediment-starved [*Panin and Jipa*, 2002]. This is the result of the strong (>50 $cm \cdot s^{-1}$) cyclonic "Rim Current" [*Oguz and Besiktepe*, 1999], which transports most of the suspended sediments along the coast towards the deep-sea region [*Panin and Jipa*, 2002] (Fig.1). Therefore, Holocene sediments are only present as a very thin cover or absent on this part of the shelf.

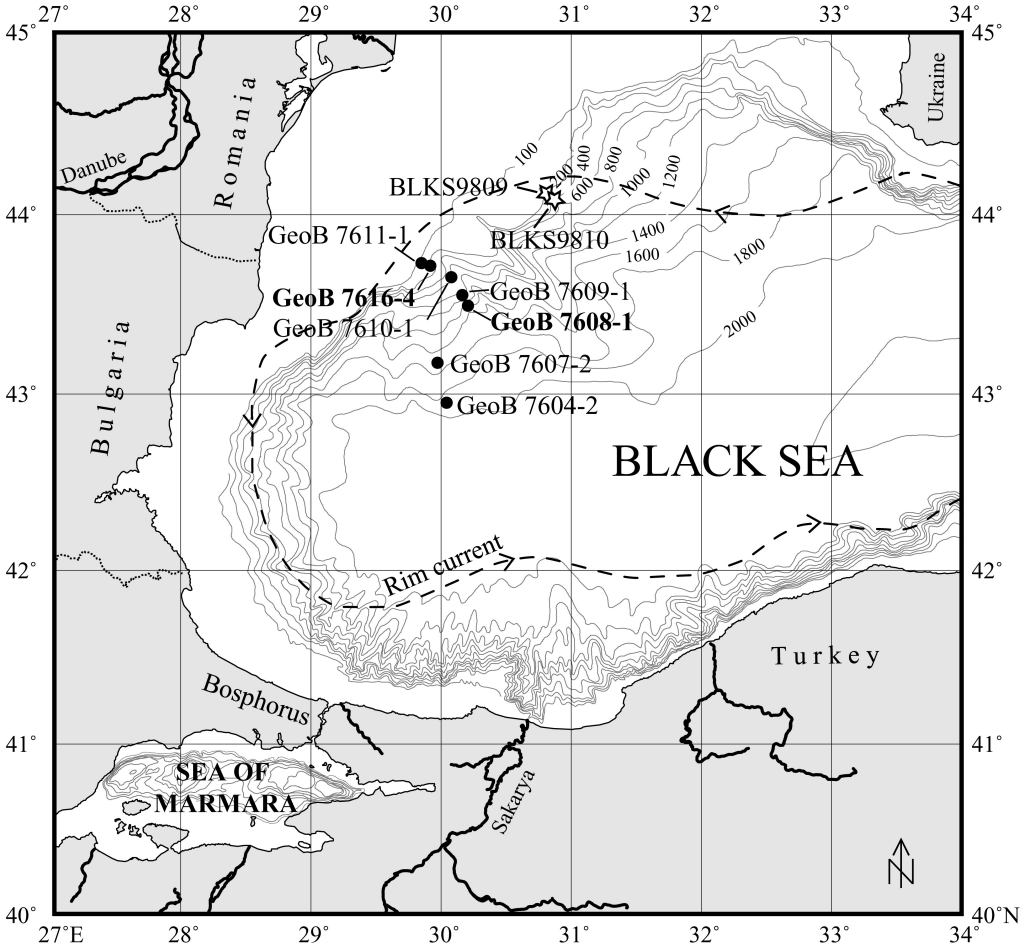

Fig. 1 Location of gravity cores recovered during *RV Meteor* cruise M51-4 (circles) and location of two cores presented in a previous study [*Major et al.,* 2002] (stars). Also indicated is the approximate position of the Black Sea rim current (after [*Oguz et al.*, 1993]).

The sediment transported by the Danube is derived from a large drainage area in southeastern Europe. In its middle and lower course, the Danube flows through the Quaternary fluvial and eolian deposits of the Hungarian and Walachian lowlands, through Cretaceous and Tertiary flysch and molasse of the northern Carpathian Mountains and through gneiss and crystalline schists of the southern Carpathian Mountains. The southern drainage area is mostly dominated by granites and crystalline schists of the Balkans [*Müller and Stoffers*, 1974]. Sediment input

from the regions north of the Black Sea by the rivers Dniester, Dniepr and Don is of minor importance today. But, as discussed later, it may have been larger during the deglacial.
Climatically the western Black Sea is situated in the transition between the humid climatic regime of the mid-latitudes in SE Europe with a temperate mixed forest and precipitation >1000 $mm \cdot yr^{-1}$, a more continental climate in the northern part of the Black Sea and the eastern Danube lowlands with savannah grasslands and <600 mm annual rainfall and, third, the Mediterranean climate region in the south towards the Sea of Marmara [*Mudie et al.*, 2002b].

3. Material and Methods

3.1. Material

7 gravity cores retrieved during the RV Meteor-cruise M51-4 in December 2001 were chosen for the present study (Tab. 1). All sediment cores from the continental slope show the subdivision in three units typical for sediments from the Black Sea basin [*Ross and Degens*, 1974]: the marine units I (finely laminated coccolith ooze) and II (sapropelic sediments) at the top with a fairly constant thickness of together ca. 45 cm, and the lowermost Unit III, which consists of homogeneous to (mostly) cm-scale laminated muddy clay deposited under lacustrine conditions.
The cores from the lower shelf are characterised by homogeneous to cm-scale laminated mud with abundant shells and shell fragments of bivalves and gastropods representing entirely Unit III sediments. Holocene sediments are nearly completely missing, except for the uppermost horizon of GeoB 7611-1 that revealed a late Holocene age of 2585 yr BP.

3.2. Methods

3.2.1. Profiling measurements

A Minolta CM - 2002™ hand-held spectrophotometer was used to measure percent reflectance values of sediment color at 31 wavelength channels over the visible light range (400-700 nm). The digital reflectance data of the spectrophotometer readings were obtained from the surface (measured in 1 cm steps) of the split cores. The red/blue ratio was calculated as the ratio between the 700 nm and 450 nm wave lengths.

All cores listed in Tab. 1 except GeoB 7611-1 were scanned in 1 cm intervals with a X-ray fluorescence scanner at the University of Bremen, Germany. The XRF-core scanner, developed at the Netherlands Institute for Sea Research, Texel, measures the bulk intensities of major elements (e.g., K, Ca, Ti, Mn, Fe, Cu and Sr) on split sediment cores [*Jansen et al*., 1998; *Röhl and Abrams*, 2000]. These data were used to correlate the cores along the slope transect.

3.2.2. Radiocarbon dating

For AMS ^{14}C-dating on the shallow water core GeoB 7616-4, 6 samples containing shells of the bivalve species *Dreissena rostriformis* were collected. Due to the absence of *Dreissena rostriformis,* we used 7 samples with ostracods and/or molluscs shells for dating the deeper core GeoB 7608-1 (Tab. 2). Carbonate hydrolysis and CO_2-reduction of the samples were performed at the University of Bremen, Germany; the AMS measurements were done at the Leibniz-Labor in Kiel, Germany [*Nadeau et al*., 1997].

Table 2
Radiocarbon ages from gravity cores GeoB 7608-1 and 7616-4. For GeoB 7608-1 a correction of 1000 yrs was applied before calibrating, in GeoB 7616-4 calendar ages were calculated with 0 yrs correction.

Lab.-ID	Core depth	^{14}C age (yr BP)	Calendar age (yr BP)	Material
GeoB 7608-1				
KIA 21464	34 cm	7735 ± 50	7607 ± 40	Ostracods
KIA 21463	88 cm	11 460 ± 70	12 342 ± 215	Gastropod
KIA 21461	158 cm	13 350 ± 80	14 469 ± 365	Gastropod
KIA 21460[a]	243 cm	17 080 + 150 / -140	18 563 ± 320	Ostracods and bivalves
KIA 21866	436 cm	16 360 ± 70	17 951 ± 285	Ostracods and bivalves
KIA 21459	596 cm	20 140 + 180 / - 170	22 499 ± 265	Gastropod
KIA 21457	652 cm	24 970 + 310 / -300	26 891 ± 480	Mixed mollusc shells
GeoB 7616-4				
KIA 18212	2 cm	10 470 ± 60	12 360 ± 200	*Dreissena rostriformis*
KIA 19681	184 cm	10 945 ± 60	12 855 ± 50	*Dreissena rostriformis*
KIA 19680	386 cm	11 250 ± 60	13 055 ± 90	*Dreissena rostriformis*
KIA 19678	579 cm	11 670 ± 80	13 435 ± 140	*Dreissena rostriformis*
KIA 19677	802 cm	12 040 ± 130	13 824 ± 220	*Dreissena rostriformis*
KIA 18213	899 cm	13 105 ± 55	15 452 ± 105	*Dreissena rostriformis*

[a] The date from 243 cm depth in GeoB 7608-1 was discarded because of its high age.

3.2.3. Stable isotopes measurements

For stable isotope analyses ($\delta^{18}O$ and $\delta^{13}C$) on core GeoB 7616-4, a total of 288 samples recovered in 4 cm intervals were collected and wet sieved with 63 and 150 µm mesh size. From the fraction >150 µm we collected 5 to 7 juvenile shells of the freshwater bivalve *Dreissena rostriformis* and analysed them at the Geoscience Department at the University of Bremen using a Finnigan MAT 251 mass spectrometer with an automated carbonate preparation device. The ratio of $^{18}O/^{16}O$ is given in ‰ relative to the PDB standard. Analytical long-time standard deviation is about ±0.07‰ PDB.

All data are available under the name of the corresponding author through the PANGAEA server (www.pangaea.de/PangaVista).

4. Chronology

The stratigraphies of GeoB 7608-1 and GeoB 7616-4 are principally based on the linear interpolation between 6 AMS ^{14}C dates for each core (Tab. 2). For calibration to calendar years BP (1950) we used the program CALPAL (Version 2003 [*Weninger and Jöris*, 2003]) mainly based on the INTCAL-98 [*Stuiver et al*., 1998] calibration set. The date at 243 cm depth in GeoB 7608-1 was discarded because its age was regarded as too old, probably because it contains reworked shell material. The stratigraphy of GeoB 7608-1 was further refined by using the 2700 yr BP Unit I/Unit II boundary [*Jones and Gagnon*, 1994] at 8 cm core depth and 7540 yr BP for the Unit II/Unit III boundary [*Jones and Gagnon*, 1994] at 31 cm core depth as additional time markers. Although our dating of 7600 yr BP from 34 cm core depth (directly below the Unit II/Unit III boundary) is in good agreement with the published data for this boundary we decided to use only the well-founded 7540 yr BP date. Since the upper part of Unit I is not preserved in GeoB 7608-1, an age of 1380 yr BP was calculated for the core top through extrapolation using the sedimentation rate computed for Unit II.

A central problem when working on the last glacial lacustrine sediments of the Black Sea is the construction of a consistent stratigraphy, primarily for the reason that radiocarbon dates do not allow precise age assignments because of an unknown reservoir age. *Major et al*. [2002] based their stratigraphy on ^{14}C-dates on individual mollusc shells assuming a 0 yrs reservoir correction and correlations with marker horizons from the Caspian Sea (see introduction). In

order to prove the validity of our radiocarbon dates, especially those on shell debris from GeoB 7608-1, we tried to link our cores with those studied by *Major et al.* [2002], which are located adjacent to our study area (cores BLKS9809 and 9810, Fig. 1).

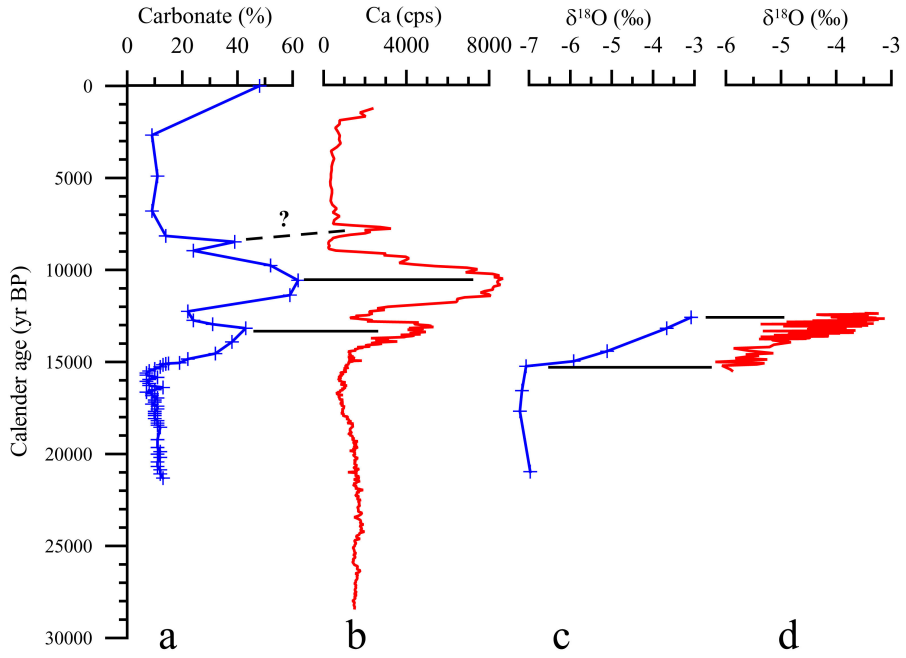

Fig. 2 Correlation of (**a**) the carbonate content of core BLKS9810 after *Major et al.* [2002] with (**b**) the XRF-Ca content in GeoB 7608-1 and (**c**) the $\delta^{18}O$ of mollusc shells in cores BLKS9809 and BKLS 9810 after *Major et al.* [2002] with (**d**) $\delta^{18}O$ measurements on *Dreissena rostriformis* juv. in GeoB 7616-4. For (b) an age correction of 1000 yrs was applied before calibrating, all other curves are calibrated to calendar years with 0 yrs age correction.

The XRF Ca-curve from GeoB 7608-1 and the carbonate content published by *Major et al.* [2002] are fairly congruent, if an age correction of 1000 yrs is applied to the measurements on GeoB 7608-1 (Fig. 2). In contrast, the oxygen isotope data from GeoB 7616-4 and those given by *Major et al.* [2002] seem to fit without any age correction, although the low number of values in the published record only allows a rough comparison (Fig. 2). This discrepancy might be explained by the different dating material: because of the scarcity of material in GeoB 7608-1, a mixture of ostracodes and shell debris was pooled for dating (Tab. 2); this may have introduced older material in the samples. Because the radiocarbon dates in *Major et al.* [2002] and GeoB 7616-4 are both based on adult mollusc shells, the probability of contamination with older material is smaller. Furthermore, the specimens of *Dreissena rostriformis* used for dating GeoB 7616-4 were found articulated and in living position and thus may be considered to be autochthonous. As a consequence we adopted the published

stratigraphy by *Major et al.* [2002] and applied the suggested age correction of 1000 yrs for GeoB 7608-1.

It is worth noting that the offset of 1000 yrs is fairly constant throughout the core GeoB 7608-1. This could be coincidence, but may alternatively be explained by a stratification of the ancient Black Sea lake: at least the upper 400 m (the present water depth of the cores published by *Major et al.* [2002] are 240 m for BLKS98109 and 378 m for BLKS9810) of the water column were ventilated and therefore show no reservoir age, whereas GeoB 7608-1 from 1202 m water depth may contain signals of an older, not ventilated water mass. This assumes that a permanent stratification persisted throughout the glacial and deglacial period.

5. Results

5.1. Slope transect

The correlation of the five cores along the slope transect was done using the Ca-intensity to track the Unit I/II boundary and the carbonate peaks in the upper 1-2 m of the cores. In the lower part of the cores (especially for the red layers) Fe, Ti, K-intensities, Fe/Ca, Ti/Ca, K/Ca ratios and the spectral red/blue ratio were the most useful parameters for correlation (Ca and Ti/Ca are shown in Fig. 3). The identification of the carbonate peaks in GeoB 7610-1 is difficult, because the high amount of terrigenous material dilutes the Ca-signal.

The thickness of the Holocene units I and II is fairly constant in all cores, while the limnic sediments show an at least fourfold increase in sedimentation rate towards shallower water depths. This increase is most pronounced in the interval between the end of the carbonate peaks and the onset of the red layers, but weakens during the deposition of the red layers (Fig. 4).

GeoB 7608-1 was chosen for further investigation because it has a continuous sediment record without any turbidites and represents a good compromise between deep penetration and high resolution.

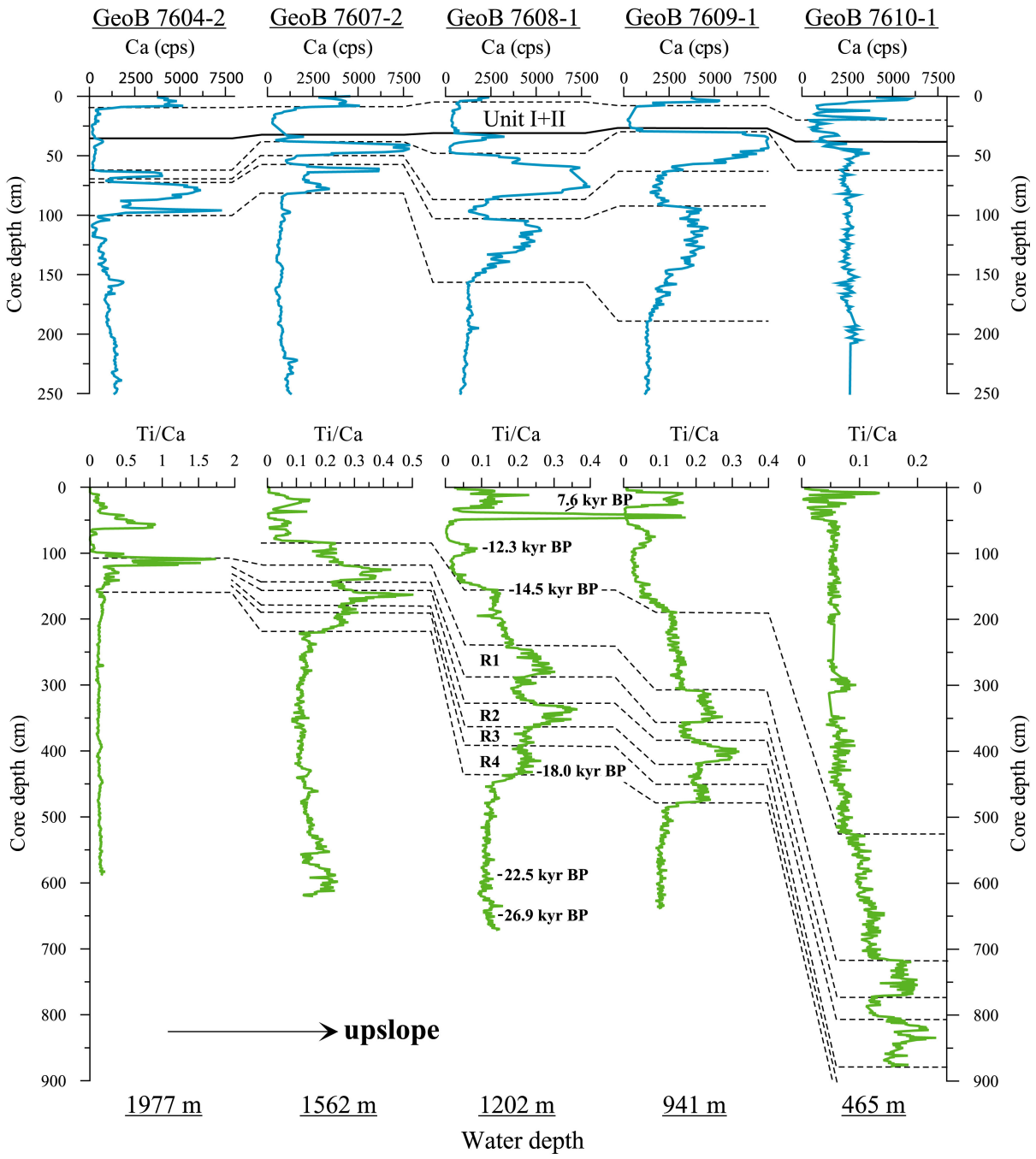

Fig. 3 Correlation of gravity cores from the slope transect in the northwestern Black Sea using the XRF-Ca-intensity (upper graph) and Ti/Ca ratio (lower graph). For GeoB 7608-1 the radiocarbon dates are indicated in calendar years. R1 to R4 indicate the red layers.

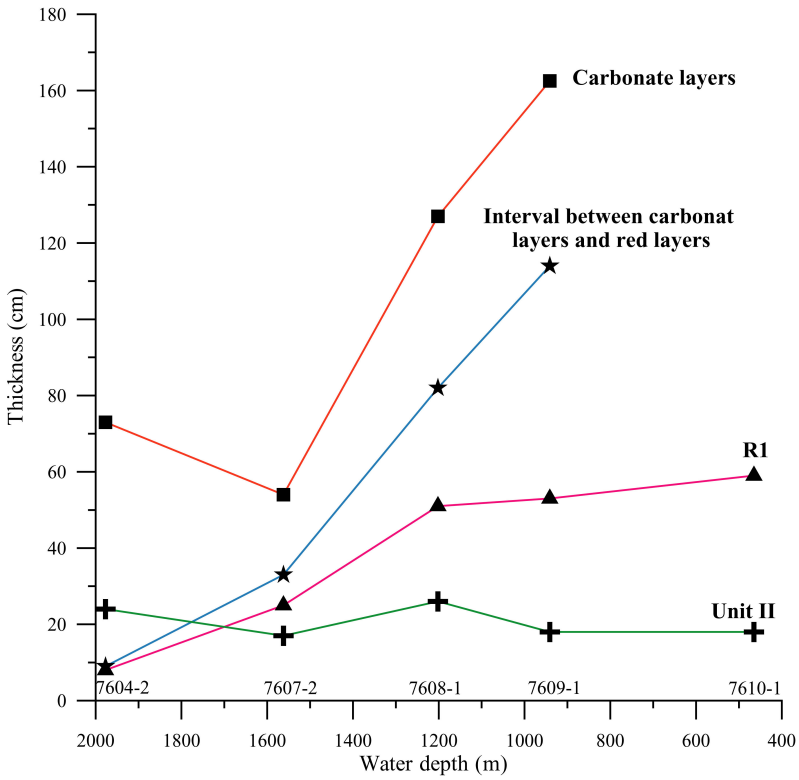

Fig. 4 Thickness of particular horizons along the slope transect. (R1 = uppermost red layer).

5.2. Sedimentological data from GeoB 7608-1

From the stratigraphy presented in chapter 4, the core covers a continuous sequence since 30 kyr BP. An overview about different parameters measured in GeoB 7608-1 is presented in Fig. 5, together with $\delta^{18}O$ values from the GRIP ice core and $\delta^{13}C$ values of core GeoB 7616-4.

As mainly reflecting biogenic and/or authigenic precipitated carbonate, Ca-intensities are inversely related to the Fe, Ti and K-intensities, which are linked to siliciclastic components. Since Fe, Ti and K-intensities are very similar throughout the record and Ti is inert against diagenetic alterations, the Ti/Ca ratio was chosen as a representative indicator for variations in the relative proportion of terrestrial and carbonate sedimentation.

The Ti/Ca-ratio is fairly constant during the LGM while the bulk grain size shows a rather high sand content with a declining trend up to 18 kyr BP. A peak in the sand content around 21 kyr BP is mainly produced through the presence of a large amount of sulphidic concretions.

The on the whole stable period from 30 to 18 kyr BP is terminated at ca. 18 kyr BP by the occurrence of four reddish-brown layers, spanning a time of roughly 2500 yrs. The terrigenous input sharply increased during the deposition of these red layers, while the sand

content shows a declining trend, indicating that most of the terrigenous minerals were transported in the silt and clay fraction. The high sediment input is also reflected by a two-fold increase in sedimentation rate from 0.35 to 0.8 m·kyr^{-1}. After this episode of high terrigenous input the sedimentation rate decreased again to a moderate value (ca. 0.33 m·kyr^{-1}) and successively declined to 0.05 m·kyr^{-1} in the late Holocene. Ca. 1000 yrs after the occurrence of the uppermost red layer, contemporaneous to the Bølling warm period, the Ca-intensity shows the first of three separated maxima, which are related to an increased carbonate content. While in the lower part of the record most of the carbonate in GeoB 7608-1 consists of biogenic components (mollusc or ostracod shells and subordinate detritical carbonate) all three Ca-maxima are produced by a high quantity of silt-sized, rhombohedric authigenic calcite that were clearly identified in smear slides.

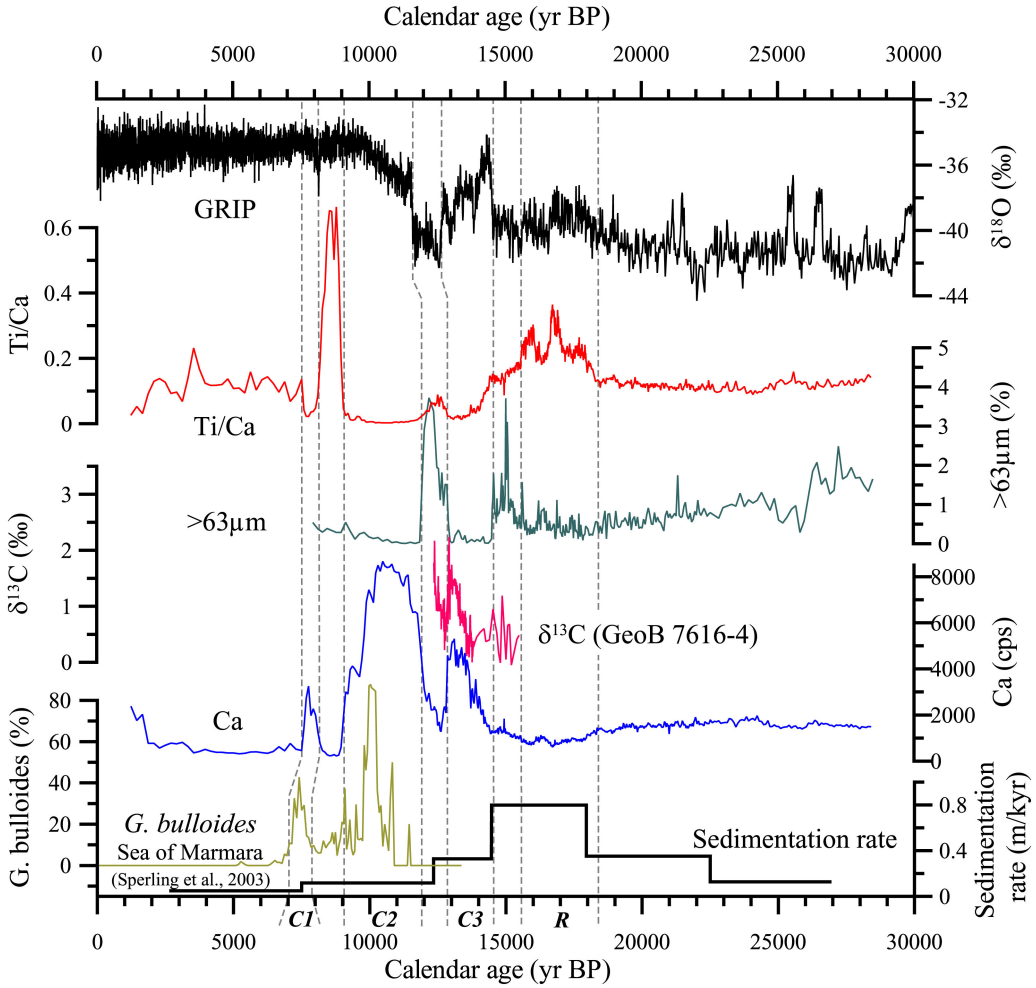

Fig. 5 Overview about parameters measured on GeoB 7608-1. Plotted are the XRF Ti/Ca ratio, the spectral red/blue ratio, bulk grain size, and sedimentation rate. For comparison the $\delta^{13}C$ from core GeoB 7616-4 and counts (in percent) of the planktic foraminifer *G. bullides* from the Sea of Marmara [*Sperling et al.*, 2003]. Marked are a sequence of reddish-brown clay layers (R) and three Ca-peaks (C1 to C3) and their potential correlation to the GRIP ice-core.

During the Ca-troughs the Ti/Ca-ratio increases, especially in the upper Ca-trough at around 8 ka, where it reaches its absolute maximum. The Holocene period after the uppermost Ca-peak is characterised by a relatively high Ti/Ca ratio with distinct fluctuations. The final increase in the Ca-intensity marks the beginning of the carbonate-rich Unit I (laminated coccolith ooze).

5.3. Stable isotopes

$\delta^{18}O$ values from core GeoB 7616-4 are in the range of the values reported by Major et al. (2002) with a trend from values around -6‰ at 14 kyr BP towards lighter values around -3.5‰ at 11 kyr BP (Fig. 2). $\delta^{13}C$ values are enriched (up to +2.24‰) during the maximum of the lowermost Ca-maximum and depleted (around +0.25‰) before and afterwards (Fig. 5).

6. Discussion

The comparison of data measured on six cores from the slope transect in the northwestern Black Sea (Fig. 3) shows that the results obtained on GeoB 7608-1 are representative for the regional sedimentary history. The distinct increase in the pre-Holocene sedimentation rate towards the upper slope indicates a proximal position of the core to the ancient Danube delta and higher river suspension load compared to the marine Holocene deposits which are constant in thickness along the entire slope (Unit II in Fig. 4; due to core loss Unit I is not entirely preserved in all cores).

6.1. Last glaciation (28 500 – 18 000 yr BP)

The sedimentological parameters measured on core GeoB 7608-1 show that climatic conditions have been relatively stable throughout the LGM. The high sand content between 28.5 and 25 kyr BP may reflect a more proximal position relative to the Danube delta as it prograded towards the basin interior during this period of low Black Sea lake-level.

6.2. Deposition of the red layers (18 000 – 15 500 yr BP)

Between ca. 18 and 15.5 kyr BP a series of reddish-brown clay layers were deposited at all locations on the slope. To confine the source of the red clays, it is important to distinguish between meltwater delivery of alpine and Scandinavian/Siberian provenance. The retreat of

alpine ice domes started at ca. 17.7 kyr BP and finished around 17.3 kyr BP [*Denton et al*., 1999], while 17.2 kyr BP marks the end of meltwater delivery from glaciers in northeastern Europe through the Dniepr watershed [*Major et al*., 2002]. The termination of the Caspian overflow is disputed, but may not have persisted beyond 15.8 kyr BP [*Svitoch*, 1999]. Therefore, alpine meltwater can only account for the increase in sedimentation rate and terrigenous material between 18 and 17.3 kyr BP, not for the entire period of 2500 yrs during the deposition of the red layers. Taken together, the lesser increase in sedimentation rate upslope compared to the subsequent deposits (Fig. 4), the small grain size, wide-spread occurrence of the red layers, and similarity to contemporaneous Caspian deposits (see below) favour a distal sediment source such as the Caspian Sea – Black Sea drainage corridor (Manych-depression).

Ryan et al. [2003] suggested a possible link of the reddish-brown layers to the "Early Khvalynian transgression" in the Caspian Sea during the late glacial induced by meltwater pulses from glaciers in Fennoscandia and/or Siberia that led to a lake-level rise in the Caspian Sea [*Kroonenberg et al*., 1997; *Grosswald and Hughes*, 2002]. Thus, the Manych-depression would represent one possible spillway for Scandinavian and/or Siberian meltwater during the deglaciation [*Ryan et al*., 2003]. The height of former beach terraces in the Caspian Sea indicates +50 m (above the present lake level) as the maximum highstand during the deglacial [*Kroonenberg et al.,* 1997]. This allowed the flooding of the Manych-depression between the Caspian and Black Sea that is today +25 m above sea-level [*Popov*, 1983; *Mangerud et al*., 2001]. During the maximum stage of the Early Khvalynian transgression, brownish "Chocolate Clays" were deposited in the Caspian Sea (e.g., [*Kroonenberg et al*., 1997]), resembling the colour of the red layers in the Black Sea. The timing of the Early Khvalynian transgression is uncertain - estimates are from 70 kyr BP (thermoluminescence dating) to ca. 9000 yr BP (^{14}C and U-Th-dates [*Kroonenberg et al*., 1997; *Svitoch,* 1999]). Within our stratigraphy and considering the dates of our red layers in GeoB 7608-1, the transgression occurred between 15.5 and 18 kyr BP.

The origin of meltwater flowing into the Caspian Sea, i.e., whether it is derived from the Barents-Kara ice sheet or the eastern Scandinavian ice sheet, is still discussed controversially. It is known that during the last glacial period huge ice masses blocked the rivers flowing into the Arctic Ocean, diverted them to the south, and dammed extensive lakes in northern Siberia [*Grosswald and Hughes*, 2002]. However, there is disagreement about the spatial advance of the Barents-Kara ice sheet during the LGM. Some authors (e.g., [*Grosswald*, 1998; *Grosswald and Hughes*, 2002]) claim that the Barents-Kara ice sheet existed throughout the

LGM and meltwater drained into the Caspian Sea, but recently published results [*Mangerud et al*., 2004] show that the Barents-Kara ice sheet was most likely restricted to the shelf areas of the Arctic Ocean and the ice was unable to block the northward flowing rivers. Instead, the Scandinavian ice sheet reached its maximum extent at ca. 17-18 kyr BP and diverted rivers and meltwater from the Baltic Basin to the River Volga and further to the Caspian Sea [*Mangerud et al*., 2004], which is contemporaneous to the development of the Black Sea red layers.

Our data indicate four major episodes (equivalent to four layers) of Caspian water spilling into the Black Sea. Additionally, each red layer has a complex internal structure with mm-scale laminations, which may represent interannual or even annual pulses of meltwater discharge. The occurrence of the red layers may be linked to high latitude climate variations as the red layers and the accompanying increase in the terrigenous components correspond to periods of slightly increased $\delta^{18}O$ (reflecting warmer conditions) during the GS-2 (Greenland Stadial 2) as recorded in the GRIP ice-core record (Fig. 6). This may indicate that the Scandinavian glaciers and ice-dammed lakes reacted very sensitive to climate forcing also on short time scales and, as also demonstrated by modelling studies [*Krinner et al*., 2004], had themselves effects on the climate dynamics in northern Eurasia.

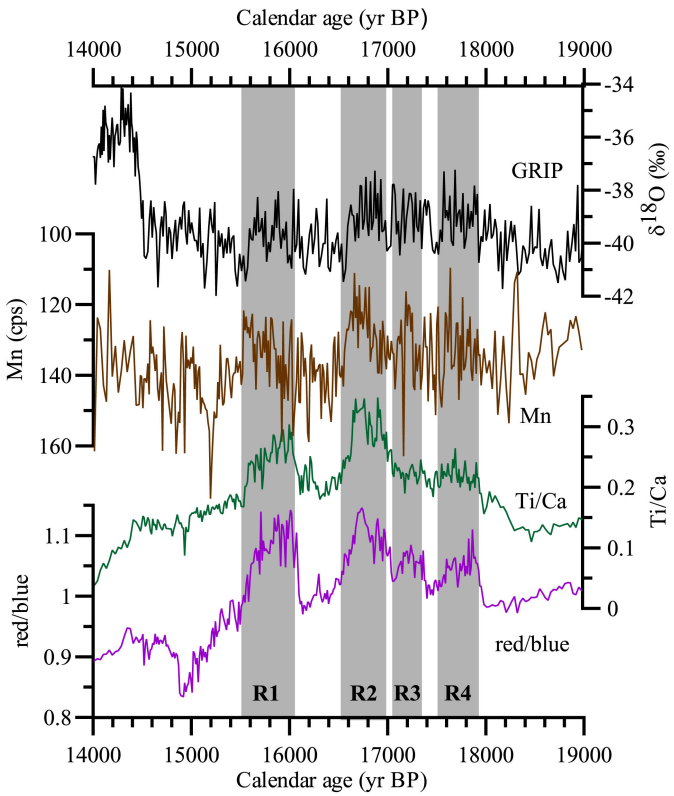

Fig. 6 Relation of the occurrence of the red layers in the Black Sea to periods of warmer condition recorded in the oxygen isotope record of the GRIP ice core. The four red horizons, indicated by grey background shadings, are labelled R1, R2, R3 and R4. Plotted are the spectral red/blue ratio, the Mn-intensity and the Ti/Ca-ratio. Please note the reversed scale for the Mn-intensity.

In addition, the red layer intervals are characterised by reduced Mn contents (Fig. 6). Mn contents are often used as an indicator for changing redox conditions - oxic conditions favour

MnO-precipitation, reducing conditions makes Mn^{2+} more soluble [*Peinerud*, 2000; *Tekiroglu et al.,* 2001]. Thus, the lower Mn-content would be consistent with at least temporary more oxygen depleted deep waters during enhanced freshwater input into the Black Sea (see also [*Mudie et al*., 2002a]). The at that time relative high lake level of the Black Sea [*Ryan et al.,* 2003] would have allowed the dissolved Mn^{2+} to leave the Black Sea via the Bosphorus strait.

6.3. Oldest Dryas (15 500-14 500 yr BP)

From the end of the red layer deposition till the onset of the Bølling, a marked increase in bulk grain size at relative constant Ti/Ca ratios occurs. Beside abundant iron sulphide concretions, the bulk grain size changes mainly relate to an increase in the accumulation of quartz grains. This interval also shows a huge upslope increase in sedimentation rates along the slope transect, indicating a more proximal position to the Danube Delta during a relatively low Black Sea level.

There is a lag of around 300 yrs between the steady decline in the Ti/Ca-ratio when compared to the abrupt drop of bulk grain size at the Oldest Dryas/Bølling transition at ca. 14.5 kyr BP (Fig. 5). We interpret the lag as an impact of delayed reforestation, which occurred around 200 years after the onset of warming in the Alps [*Denton et al*., 1999; *Magny et al*., 2003b] as e.g. indicated by the Gerzensee $\delta^{18}O$-record [*von Grafenstein et al*., 2000]. The decrease in meltwater supply and surface run-off (through developing vegetation) could have been responsible for an abrupt decline in transported grain sizes, while the subsequent onset of forest growth, increasing chemical weathering, and pedogenesis decreased the amount of terrigenous material supplied by the rivers.

6.4. Bølling/Allerød, Younger Dryas, and Holocene (14 500 – 1500 yr BP)

A typical process in lakes causing authigenic carbonate precipitation is CO_2-assimilation and pH-increase by phytoplankton blooms during warm periods such as the Bølling/Allerød and early Holocene [*Leng and Marshall*, 2004]. High $\delta^{13}C$ values in GeoB 7616-4 parallel the lowermost calcite-peak and support this relationship since the preferred uptake of the stable isotope ^{12}C during photosynthesis enriches ^{13}C in the water. The two phases of low Ca-content during the Younger Dryas and around 8200 yr BP could then be attributed to periods of cold conditions and reduced phytoplankton activity. Dating is not exact enough to constrain

the duration of the upper Ca-trough, but the high amount of terrigenous material implies that the sedimentation rate might have been higher than computed from the AMS ^{14}C-dates shortening its duration to considerably less than 1000 yrs. This would go conform to the short duration of the well known "8200 yr BP cold event" in Europe [e.g., *Magny et al*, 2003a]. Interestingly, records from the Sea of Marmara published by *Sperling et al*. [2003] show an increase in paleoproductivity (inferred from high abundances of the productivity-related planktic foraminifera *Globigerina bulloides*) paralleling the upper and middle Ca-maxima in GeoB 7608-1 (Fig. 5). This indicates that climatic conditions were changing synchronously in both areas.

A diatomaceous horizon, also described in *Ryan et al.* [2003], was found at the base of the lower Ca-trough (constituting the lower half of the peak in bulk grain size). These authors propose a connection between the Black and Caspian Sea during the Younger Dryas, based on the occurrence of a similar diatomaceous horizon in the Caspian Sea. But while the breeching of the spillway between the Caspian and Black Sea was easily possible during the Early Khvalynian transgression with a lake level of +50 m, it seems unlikely that there was a later connection between both basins because the Caspian lake level only reached -20 m during the Late Khvalynian transgression [*Kroonenberg et al*., 1997], contemporaneous to the Younger Dryas. Therefore it is more likely that both diatom-rich horizons were synchronous because of similar climatic conditions but not a result of an interconnection between both areas.

A heavily disputed keypoint concerning the question of an early Mediterranean-Black Sea connection is the depth of the Bosphorus at that time (e.g., [*Cagatay et al*., 2000; *Major et al*., 2002; *Ryan et al.*, 2003]). A deep Bosphorus (-80 m) would allow inflow of Mediterranean water as early as 14 kyr BP. A shallow, sediment-filled Bophorus with ca. -35 m depth would only permit entrance of Mediterranean waters at around 9500 to 9800 yr BP [*Jones and Gagnon*, 1994]. *Myers et al.* [2003] refuted the idea of a deep Bosphorus with respect to the first occurrence of marine fauna in the Sea of Marmara at around 13.7 kyr BP. Salinification of the Sea of Marmara at that point of time requires a low outflow from the Black Sea. This means a very early salinification of the Black Sea at around 11.0 to 11.8 kyr BP, a long time before the onset of sapropel development at 7500 yr BP [*Jones and Gagnon*, 1994]. A high outflow coming from the Black Sea into the Sea of Marmara would prolongate the influx of marine water into the Black Sea to a later point, but would also delay the salinification of the Sea of Marmara beyond 13.7 kyr BP, what contradicts the faunal evidence. On the base of our

present data there is also no evidence for such an early Black Sea – Mediterranean connection.

Due to its present distal position relative to the Danube delta and the prevailing currents that transport the riverine sediments southward (see section 2), the sedimentation rate is very low during both Unit I and II. The relatively high Ti/Ca ratio indicates the dominance of detrital components over carbonate precipitation in Unit II, while the distinct variations in Ti/Ca point to fluctuations in the terrigenous sediment input related to climatic alternations during the middle and late Holocene.

7. Conclusions

High-resolution studies on cores from the northwestern Black Sea continental margin demonstrate the complex history of the late glacial to Holocene evolution of the Black Sea and its surrounding areas. After stable conditions throughout the LGM, the Black Sea was influenced by a series of meltwater pulses coming from the Caspian Sea between 15.5 to 18 kyr BP. These meltwater pulses were primarily initiated through meltwater from the Scandinavian ice sheet, and appear to be linked to high latitude climate variations as recorded for example in Greenland. At the onset of the Bølling warm period delayed changes in grain size and elementary composition of sediments transported by the Danube reflect the delayed reforestation of the alps, occurring around 200 yrs after temperatures started rising. During the Bølling/Allerød and the early Holocene, favourable climatic conditions led to authigenic calcite precipitation through increased phytoplankton activity, interrupted by two spells of dominant clastic sedimentation during the Younger Dryas cold period and around 8200 yr BP. The middle and late Holocene is characterised by probably climate induced changes in the terrigenous sediment input.

Acknowledgements

We thank captain and crew of the RV Meteor for their efficient support during Meteor cruise M 51-4. We also thank M. Segl, University of Bremen, and her team for performing the stable isotope analysis and U. Röhl, University of Bremen, for support in XRF measurements.

We gratefully acknowledge the helpful and constructive reviews by K.-C. Emeis and one anonymous reviewer, which helped to improve the paper. This research was founded by the

Deutsche Forschungsgemeinschaft grants no. LA 1273/2-1, LA 1273/2-2, and WE 992/47-3.

No. RCOM0239

References

Aksu, A.E., R.N. Hiscott, D. Yasar (1999), Oscillating Quaternary water levels of the Marmara Sea and vigorous outflow into the Aegean Sea from the Marmara Sea-Black Sea drainage corridor, *Mar. Geol., 153*, 275-302.

Aksu, A.E., R.N. Hiscott, D. Yasar, F.I. Isler, S. Marsh (2002a), Seismic stratigraphy of Late Quaternary deposits from the southwestern Black Sea shelf: evidence for non-catastrophic variations in sea-level during the last 10 000 yr, *Mar. Geol., 190*, 61-94.

Aksu, A.E., P.J. Mudie, A. Rochon, M.A. Kaminski, T. Abrajano, D. Yasar (2002b), Persistent Holocene outflow from the Black Sea to the Eastern Mediterranean contradicts Noah's flood hypothesis, *Geotimes, 12*, 4-10.

Bondar, C., I. Stare, D. Cernea, E. Harabagiu (1991), Water flow and sediment transport of the Danube at its outlet into the Black Sea, *Meteorology and Hydrology, 21*, 21-25.

Cagatay, M.N., N. Görür, O. Algan, C. Eastoe, A. Tchapalyga, D. Ongan, T. Kuhn, I. Kuscu (2000), Late Glacial-Holocene paleoceanography of the Sea of Marmara: timing of connections with the Mediterranean and the Black Sea, *Mar. Geol., 167*, 191-206.

Denton, G.H., C.J. Heusser, T.V. Lowell, P.I. Moreno, B.G. Andersen, L.E. Heusser, C. Schlüchter, D.R. Marchant (1999), Interhemispheric linkage of paleoclimate during the last glaciation, *Geogr. Ann., 81 A* (2), 107-153.

von Grafenstein, U., U. Eicher, H. Erlenkeuser, P. Ruch, J. Schwander, B. Ammann (2000), Isotope signature of the Younger Dryas and two minor oscillations at Gerzensee (Switzerland): palaeoclimatic and palaeolimnologic interpretation based on bulk and biogenic carbonates, *Palaeogeogr. Palaeoclimatol. Palaeoecol., 159*, 215-229.

Grosswald, M.G. (1998), Late-Weichselian ice sheets in Arctic and Pacific Siberia, *Quat. Int., 45/46*, 3-18.

Grosswald, M.G., T.J. Hughes (2002), The Russian component of an Artic ice sheet during the Last Glacial Maximum, *Quat. Sci. Rev., 21*, 121-146.

Hay, B.J., M.A. Arthur, W.E. Dean, E.D. Neff, S. Honjo (1991), Sediment deposition in the Late Holocene abyssal Black Sea with climatic and chronological implications, *Deep Sea Res., 38, Suppl. 2,* S1211-S1235.

Jansen, J. H. F., S.J.Van der Gaast, B. Koster, A.J. Vaars (1998), CORTEX, a shipboard XRF-scanner for element analyses in split sediment cores, *Mar. Geol., 151*, 143-153.

Jones, G.A., A.R. Gagnon (1994), Radiocarbon chronology of Black Sea sediments, *Deep Sea Res. I, 41* (3), 531-557.

Krinner, G., J. Mangerud, J. Jakobsson, M. Crucifix, C. Ritz, J.I. Svendsen (2004), Enhanced ice sheet growth in Eurasia owing to adjacent ice dammed lakes*, Nature, 427*, 429-432.

Kroonenberg, S.B., G.V. Rusakov, A.A. Svitoch (1997), The wandering of the Volga delta: a response to rapid Caspian sea-level change, *Sediment. Geol., 107*, 189-209.

Lane-Serff, G.F., E.J. Rohling, H.J. Bryden, H. Charnock (1997), Postglacial connection of the Black Sea to the Mediterranean and its relation to the timing of sapropel formation, *Paleoceanography*, *12* (2), 169-174.

Leng, M.J., J.D. Marshall (2004), Palaeoclimate interpretation of stable isotope data from lake sediment archives, *Quat. Sci. Rev., 23*, 811-831.

Magny, M., C. Bégeot, J. Guiot, O. Peyron (2003a), Contrasting patterns of hydrological changes in Europe in response to Holocene climate cooling phases, *Quat. Sci. Rev., 22*, 1589-1596.

Magny, M., N. Thew, P. Hadorn (2003b), Late-glacial and early Holocene changes in vegetation and lake level at Hauterive/Rouges-Terre, Lake Neuchâtel (Switzerland), *J. Quat. Sci., 18* (1), 31-40.

Major, C., W. Ryan, G. Lericolais, I. Hajdas (2002), Constraints on Black Sea outflow to the Sea of Marmara during the last glacial-interglacial transition, *Mar. Geol., 190*, 19-34.

Mangerud, J., V. Astakhov, M. Jakobsson, J.I. Svendsen (2001), Huge Ice-age lakes in Russia, *J. Quat. Sci., 16* (8), 773-777.

Mangerud, J., M. Jakobsson, H. Alexanderson, V. Astakhov, G.K.C. Clarke, M. Henriksen, C. Hjort, G. Krinner, J.-P. Lunkka, P. Möller, A. Murray, O. Nikolskaya, M. Saarnisto, J.I. Sevendsen (2004), Ice-dammed lakes and rerouting of the drainage of northern Eurasia during the Last Glaciation, *Quat. Sci. Rev., 23*, 1313-1332.

Mudie, P.J., A. Rochon, A.E. Aksu, H. Gillespie (2002a), Dinoflagellate cysts, freshwater algae and fungal spores as salinity indicators in Late Quaternary cores from the Marmara and Black seas, *Mar. Geol., 190*, 203-231.

Mudie, P.J., A. Rochon, A.E. Aksu (2002b), Pollen stratigraphy of late Quaternary cores from Marmara Sea: land-sea correlation and paleoclimatic history, *Mar. Geol., 190*, 233-260.

Müller, G., P. Stoffers (1974), Mineralogy and petrology of Black Sea basin sediments. In: E.T. Degens and D. Ross (Editors), *The Black Sea – Geology, Chemistry and Biology*. AAPG Memoir 20, Tulsa, pp. 200-248.

Myers, P.G., C. Wielki, S.B. Goldstein, E.J. Rohling (2003), Hydraulic calculations of postglacial connections between the Mediterranean and the Black Sea, *Mar. Geol., 201*, 253-267.

Nadeau, M.J., M. Schleicher, P.M. Grootes, H. Erlenkeuser, A. Gottdang, D.J.W. Mous, J.M. Sarnthein, H. Willkomm (1997), The Leibniz-Labor AMS facility at the Christian-Albrechts University, Kiel, Germany, *Nuclear Instruments and Methods in Physics Research Section B: Beam Interactions with Materials and Atoms, 123* (1-4), 22-30.

Oguz, T., V.S. Latun, M.A. Latif, V. Vladimirov, H.I. Sur, A.A. Markov, E. Öszoy, B.B. Kotovschikov, V.V. Eremeev, Ü. Ünlüata (1993), Circulation in the surface and intermediate layers of the Black Sea, *Deep Sea Res. I, 40*, 1597-1612.

Oguz, T., S. Besiktepe (1999), Observations on the Rim Current structure, CIW formation and transport in the western Black Sea, *Deep Sea Res. I, 46* (10), 1733-1754.

Panin, N., D. Jipa (2002), Danube River Sediment input and its interaction with the northwestern Black Sea, *Estuar. Coastal Shelf Sci., 54*, 551-562.

Peinerud, E.K. (2000), Interpretation of Si concentrations in lake sediments: three case studies. *Environ. Geol., 40* (1-2), 64-72.

Pilskaln, C.H., J. Pike (2001), Formation of Holocene sedimentary laminae in the Black Sea and the role of the benthic flocculent layer, *Paleoceanography, 16* (1), 1-19.

Popov, G.I. (1983), *Pleistocene of the Black Sea-Caspian straits*. Nauka, Moscow. *(in Russian)*

Röhl, U., L.J. Abrams (2000), High-resolution, downhole, and nondestructive core measurements from sites 999 and 1001 in the Caribbean Sea: application to the late Paleocene thermal maximum. In: Leckies, R.M., Sigurdsson, H., Acton, G.D., Draper, G. (Editors), *Proc. ODP Sci. Res. 165*, pp. 191–203.

Ross, D.A., E.T. Degens (1974), Recent sediments of the Black Sea. In: E.T. Degens and D.A. Ross (Editors), *The Black Sea: Geology, Chemistry, and Biology*. AAPG, Tulsa, OK, pp. 183-199.

Ryan, W.B.F., W.C. Pitman III, C. Major, K. Shimkus, V. Moskalenko, G.A. Jones, P. Dimitrov, N. Görür, M. Sakinc, H. Yüce (1997), An abrupt drowning of the Black Sea shelf, *Mar. Geol., 138*, 119-126.

Ryan, W.B.F., C. Major, G. Lericolais, S. Goldstein (2003), Catastrophic flooding of the Black Sea, *Annu. Rev. Earth Planet. Sci., 31*, 525-554.

Sperling M., G. Schmiedl, C. Hemleben, K.C. Emeis, H. Erlenkeuser, P.M. Grootes (2003), Black Sea impact on the formation of eastern Mediterranean sapropel S1? Evidence from the Marmara Sea, *Palaeogeogr. Paleaeoclimatol. Palaeoecol., 190*, 9-21.

Stuiver, M., P.J. Reimer, E. Bard, J.W. Beck, G.S. Burr, K.A. Hughen, B. Kromer, G. McCormac, J. van der Plicht, M. Spurk (1998), INTCAL98 radiocarbon age calibration, 24,000–0 cal BP, *Radiocarbon, 40*, 1041–1084.

Svitoch, A.A. (1999), Caspian Sea level in the Pleistocene: hierarchy and position in the paleogeographic and chronological records, *Oceanology, 39*, 94-101.

Tekiroglu, S.E., V. Ediger, S. Yeminocioglu, S. Kapur, E. Akca (2001), The experimental analysis on the Late Quaternary deposits of the Black Sea, *Oceanol. Acta, 24* (1), 51-67.

Weninger, B., O. Jöris (2003), CALPAL version 2003 (software). Cologne University, Germany.

Winguth, C., H.K. Wong, N. Panin, C. Dinu, P. Georgescu, G. Ungureanu, V.V. Krugliakov, V. Podshuveit (2000), Upper Quaternary water level history and sedimentation in the northwestern Black Sea, *Mar. Geol., 167*, 127-146.

Zhakovshchikova, T.K. (1968), Diatoms in the bottom of the bottom deposits of the middle Caspian, *Vest. Lening. Gos. Univ., 21*, 1-8.

MANUSCRIPT 2

Late glacial to Holocene paleoenvironmental evolution of the Black Sea, reconstructed with stable oxygen isotope records obtained on ostracod shells

André Bahr[a], Helge W. Arz[b], Frank Lamy[b], Gerold Wefer[a]

[a] Universität Bremen, Fachbereich 5 – Geowissenschaften, Postfach 33 04 40, D-28334, Bremen, Germany

[b] GeoForschungsZentrum Potsdam, Section 3.3, Telegrafenberg, D-14473 Potsdam, Germany

(submitted to *Earth and Planetary Science Letters*)

Abstract

High-resolution stable oxygen isotope ($\delta^{18}O$ on ostracod shells), XRF-scanning and bulk grain-size data obtained on a transect of 6 gravity cores from the continental slope in the northwestern Black Sea give new insight into the hydrological evolution of the Black Sea since the Last Glacial Maximum (LGM). Stable climatic conditions during the LGM were followed by a series of meltwater pulses between 18 and 15.5 kyr BP that resulted in temporary isotopic depletion of the Black Sea waters. Subsequently, steadily increasing $\delta^{18}O$ values in all cores are mainly caused by isotopically enriched precipitation at the onset of the Allerød/Bølling warm period. A comparison of the major trends in $\delta^{18}O$ at different water depths suggests evaporation-driven deep water formation since ~ 14.5 kyr BP, while the two shallowest cores from 168 m and 465 m water depth were under the influence of increased warming in the upper water column since 14.5 and 12.5 kyr BP, respectively. The core from 168 m depth seems to be additionally influenced by freshwater input of the Danube. This core provides a high-resolution record from the Younger Dryas/Allerød boundary and suggests that a NAO-like climate mode was governing the interannual variability in the run-off of the Danube, which implies that this climate mode has been a persistent climatic feature over central Europe. The inflow of saline Mediterranean waters occurs between 9 and 8 kyr BP, where a merging of all $\delta^{18}O$ records signals an initial homogenisation of the water column.

Keywords
Black Sea, paleohydrology, late glacial, oxygen isotopes, ostracods, NAO

1. Introduction

The late glacial and Holocene evolution of the Black Sea-Marmara Sea area received increasing scientific and public attention during the past decades, especially after *Ryan and Pitman* [1997] published their theory of a catastrophic flooding of the Black Sea shelf through inflowing Mediterranean waters ca. 7500 yrs ago (later corrected to 9.4 kyr BP [*Ryan et al.*, 2003]; ages calibrated to calendar years), also known as "Noah's Flood hypothesis". In order to test this hypothesis, numerous researchers tried to reconstruct the hydrologic evolution of the Black Sea. Hydraulic modeling studies [*Lane-Serff et al.*, 1997; *Myers et al.*, 2003] added some skepticism concerning the physical plausibility of such a flood. *Myers et al.* [2003] do however not exclude the possibility of a (in geologic terms) fast filling of the Black Sea within a few decades and *Sidall et al.* [2004] stated that the morphological features for a very rapid inflow of Mediterranean water as expected from their model could indeed be found on the sea-floor near the Bosphorus entrance into the Black Sea. Paleoenvironmental reconstructions using pollen analysis [*Mudie et al.*, 2002a], seismic stratigraphy [*Aksu et al.*, 2002b], as well as foraminiferal and isotopic indicators [*Aksu et al.*, 2002a] raised serious doubts about a catastrophic flooding of the Black Sea, while the finding of submerged shorelines at -155 m water depth [*Ballard et al.*, 2000] and salinity-reconstructions from the Sea of Marmara [*Sperling et al.*, 2003] seem to support the theory.

Stable oxygen isotope records from the Black Sea itself could give valuable insight into the salinification history. However, rather few records are presently available [*Deuser*, 1972; *Major et al.*, 2002; *Ryan et al.*, 2003], and most of them reveal a rather low time resolution. The main reason is that stable isotope studies in the Black Sea are hampered by the scarcity of appropriate biogenic material and dating uncertainties because of unknown reservoir effects for the pre-marine sediments. For the present study, we obtained $\delta^{18}O$ records on ostracod shells on different cores from a NW Black Sea outer shelf to slope transect (168 m – 1977 m water depth) that provide information about the development of the Black Sea water column between 28.5 and 8 kyr BP.

In addition to the Holocene connection with the Sea of Marmara, the Black Sea experienced a period of connection to the Caspian Sea, when meltwater from Scandinavian ice sheets rose the water level of the Caspian Sea over the height of the Manych depression [*Leonov et al.*,

2002; *Ryan et al.*, 2003; *Mangerud et al.*, 2004]. This period is documented in the Black Sea by the deposition of a series of reddish-brown clay layers [M*ajor et al.*, 2002; *Bahr et al.*, 2005], roughly contemporaneous to Heinrich Event 1, when major parts of the Laurentide and other Northern Hemisphere ice sheets started to collapse [*Elliot et al.*, 2001]. To evaluate the sensitivity of the Black Sea towards such freshwater inflow is another important subject of this study.

The oxygen isotopic composition of lake water depends on several factors such as the isotopic composition of precipitation ($\delta^{18}O_{prec}$) and runoff ($\delta^{18}O_{run\text{-}off}$) entering the lake as well as the isotopic composition of the evaporated water, which again is dependent on factors like relative humidity, temperature and the $\delta^{18}O$ of atmospheric water vapour above the lake surface. Quantification of these parameters for the pre-Holocene Black Sea is hardly possible because the present hydrology of the Black Sea basin is considerably different from its pre-Holocene state: today the Black Sea has a connection to the Mediterranean Sea via the Sea of Marmara and shows a stable two-layer stratification with permanent anoxia in the deep basin [*Öszoy and Ünlüata*, 1997], while the ancient Black Sea is generally thought to have been a freshwater lake, disconnected from the open ocean without permanent anoxia. Although quantitative estimations might be difficult to asses, stable oxygen isotopes provide useful qualitative insights into the changes the Black Sea underwent during the last ca. 30 000 years.

2. Study area

The study area is situated in the NW Black Sea south of the Danube delta (Fig. 1) and comprises a transect of gravity cores from the outer shelf in 118 m water depth down to 1977 m on the lowermost slope (Tab. 1).

Table 1
Location and length of the investigated gravity cores.

Core name	Latitude N	Longitude E	Water depth	Core length
GeoB 7604-2	42°56.2'	30°01.9'	1977 m	592 cm
GeoB 7607-2	43°09.7'	29°57.7'	1562 m	636 cm
GeoB 7608-1	43°29.2'	30°11.8'	1202 m	685 cm
GeoB 7609-1	43°32.8'	30°09.2'	941 m	655 cm
GeoB 7610-1	43°38.9'	30°04.1'	465 m	880 cm
GeoB 7616-4	43°41.0'	30°02.5'	168 m	916 cm
GeoB 7611-1	43°41.8'	30°00.1'	118 m	634 cm

The NW Black Sea shelf includes almost 94% of the total shelf area in the Black Sea [*Panin and Jipa*, 2002]. The continental slope is very gentle and shaped by the morphology of the pre-Holocene Danube delta fan, which reaches far out towards the centre of the western Black Sea basin. Although the Danube transports 51.7 million tons per year (multi-annual mean [*Bondar et al.*, 1991]) of sediments to the NW Black Sea, the outer shelf is covered only by a very thin blanket of Holocene sediments and in some parts the Holocene is completely absent. This is caused by the strong (>50 cm s^{-1}) cyclonic "Rim Current" [*Oguz and Besiktepe*, 1999], which transports most of the suspended sediments alongside the coast to the south [*Panin and Jipa*, 2002] (Fig. 1).

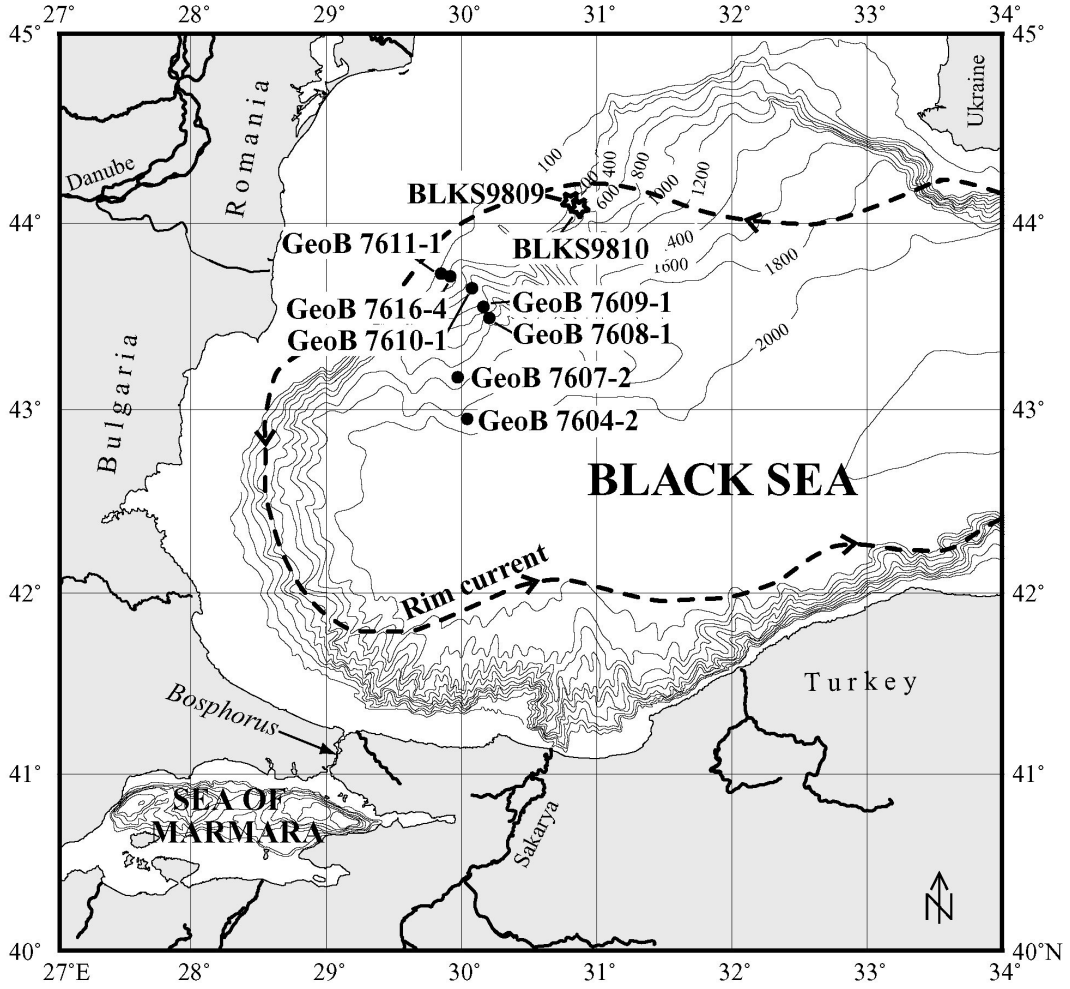

Fig. 1 Location of gravity cores recovered during *RV Meteor* cruise M51-4 in December 2001 (circles) and location of the two cores presented in *Major et al.* [2002] (stars). Also indicated is the approximate position of the present Black Sea rim current [*Aksu et al.*, 2002b].

The western Black Sea is influenced by three different climate regimes: first by the humid conditions of SE Europe with an annual precipitation >1000 mm·yr^{-1}; second by the more continental climate in the northern part of the Black Sea and the eastern Danube lowlands

with <600 mm·yr^{-1} rainfall and, third, by the Mediterranean climate regime with winter rainfall in the south towards the Sea of Marmara [*Mudie et al.*, 2002a]. Today the Black Sea has a positive water balance, i.e. the input by freshwater sources (300 km³·yr^{-1} precipitation; 350 km³·yr^{-1} runoff waters) exceeds the loss by evaporation (350 km³·yr^{-1}); the net-difference in the freshwater budget is compensated by the net flux through the Bosphorus [*Öszoy and Ünlüata*, 1997]. The hydrography of the Black Sea is characterised by a stable pycnocline between 100 and 200 m water depth that separates less saline near-surface water (18‰ salinity) from the more saline (22.5‰) deep water of Mediterranean origin. Since there is almost no exchange between both water masses, anoxia prevails below ca. 150 m, although the oxic/anoxic boundary can shift tens of meters in a few years [*Murray et al.*, 1989].
δ^{18}O-values of Black Sea waters mirror the present hydrological state: they vary around -2.8‰ in the upper 50 m and -1.8‰ in depths >500 m [*Öszoy et al.*, 2002]. The area of investigation is substantially influenced by the freshwater input of the Danube with a multiannual mean water discharge of 190.7 km³·yr^{-1} (before damming of the river [*Panin and Jipa*, 2002]), which accounts for more than 50% [*Öszoy and Ünlüata*, 1997] of the total river-runoff flowing into the Black Sea. The freshwater influence leads to considerably depleted δ^{18}O values of -10.5‰ near the Danube river mouth and -3‰ on the NW Black Sea shelf close to our coring sites [*Öszoy et al.*, 2002].

3. Material and Methods

Our study is based on seven gravity cores from the NW Black Sea retrieved during RV Meteor cruise M51-4 [*Jørgensen*, 2003] that are located on a depth transect ranging from the outer shelf to the lower continental slope (Tab. 1). The cores from the slope (GeoB 7604-2, 7607-2, 7608-1, 7609-1, 7610-1) reveal an undisturbed sequence of the marine units I (finely laminated coccolith ooze) and II (sapropelic sediments) at the top, with a relatively constant combined thickness of ca. 45 cm. The lower parts of the cores consist of homogeneous to (mostly) mm-scale laminated muddy clay (lacustrine unit III). The shelf cores GeoB 7611-1 and GeoB 7616-4 do not contain Holocene sediments (except for a shelly horizon at the top of GeoB 7611-1 with a late Holocene age of 2585 yr BP) and thus represent nearly entirely the lacustrine unit III. Sedimentologically, the two cores are characterised by mm to cm-scale laminated mud with abundant shells and shell fragments of bivalves and gastropods. All cores listed in Tab. 1 except GeoB 7611-1 were XRF-scanned in high resolution (for further details see *Bahr et al.* [2005]).

Table 2

Radiocarbon ages for gravity cores GeoB 7608-1 and 7616-4. For GeoB 7608-1 a correction of 1000 yrs was applied before calibrating, in GeoB 7616-4 calendar ages were calculated with 0 yr correction.

Lab.-ID	Core depth	^{14}C age (yr BP)	Calendar age (yr BP)	Material
GeoB 7608-1				
KIA 21464	34 cm	7735 ± 50	7607 ± 40	Ostracods
KIA 21463	88 cm	11460 ± 70	12342 ± 215	Gastropod
KIA 21461	158 cm	13350 ± 80	14469 ± 365	Gastropod
KIA 21460*	243 cm	17080 + 150 / -140	18563 ± 320	Ostracods and bivalves
KIA 21866	436 cm	16360 ± 70	17951 ± 285	Ostracods and bivalves
KIA 21459	596 cm	20140 + 180 / - 170	22499 ± 265	Gastropod
KIA 21457	652 cm	24970 + 310 / -300	26891 ± 480	Mixed mollusc shells
GeoB 7616-4				
KIA 18212	2 cm	10470 ± 60	12360 ± 200	*Dreissena rostriformis*
KIA 19681	184 cm	10945 ± 60	12855 ± 50	*Dreissena rostriformis*
KIA 19680	386 cm	11250 ± 60	13055 ± 90	*Dreissena rostriformis*
KIA 19678	579 cm	11670 ± 80	13435 ± 140	*Dreissena rostriformis*
KIA 19671	802 cm	12040 ± 130	13824 ± 220	*Dreissena rostriformis*
KIA 18213	899 cm	13105 ± 55	15452 ± 105	*Dreissena rostriformis*

* The date from 243 cm depth in GeoB 7608-1 was discarded because of the high amount of broken and probably reworked shells in the sample.

The age models of the individual cores have been recently published [*Bahr et al.*, 2005]. They are based on 6 AMS ^{14}C dates for each of the cores GeoB 7608-1 and 7616-4 (Tab. 2). The age models could be transferred to the other cores through detailed correlations using XRF and colour data (Ti/Ca shown in Fig. 2). For calibration to calendar years BP (1950) we used the program CALPAL (Version 2003 [*Weninger and Jöris*, 2003]) which uses the INTCAL-98 [*Stuiver et al.*, 1998] calibration set. Based on the correlation with the two published cores BLKS9809 and 9810 [*Major et al.*, 2002] (Fig. 3) we calculated calendar years applying a 1000 yrs age correction for GeoB 7608-1 and a 0 yr correction for GeoB 7616-4 (for further details see *Bahr et al.* [2005]).

For stable isotope analyses (δ^{18}O and δ^{13}C) on core GeoB 7616-4 a total of 288 samples in 4 cm intervals were collected and wet sieved. Subsequently 5 to 7 juvenile shells of the freshwater bivalve *Dreissena rostriformis* were hand-picked and analysed at the University of Bremen using a Finnigan MAT 251 mass spectrometer with an automated carbonate preparation device. For GeoB 7608-1 we took 319 samples in 2 cm intervals and prepared 5-8 shells of juvenile ostracods belonging to the genus *Candona* spp. (*C. schweyeri* and *C. angulata*) for stable isotope measurements. Additionally a total of 50 samples with *Candona* spp. from the cores GeoB 7604-2, 7607-2, 7609-1 and 7610-1 were analysed. The ratio of

$^{18}O/^{16}O$ is given in ‰ relative to the PDB standard. Analytical long-time standard deviation is about ±0.07‰ PDB and ±0.26‰ the analytical precision from 18 replicated measurements.

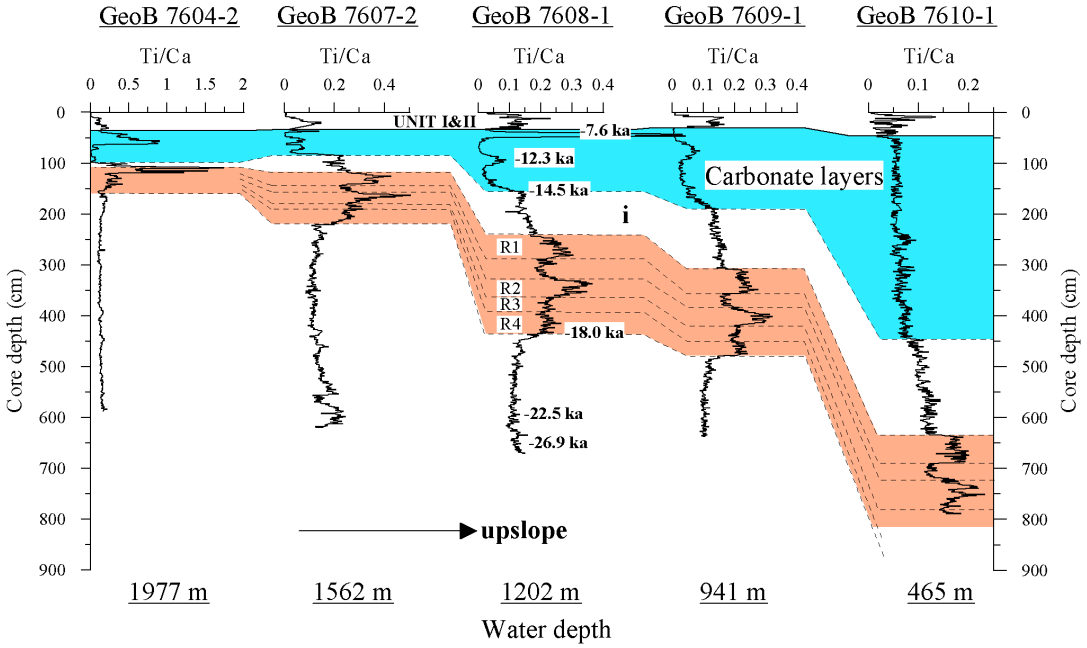

Fig. 2 Correlation of gravity cores from the slope transect in the NW Black Sea using the Ti/Ca ratio. For GeoB 7608-1 the radiocarbon dates are given in calendar years. The rather uniform thickness of the marine unit I contrasts the varying thickness of the red clay layers (in red, labelled R1 to R4) and the carbonate layers (in cyan, see also Ca-peaks in Fig. 4). The interval between the red layers and carbonate layers is labelled as "i".

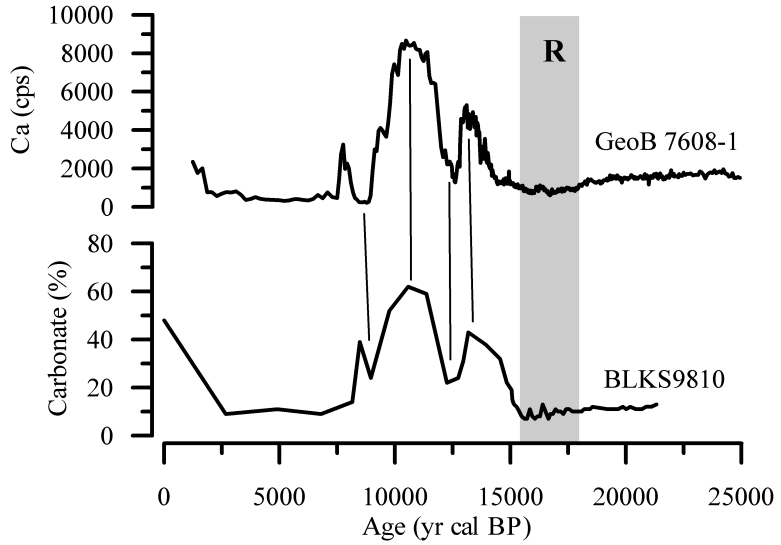

Fig. 3 Correlation of the XRF-Ca content in GeoB 7608-1 from 1202 m water depth and the carbonate content of core BLKS9810 from 378 m (from *Major et al.* [2002]). For GeoB 7608-1 a 1000 yrs age correction was applied before calibrating the radiocarbon dates. BLKS9810 was calibrated to calendar years with a reservoir age correction of 0 yr. R indicates the occurrence of reddish-brown clay layers.

Spectral analyses were performed with the program AnalySeries [*Paillard et al.*, 1996] using the Blackman-Tukey method. This algorithm first computes the autocovariance of the data, applies then a Tuckey window and finally computes the power spectrum by Fourier-transforming covariance functions. Before analysing we detrended the data to further pronounce the interannual to decadal variability in the records.

All data are available under the name of the corresponding author through the PANGAEA server (www.pangaea.de/PangaVista).

4. Results

4.1. Sedimentological characteristics

A detailed description of the sedimentological characteristics of GeoB 7608-1 was already given in *Bahr et al.* [2005], thus only a short overview over the most important features will be presented here. Sedimentological data including the Ti and Ca-intensity and bulk grain size from GeoB 7608-1 for the time interval of 5 to 28.5 kyr BP are presented in Fig. 4.

The Ti and Ca contents mainly reflect the varying contribution of biogenic and/or authigenic precipitated calcite (Ca) versus siliciclastic terrigenous input (Ti). After a period of rather constant Ti and Ca intensities before ca. 18.5 kyr BP, the terrigenous input (represented by high Ti) increases sharply until ca. 15.5 kyr BP, equivalent to a series of four distinct reddish-brown clay-layers. About 1000 yrs later, contemporaneous to the Bølling warm period, the Ca intensity shows the first of three separated maxima, reflecting high amounts of authigenically precipitated calcite.

Sand content is as high as 2.4% until 26 kyr BP but steadily drops to values between 0.2 and 1% during the red layer deposition. The grain size rises subsequently towards a first maximum (up to 3.6 wt.%) which terminates abruptly at the onset of the Bølling at 14.5 kyr BP; a second maximum (3.6 wt.%) could be observed during the lower Ca-trough, contemporaneous to the Younger Dryas (YD).

The cores from the slope (except GeoB 7616-4) could be correlated using XRF and colour scan data (Ti/Ca is shown in Fig. 2). In contrast to the Holocene units I and II, that have a fairly constant thickness in all cores, the sedimentation rate of the limnic sediments increases at least fourfold towards shallower water depths. This increase is most pronounced in the

interval between the end of the red layers and the onset of the carbonate peaks, but is less pronounced during the deposition of the red layers (Fig. 2).

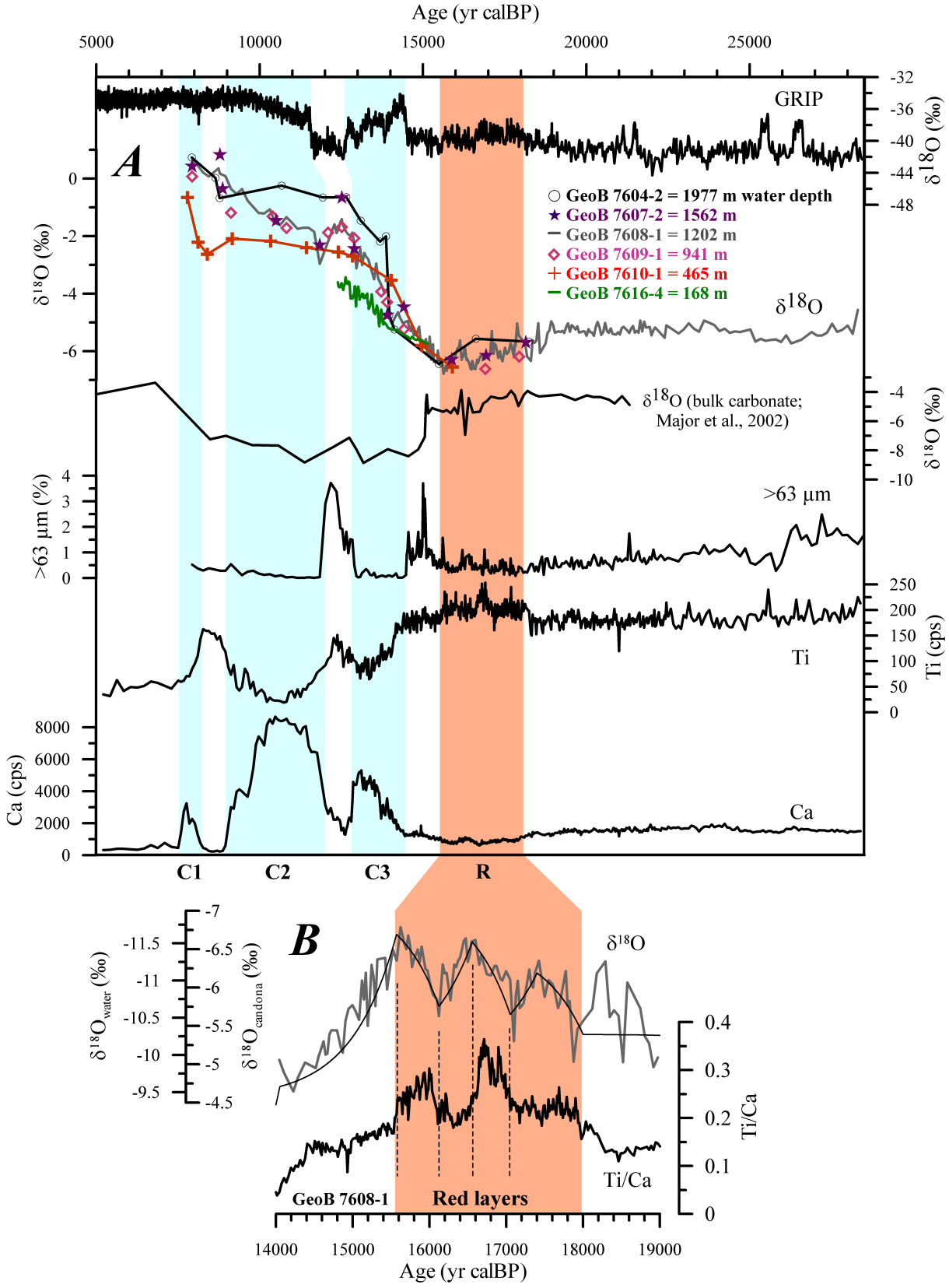

Fig. 4 (**A**) $\delta^{18}O$ data (uncorrected for vital offsets) measured on *Candona* spp. from cores GeoB 7604-2, 7607-2, 7608-1, 7609-1, 7610-1, and 7616-4 (measured on *Dreissena rostriformis* juv., 7-point running average), $\delta^{18}O$ (bulk) from core BLKS9810 [*Major et al.*, 2002]; bulk sand content, XRF Ti and Ca-intensity measured on core GeoB 7608-1 from the NW Black Sea slope and their suggested correlation with the GRIP ice-core $\delta^{18}O$ record. Marked are the occurrence of the red clay layers (R) and the Ca-peaks (C1-3). Note the different scale used for $\delta^{18}O$ of bulk carbonate and shell material. (**B**) Ostracod $\delta^{18}O$ record from core GeoB 7608-1 (grey line), modelled $\delta^{18}O$ of the Black Sea water (black line) and XRF Ti/Ca ratio from GeoB 7608-1 for the interval covering the red layer deposition. Red shading shows the termination of the red layers; dashed lines border the periods with peak Ti/Ca ratio that were incorporated into the isotopic balance model (see Tab. 3 for details). The scale for $\delta^{18}O_{water}$ was adjusted to the corresponding values of $\delta^{18}O_{ostracod}$, calculated for a constant water temperature of 4°C.

4.2. Stable isotopes

Ostracods are widely used for reconstructing paleoenvironmental changes, especially in lakes. It is known that ostracods do not calcify in equilibrium with the ambient water but show constant, temperature-independent offsets. *Von Grafenstein et al.* [1999] calculated this offset to be +2.2 ± 0.15‰ for all Candoninae with respect to the equilibrium calcite. Because of the scarcity of material in our cores we had to combine juvenile instars (A-1 to A-4; A-1 refers to the juvenile stage prior to adulthood, A-2 to the previous stage etc.) of different species of *Candona* (*C. schweyeri* and *C. angulata*) in one sample, assuming the same vital offset for all species.

$\delta^{18}O$ measurements on juvenile *Candona* spp. from GeoB 7608-1 (Fig. 4A) reveal a relatively stable level during the glacial interval of our records with values around -5.6‰ between 28 and 25 kyr and -5.2‰ BP between 25 and 18.5 kyr BP. A significant depletion is observed during the deposition of the red layers between 18.5 and 15.5 kyr BP, where $\delta^{18}O$-values decrease down to -6.5‰. The distinct terrigenous pulses during this period [*Bahr et al.*, 2005] are mirrored by the almost contemporaneous negative peaks in the $\delta^{18}O$-record. After 15.5 kyr BP values start to increase and reach their LGM-level with the onset of the Bølling warm period. Thereafter, we observe a stepwise shift towards enriched values. The steepest increase (from -5.0‰ to -1.95‰) takes place between 14.0 and 12.9 kyr BP, followed by a period of more stable values between 12.9 and 11.1 kyr BP including two significant negative excursion of -3.0‰ at ca. 12.9 and 11.8 kyr BP. Finally, $\delta^{18}O$ increases from -1.75‰ at 11.1 kyr BP towards +0.68‰ at 8 kyr BP.

$\delta^{18}O$ values measured on *Dreissena rostriformis juv*. from GeoB 7616-4 show a general increasing trend from -5.7‰ at ca. 15.2 kyr BP towards heavier values around -3.5‰ at 12.5 kyr BP but are highly variable with fluctuations of ~1‰ or more on multidecadal and centennial time-scales.

Comparing the major trends in $\delta^{18}O$ at different water depths, the records appear to diverge since ca. 14.5 kyr BP. While cores from intermediate water depths (1562 to 465 m) have $\delta^{18}O$ values in the range of GeoB 7608-1 (1202 m), the shallow core GeoB 7616-4 (168 m) shows a trend to values up to 1.5‰ lighter than GeoB 7608-1. $\delta^{18}O$ from the deepest core GeoB 7604-2 (1977 m), on the other hand, is up to 2‰ heavier than those in GeoB 7608-1 since 14.5 kyr BP. This difference diminishes between 9 and 8 kyr BP where the $\delta^{18}O$-records seem to merge. Another diverging trend is noticeable since ca. 12.5 kyr BP, when GeoB 7610-1 from 465 m water depth starts to show depleted values relative to GeoB 7608-1.

5. Discussion

By combining our isotope records at different water depths with sedimentological evidence [*Bahr et al.*, 2005], we can provide a detailed picture of the hydrological evolution of the Black Sea over the last glacial and deglaciation. In addition, high resolution isotope data from the shelf core GeoB 7616-4 allow to discuss short-term fluctuations during the Bølling/Allerød (B/A) and YD intervals.

5.1. The paleohydrological evolution of the Black Sea

5.1.1. Evolution between 28.5 to 14.5 kyr BP

Beside of some minor fluctuations, the stable $\delta^{18}O$ record before 18.5 kyr BP indicates that the Black Sea was in a state of isotopic equilibrium. This steady state was terminated by the observed 1‰-drop in $\delta^{18}O$ between ca. 18 and 15 kyr BP. During the time of the red layer deposition the Scandinavian Ice Sheet dammed large lakes and diverted rivers and meltwater drainage southward towards the River Volga and into the Caspian Sea. These (melt)waters caused the Caspian Sea to overflow over the Manych depression (+26 m a.s.l.) into the Black Sea [*Leonov et al.*, 2002; *Mangerud et al.*, 2004]. The low $\delta^{18}O$ values observed in the Black Sea could therefore be explained by the contribution of this isotopically depleted water. On a

finer scale, the observed changes in the ostracod oxygen isotopes are characterised by a saw-tooth pattern (Fig. 4B). The $\delta^{18}O$ values are getting gradually more depleted during each phase of meltwater input (displayed by a high Ti/Ca ratio), but rise again relatively rapidly when the meltwater supply ceases (low Ti/Ca). This leads to apparent lags of the maxima and minima in the $\delta^{18}O$ data relative to the Ti/Ca record, reflecting the time the Black Sea basin needs to adjust to hydrological changes. The tendency towards heavier isotopic values after the termination of each meltwater inflow is related to the temporary reduction of the meltwater inflow.

To assess the sensitivity of the Black Sea towards changes in amount and isotopic composition of river run-off, we performed a simple mass balance calculation. Our model is primarily based on the considerations underlying the hydrologic-isotope-balance model (HIBAL) by *Benson and Paillet* [2002], although with the simplification that we assumed a fully mixed Black Sea with a constant volume for the period prior to 14.5 kyr BP and the simulations were run by year not by month (boundary conditions are summarised in Tab. 3). Considering the values used for computing the pre-red layer steady state, it is striking that a very negative $\delta^{18}O_{run\text{-}off}$ is needed to reach the ca. -10.2‰ for $\delta^{18}O_{water}$. This might be explained by a greater portion of isotopic depleted water entering the Black Sea from the northern drainage area.

Table 3
Hydrologic and climatic boundary conditions for the isotopic balance model

Time slice (kyr BP)	V (km^3)	Q_r ($km^3 \cdot yr^{-1}$)	$\delta^{18}O_r$ (‰)	Q_p ($km^3 \cdot yr^{-1}$)	$\delta^{18}O_p$ (‰)	Q_e ($km^3 \cdot yr^{-1}$)	T (°C)	h (%)
25-18	537000	450	-20	230	-11.5	205	4	76
18-17.4	537000	550	-21.5	230	-11.5	230	4	76
17.4-15[a]	537000	570	-22.3	230	-11.5	230	4	76
17.4-15[b]	537000	460	-20.2	230	-11.5	230	4	76
15-14.5	537000	450	-20	230	-11.5	240	4	76
modern[c]	537000	350	-10	230	-8	280	11.2	78

V – lake volume; Q_r – volume of run-off; $\delta^{18}O_r$ – $\delta^{18}O$ of run-off; Q_p – volume of on-lake precipitation; $\delta^{18}O_p$ – $\delta^{18}O$ of precipitation; Qe – volume of evaporation; T – temperature of lake surface; h – relative humidity
[a] values for periods with peak Ti/Ca (see Fig. 4)
[b] values for periods with average Ti/Ca (see Fig. 4)
[c] values from *Swart et al.* [1991]

It becomes apparent that a relatively small change in run-off and $\delta^{18}O_{run\text{-}off}$ is sufficient to simulate the magnitude of the observed isotopic excursions (Tab. 3; Fig. 4B). To compare

both model and observation we calculated $\delta^{18}O_{ostracod}$ from the modelled $\delta^{18}O$ of the Black Sea water using the formula [*Rösler and Lange*, 1976]

$$\delta^{18}O_{ostracod}=(2.6229\cdot10^{6}\cdot(273.15+T)^{-2}+0.97002\cdot\delta^{18}O_{water}-31.7648)+2.2;$$

T was set to 4°C, $\delta^{18}O_{ostracod}$ is given relative to the PDB standard, $\delta^{18}O_{water}$ to SMOW.
The two negative $\delta^{18}O$-excursions before the start of the red layer interval indicate that there must be a second source (e.g., Dnestr and Dnepr) for isotopic depleted water beside the one that is responsible for the red clays.
As proposed by other authors [*Kvasov*, 1975; *Ryan et al.*, 2003; *Smith et al.*, 2005], the Black Sea could have possibly spilled via the Sea of Marmara into the Aegean Sea during this time. This scenario is supported by studies of dinoflagellate cysts, freshwater algae and fungal spores [*Mudie et al.*, 2002b] that suggest freshwater to brackish conditions in the Sea of Marmara during this period.
The $\delta^{18}O$ values of all cores GeoB 7604-2, 7607-2, 7609-1 and 7610-1 are in the range of GeoB 7608-1, implying that the lake has not been stratified. *Bahr et al.* [2005] suggested that a stratification of the ancient Black Sea is responsible for the persistent 1000 year age correction in our age model. As shown in the following section, this might be the case after 14.5 kyr BP; however, the $\delta^{18}O$ record does not support this assumption for the period before 14.5 kyr BP.

5.1.2. Evolution between 14.5 to 8 kyr BP

The pronounced trend towards heavier values for $\delta^{18}O$ in GeoB 7608-1 since the end of the red layers is primarily the effect of increasing $\delta^{18}O$ of run-off and on-lake precipitation as well as enhanced evaporation. The well-documented 3.5‰ increase in $\delta^{18}O$ of atmospheric precipitation between Oldest Dryas and B/A in central Europe [*von Grafenstein et al.*, 1999a] could almost account alone for the whole shift of ca. 4‰ that occurred in our record since the end of the red layer period and the begin of the YD. It is therefore not surprising that the return to almost LGM-values in $\delta^{18}O_{prec}$ during the YD [*von Grafenstein et al.*, 1999a] interrupted the increasing $\delta^{18}O$ trend in core GeoB 7608-1. The $\delta^{18}O$-peak at the end of the YD is questionable, because it consists only of one measurement. Nevertheless, re-measuring confirmed this value and GeoB 7607-2 shows also a value almost as low as in 7608-1. The peak occurred shortly after the maximum in bulk grain size, thus seems no to be related to

high river discharge and freshwater input. On the other hand, alpine lake level records show a short (200 to 300 yrs) phase of high lake level at the YD termination (the so-called Onoz 3 phase at ca. 11.7 kyr BP [*Magny et al.*, 2001]) what might argue in favour of a highly increased run-off at that time.

The in relation to the other cores relatively heavy $\delta^{18}O$-values from the deepest core GeoB 7604-2 (1977 m water depth) strongly suggest the existence of a denser bottom layer in the Black Sea during the B/A warm period, most likely produced through evaporation accompanied by biogenic calcite-precipitation forming the Ca-peaks (Fig. 4A). Another supporting evidence for increased evaporation as a cause for deep water formation is a sudden decrease in $\delta^{18}O$ of bulk carbonate at ca. 15 kyr BP [*Major et al.*, 2002] (Fig. 4A). The carbonate fraction mostly consists of authigenically precipitated calcite produced by high phytoplankton activity [*Major et al.*, 2002; *Bahr et al.*, 2005] - low $\delta^{18}O$ of bulk carbonate should therefore reflect higher temperatures.

Although the values and the trend in $\delta^{18}O$ of core GeoB 7604-2 are decoupled from the shallower cores until 9 to 10 kyr BP no clear evidence for permanent anoxia could be identified in the deepest core GeoB 7604-2. This indicates that oxygen supply by deep-water formation must have been sufficient. The different trends observed in GeoB 7604-2 and the intermediate cores could mirror different rates of mixing. While a relatively small volume of deep water (presumably well below 1562 m water depth, where GeoB 7607-2 is located) would adjust relatively quickly to the increased $\delta^{18}O_{prec}$ and salinity, the upper water body reacts less rapidly to these changes due to its much larger volume. Thus, the deep water-$\delta^{18}O$ of 7604-2 reaches more or less constant values around –0.6‰ as early as 12.5 kyr BP, while in 7608-1 such values are observed later (at ca. 9.5 kyr BP).

While cores GeoB 7607-2, 7608-1, 7609-1, and 7610-1 show comparable values during the B/A, GeoB 7616-4 exhibits a trend towards lighter $\delta^{18}O$ at least since ca. 14 kyr BP. Although it should be noted that the values are measured on bivalve shells and not on ostracod valves, potential vital offset between both benthic organisms should not affect the trends observed in $\delta^{18}O$. Increasing temperatures would counteract the trend towards heavier $\delta^{18}O$ values in GeoB 7616-4, since it is located in a relatively shallow water depth of 168 m or perhaps an even shallower one, if the Black Sea level was lowered during the B/A by evaporative drawdown [*Major et al.*, 2002]. A second important factor is the influence of the Danube's freshwater plume, that today leads to a depletion of $\delta^{18}O$ values on the NW Black Sea shelf (see section 2). The trend towards isotopic values lighter than those in the deeper cores might point to a progradation of the delta to the shelf edge during a period of low sea level, shifting

GeoB 7616-4 gradually to a more proximal position to the freshwater source, thus enhancing the influence of the Danube. The assumption of a low lake level and a progradation of the Danube delta is further corroborated by the strong upslope increase of the sedimentation rates during the deposition of the lowermost Ca-peak [*Bahr et al.*, 2005].

Another question is connected to the cause for the lighter $\delta^{18}O$ values of core GeoB 7610-1 relative to the deeper cores since the YD: Although 7610-1 is located closer to the Danube delta than the deeper cores, it seems on the first sight unlikely that increased freshwater influence plays a major role, because in this case core GeoB 7610-1 should also have shown a trend towards lighter values relative to the other cores as observed in the shallowest core 7616-4 during B/A, where a proximal position to the Danube is proposed to have lowered the local $\delta^{18}O$ signal (see above). Increased water temperatures in the upper 465 m (or less, if the lake level was considerably reduced during this period [*Major et al.*, 2002]) might have lowered the $\delta^{18}O$ of GeoB 7610-1. The difference between $\delta^{18}O$ in core GeoB 7610-1 and core GeoB 7608-1 from 1202 m water depth is 2‰ at maximum (or even 2.7‰ at 8.7 kyr BP), which would account for a temperature difference of ca. 8 to 10.8°C. This seems to be unrealistically high, a combination of both temperature and Danube-influence might account for the whole difference.

5.2. High-frequent variability of the Danube's discharge during the late glacial

Today, the Danube river run-off is closely linked to the North Atlantic Oscillation (NAO) [*Stanev and Peneva*, 2001; *Rimbu et al.*, 2002], which exerts a strong influence on the precipitation-pattern over Europe on interannual to decadal timescales. Our high-resolution records obtained on the shallow core GeoB 7616-4 provide a good opportunity to determine if there is any evidence that a NAO-like climatic mode also prevailed during the last deglaciation.

In section 5.1.2. we argued that core GeoB 7616-4 is under direct influence of the freshwater input by the Danube. In fact, the high variability in its $\delta^{18}O$-record most likely mirrors pronounced short-term oscillations in the Danube's discharge. This assumption is based on the comparison of the $\delta^{18}O$ record and grain size fluctuations from this core. Negative excursions in $\delta^{18}O$, interpreted to represent freshwater pulses, often correspond to positive excursions in the sand content, which are thought to represent maxima in the fluvial input (Fig. 5A).

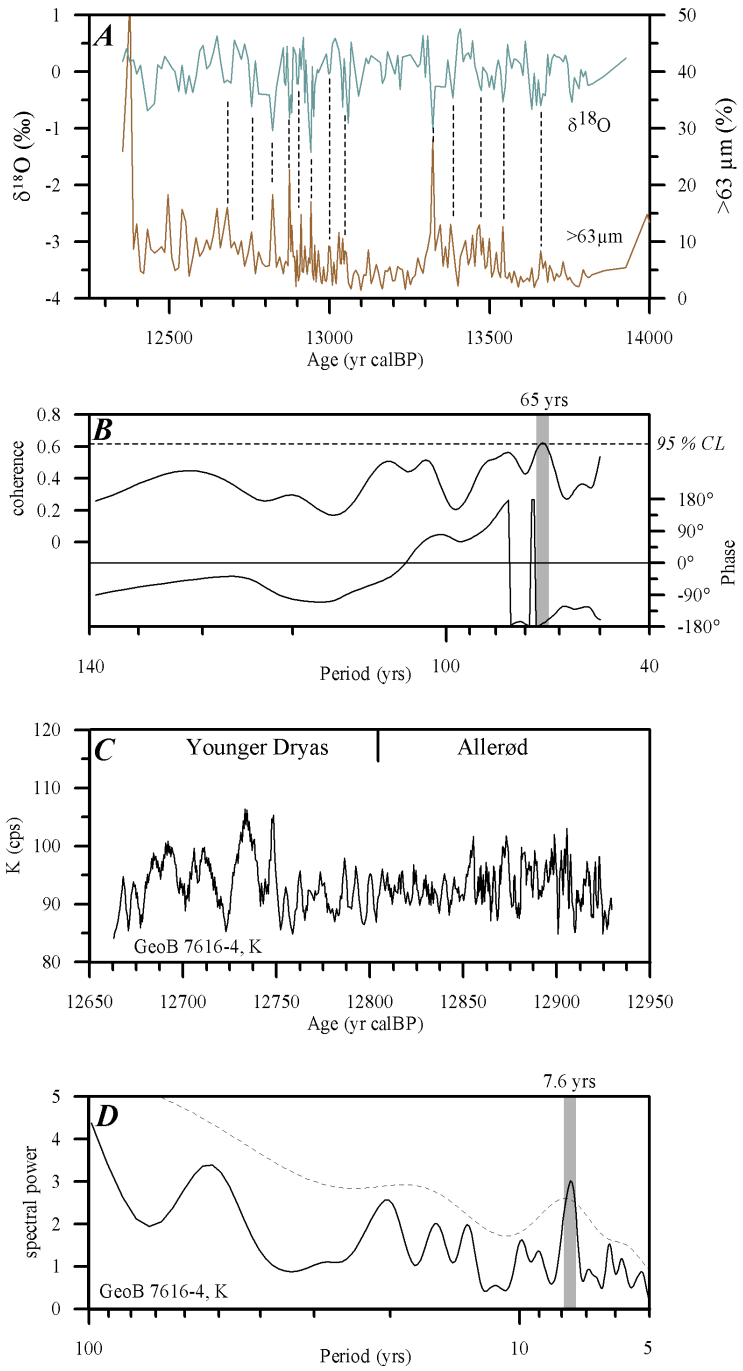

Fig. 5 (**A**) $\delta^{18}O$ values (detrended through subtraction from a 60 point adjacent average) measured on *Dreissena rostriformis* juv. and bulk sand content from GeoB 7616-4. Dashed lines delineate peaks of high sand content (high fluvial discharge) that correspond to negative excursions in the $\delta^{18}O$ record (lowered salinity). (**B**) Blackman-Tukey cross-spectral coherence and phasing between $\delta^{18}O$ and sand content at the 95 % confidence level. The major coherent phase of 65 yrs with a ca. 180° phasing is indicated. CL indicates "confidence level". (**C**) 5-point average of K measured in 2 mm intervals on a section of core GeoB 7616-4. Please note the different time scales used in (A) and (C). (**D**) Blackman-Tukey spectrum of the detrended K values from core GeoB 7616-4 for the interval between 12659-12931 yr BP. Analyses were performed with the Analyseries software [*Paillard et al.*, 1996] using a 0.5 yr sampling interval, 272 lags and 0.01103 bandwidth (straight line: one sided confidence interval at the 80% level) and 54 lags and 0.05558 bandwidth (dashed line: low-resolution spectrum). Indicated is the major NAO-related 7.6 yr-period.

A spectral coherency calculation between both records shows that the main common periodicity at the 95 % confidence level is 65 years, with a ca. 180° phase lag (the sampling interval lies between 7 an 11 years and is therefore sufficient to resolve a periodicity of 65 yrs), consistent with the above mentioned inverse correlation between sand content and $\delta^{18}O$. This 65 yrs cyclicity falls within the range of the 65 – 70 yrs periodicity of the North Atlantic Ocean/Northern Hemisphere climate system described by *Schlesinger and Ramankutty* [1994].

Beside this multidecadal variability, a closer inspection of a section with cm-scale alternations of coarse and fine grained material in core GeoB 7616-4 using XRF-measurements in 2 mm (equivalent to 0.2 – 0.5 yrs) resolution, reveals prominent multiannual fluctuations, as shown for example in the K record (Fig. 5C). Those fluctuations are caused by the different mineralogy of the quartz-rich coarse grained layers with a low K-concentration, and the finer grained layers with abundant mica and clay minerals and therefore high K-content. Spectral analyses of our high-resolution XRF data show a significant peak at 7.6 yrs in the Ca, Fe, Ti and K records (K is presented in Fig. 5D), which is also the most prominent period in the instrumental NAO-record [*Hurrell*, 1995]. The presence of the 7.6 and 65 yrs periods suggests that major modern modes of North Atlantic climate variability on interannual to decadal timescales affected the precipitation pattern of SE Europe likewise during the deglacial period. Additionally, the North Atlantic was also at least during parts of the deglacial period a region that exerted a major influence on the central European climate. Although the fact that the North Atlantic drives the European climate is not unexpected, the persistence of modern-day climatic features during noticeably different climatic periods is remarkable.

5.3. Implications for the timing of the first inflow of marine water into the Black Sea

Regarding the question when the reconnection of the Black Sea with the Mediterranean Sea started, it has been proposed that the Bosphorus sill was deeper than present (around -80 m [*Kvasov*, 1968] or even -100 m [*Myers et al.*, 2003]) before the flooding of the Black Sea, thus allowing an inflow of saline waters as early as 14 kyr BP. This scenario would be consistent with the divergence of $\delta^{18}O$ values in the deepest core GeoB 7604-2 that become about 1.8‰ heavier at this time (Fig. 4A). Hydrological calculations [*Myers et al.*, 2003] however showed that this idea seems unlikely with respect to the first occurrence of marine

fauna in the Sea of Marmara at around 13.7 kyr BP [*Cagatay et al.*, 2000; *Kaminski et al.*, 2002] and the onset of sapropel development in the Black Sea as late as 7500 yr BP [*Jones and Gagnon*, 1994]. Salinification of the Sea of Marmara at 13.7 kyr BP requires a low freshwater outflow from the Black Sea. If this was the case, a -80 m (or -100 m) deep Bosphorus sill would permit a salinification of the Black Sea at around 11.0 to 11.8 kyr BP, a long time before the onset of sapropel development. A high outflow of freshwater from the Black Sea into the Sea of Marmara would have delayed the salinification of the Black Sea to a more reasonable date, but would have also prevented Mediterranean water from entering the Sea of Marmara postponing the salinification of the Sea of Marmara to a considerable time after 13.7 kyr BP, which contradicts the faunal evidence [*Cagatay et al.*, 2000; *Kaminski et al.*, 2002].

The continuity of the trend towards heavier $\delta^{18}O$ in GeoB 7608-1 argues against the proposed catastrophic flooding of the Black Sea around 9.5 kyr BP [*Ryan et al.*, 2003]. The $\delta^{18}O$ in the Sea of Marmara at 9.5 kyr BP is +0.88‰ [*Sperling et al.*, 2003] measured on the planktic foraminifera *Turborotalita quinqueloba*, or an expected +3.08‰ for our record, if the vital offset of +2.2 for Candoninae is taken into consideration. Thus the inflow of considerable amounts of isotopic enriched Mediterranean water should enhance the trend towards heavier $\delta^{18}O$ values. This is not the case in core GeoB 7608-1 (Fig. 4A) but might be visible in pronounced positive shifts observed in the $\delta^{18}O$ records of the deepest cores GeoB 7604-2 and 7607-2 at ca. 9 kyr BP. It is suggestive to interpret this as a sign for dense Mediterranean water entering the deep Black Sea, but the paucity of data points makes this assumption very speculative. Additionally, the records from cores GeoB 7604-2, 7607-2, 7609-1 and especially 7610-1 show a steeper trend towards heavier $\delta^{18}O$ since ca. 9 kyr BP. The striking increase of $\delta^{18}O$ since 8.5 kyr BP recorded in GeoB 7610-1 seems to be related to the accompanying rise of the Black Sea level that diminishes the influence of depleted $\delta^{18}O$ water delivered by the Danube at this core location (see section 5.1.2.).

If, however, the reconnection started around 9.5 kyr BP in a more gradual manner, the merging of the $\delta^{18}O$ records from GeoB 7604-2, 7607-2, 7608-1, 7609-1 and 7610 -1 could be interpreted as a result of a homogeneous water column during the first inflow of saline water. The timing of the general $\delta^{18}O$ increase also corresponds to higher sea-surface salinity in the Sea of Marmara [*Sperling et al.*, 2003] after 9.5 kyr BP that was interpreted to be the result of an increased amount of saline Mediterranean water flowing through the Sea of Marmara during the flooding of the Black Sea [*Sperling et al.*, 2003]. Although a homogenized water column requires a strong inflow of Mediterranean waters and deep mixing, the rate of $\delta^{18}O$-

change itself does not appear to be high enough to support a catastrophic infill of the Black Sea within a few years.

6. Conclusions

The combination of high resolution $\delta^{18}O$ records, XRF and grain size measurements reveal the following pattern of Black Sea hydrological evolution since the Last Glacial Maximum:
After overall stable conditions during the LGM between 15.5 and 18.5 kyr BP a series of meltwater pulses derived from Scandinavian ice sheets led to a 1‰-depletion in the $\delta^{18}O$ of the Black Sea. After this interval, at the onset of the Bølling/Allerød warm period enriched $\delta^{18}O$ of atmospheric precipitation led to a gradual increase in the oxygen isotope composition of the Black Sea from –6.7 to +0.6‰, only interrupted by more constant values during the Younger Dryas cold period.
Comparison of $\delta^{18}O$-records from cores located at water depths between 168 to 1977 m along the slope showed that all record have similar values until 14.5 kyr BP, when the deepest core from 1977 m water depth starts to show $\delta^{18}O$ values at least 1‰ heavier than in the intermediate cores. This indicates the formation of isotopic enriched deep water through evaporation during warm climatic conditions which is also expressed in high amounts of authigenic precipitated calcite. The shallowest cores from 168 m and 465 m water depth on the other hand show a tendency towards lighter values compared to the deeper cores since 14.5 and ca. 12.5 kyr BP, respectively. Those trends might reflect increasing temperatures in the upper water column and an enhanced freshwater influence by the Danube during a period of lowered Black Sea lake level. High-frequent variations in the run-off of the Danube during the Younger Dryas and the Bølling indicate that a NAO-like climate mode may have governed the interannual to decadal variability also during the last deglaciation.
At 9.5 kyr BP stable oxygen isotope values from all investigated sediment cores start to merge, indicating that during the beginning inflow of saline Mediterranean waters the water column of the Black Sea was probably homogenous. However, the rate of change in $\delta^{18}O$ at this point does not support any catastrophic infill of the Black Sea within only a few years.

Acknowledgements
We thank captain and crew of the RV Meteor for their efficient support during Meteor cruise M 51-4. We also thank M. Segl, University of Bremen, and her team for performing the stable isotope analysis and U. Röhl, University of Bremen, for support in XRF measurements. We

also gratefully acknowledge the help of Ian Boomer with identifying the ostracods. The manuscript benefited from the comments of three anonymous reviewers and the editor H. Elderfield. This research was founded by the Deutsche Forschungsgemeinschaft grants no. LA 1273/2-1, LA 1273/2-2, and WE 992/47-3. No. RCOMXXXX.

References

Aksu, A. E., R. N. Hiscott, M. A. Kaminski, P. J. Mudie, H. Gillespie, T. Abrajano and D. Yasar (2002a), Last glacial-Holocene paleoceanography of the Black Sea and Marmara Sea: stable isotopic, foraminiferal and coccolith evidence, *Marine Geology*, *190*, 119-149.

Aksu, A. E., R. N. Hiscott, D. Yasar, F. I. Isler and S. Marsh (2002b), Seismic stratigraphy of Late Quaternary deposits from the southwestern Black Sea shelf: evidence for non-catastrophic variations in sea-level during the last ~10000 yr, *Marine Geology*, *190*, 61-94.

Bahr, A., F. Lamy, H. Arz, H. Kuhlmann and G. Wefer (2005), Late glacial to Holocene climate and sedimentation history in the NW Black Sea, *Marine Geology*, *214*, 309-322.

Ballard, R. D., D. F. Coleman and G. D. Rosenberg (2000), Further evidence of abrupt Holocene drowning of the Black Sea shelf, *Marine Geology*, *170*, 253-261.

Benson, L. and F. Paillet (2002), HIBAL: a hydrologic-isotopic-balance model for application to paleolake systems, *Quaternary Science Reviews*, *21*(12-13), 1521-1539.

Bondar, C., I. Stare, D. Cernea and E. Harabagiu (1991), Water flow and sediment transport of the Danube at its outlet into the Black Sea, *Meteorology and Hydrology*, *21*, 21-25.

Cagatay, M. N., N. Görür, O. Algan, C. Eastoe, A. Tchepalyga, D. Ongan, T. Kuhn and I. Kuscu (2000), Late Glacial-Holocene palaeoceanography of the Sea of Marmara: timing of connections with the Mediterranean and the Black Sea, *Marine Geology*, *167*, 191-206.

Deuser, W. G. (1972), Late-Pleistocene and Holocene History of the Black Sea as Indicated by stable-isotope studies, *Journal of Geophysical Research*, *77*(6), 1071-1077.

Elliot, M., L. Labeyrie, T. Dokken and S. Manthe (2001), Coherent patterns of ice-rafted debris deposits in the Nordic regions during the last glacial (10-60 ka), *Earth and Planetary Science Letters*, *194*(1-2), 151-163.

Hurrell, J. (1995), Decadal trends in the North Atlantic Osciclation regional temperatures and precipitation, *Science*, *296*, 676-679.

Jones, G. A. and A. R. Gagnon (1994), Radiocarbon chronology of Black Sea sediments, *Deep-Sea Research I*, *41*(3), 531-557.

Jørgensen, B. B. (2003), METEOR-Berichte, Cruise 51, Leg 4, Istanbul – Istanbul*, METEOR-Berichte 03-1, 1-57*.

Kaminski, M. A., A. Aksu, M. Box, R. N. Hiscott, S. Filipescu and M. Al-Salameen (2002), Late Glacial to Holocene benthic foraminifera in the Marmara Sea: implications for Black Sea-Mediterranean Sea connections following the last deglaciation, *Marine Geology*, *190*, 165-202.

Kvasov, D. (Editor), 1968. Paleohydrology of Eastern Europe in late Quaternary Time. Yezhegodnkkh Chetniyakh Pamyati L.S. Berga Doklady. Izd. Nauka, Leningrad, 65-81 pp.

Kvasov, D. (1975), *Late Quaternary History of Major Lakes and Inland Seas of Eastern Europe*, 248 pp., Nauka, Leningrad.

Lane-Serff, G. F., E. J. Rohling, H. L. Bryden and H. Charnock (1997), Postglacial connection of the Black Sea to the Mediterranean and its relation to the timing of sapropel formation, *Palaeogeography*, *12*(2), 169-174.

Leonov, Y. G., Y. A. Lavrushin, M. P. Antipov, Y. N. Spirididonovba, Y. V. Kuzmin, E. J. T. Jull, S. Burr, A. Jelinowska and F. Chalie (2002), New age data on sediments of the transgressive phase of the Early Khvalyn transgression of the Caspian Sea, *Doklady Earth Sciences*, *386*, 748-751.

Magny, M., J. Guiot and P. Schoellammer (2001), Quantitative Reconstruction of Younger Dryas to Mid-Holocene Paleoclimates at Le Locle, Swiss Jura, Using Pollen and Lake-Level Data, *Quaternary Research*, *56*(2), 170-180.

Major, C., W. Ryan, G. Lericolais and I. Hajdas (2002), Constraints on Black Sea outflow to the Sea of Marmara during the last glacial-interglacial transition, *Marine Geology*, *190*, 19-34.

Mangerud, J., M. Jakobsson, H. Alexanderson, V. Astakhov, G. K. C. Clarke, M. Henriksen, C. Hjort, G. Krinner, J.-P. Lunkka and P. Moller (2004), Ice-dammed lakes and rerouting of the drainage of northern Eurasia during the Last Glaciation, *Quaternary Science Reviews*, *23*(11-13), 1313-1332.

Mudie, P. J., A. Rochon and A. E. Aksu (2002a), Pollen stratigraphy of Late Quaternary cores from Marmara Sea: land-sea correlation and paleoclimatic history, *Marine Geology*, *190*, 233-260.

Mudie, P. J., A. Rochon, A. E. Aksu and H. Gillespie (2002b), Dinoflagellate cysts, freshwater algae and fungal spores as salinity indicators in Late Quaternary cores from Marmara and Black seas, *Marine Geology*, *190*, 203-231.

Murray, J. W., H. W. Jannasch, S. Honjo, F. Anderson, W. S. Reeburgh, Z. Top, E. Friederich, L. A. Codispoti and E. Izdar (1989), Unexpected changes in the oxic/anoxic interface in the Black Sea, *Nature*, *338*, 411-413.

Myers, P. G., C. Wielki, S. B. Goldstein and E. J. Rohling (2003), Hydraulic calculations of postglacial connections between the Mediterranean and the Black Sea, *Marine Geology*, *201*, 253-267.

Oguz, T. and S. Besiktepe (1999), Observations on the Rim Current structure, CIW formation and transport in the western Black Sea, *Deep-Sea Research I*, *46*(10), 1733-1754.

Öszoy, E. and Ü. Ünlüata (1997), Oceanography of the Black Sea: A review of some recent results, *Earth-Science Reviews*, *42*, 231-272.

Öszoy, E., D. Rank and I. Salihoglu (2002), Pycnocline and Deep Mixing in the Black Sea: Stable Isotope and Transient Tracer Measurements, *Estuarine, Coastal and Shelf Science*, *54*(3), 621-629.

Paillard, D., L. Labeyrie and F. Yiou (1996), Macintosh program performs time-series analysis, *Transactions of the American Geophysical Union*, *77*, 379.

Panin, N. and D. Jipa (2002), Danube River Sediment input and its interaction with the northwestern Black Sea, *Estuarine, Coastal and Shelf Science*, *54*, 551-562.

Rimbu, N., C. Boronean, C. Buta and M. Dima (2002), Decadal variability of the Danube River flow in the lower basin and its relation with the North Atlantic oscillation, *Internation Journal of Climatology*, *22*, 1169-1179.

Rösler, H. J. and H. Lange (1976), *Geochemische Tabellen*, 674 pp., Ferdinand Enke Verlag, Stuttgart.

Ryan, W. B. F., W. C. Pitman III, C. Major, K. Shimkus, V. Moskalenko, G. A. Jones, P. Dimitrov, N. Görür, M. Sakinc and H. Yüce (1997), An abrupt drowning of the Black Sea shelf, *Marine Geology*, *138*, 119-126.

Ryan, W. B. F., C. O. Major, G. Lericolais and S. L. Goldstein (2003), Catastrophic flooding of the Black Sea, *Annu. Rev. Earth Planet. Sci.*, *31*, 525-554.

Schlesinger, M. E. and N. Ramankutty (1994), An oscillation in the global climate system of period 65-70 years, *Nature*, *367*, 723-726.

Siddall, M., L. J. Pratt, K. R. Helfrich and L. Giosan (2004), Testing the physical oceanographic implications of the suggested sudden Black Sea infill 8400 years ago, *Palaeogeography*, *19*, PA1024.

Smith, J. A., G. O. Seltzer, D. L. Farber, D. T. Rodbell and R. C. Finkel (2005), Early local Last Glacial Maximum in the tropical Andes, *Science*, *308*, 678-681.

Sperling, M., G. Schmiedel, C. Hemleben, K. C. Emeis, H. Erlenkeuser and P. M. Grootes (2003), Black Sea impact on the formation of eastern Mediterranean sapropel S1? Evidence from the Marmara Sea, *Palaeogeography, Palaeoclimatology, Palaeoecology*, *190*, 9-21.

Stanev, E. V. and E. L. Peneva (2001), Regional sea level response to global climatic change: Black Sea examples, *Global and Planetary Change*, *32*(1), 33-47.

Stuiver, M., P. J. Reimer, E. Bard, J. W. Beck, G. S. Burr, K. A. Hughen, B. Kromer, G. McCormac, J. van der Plicht and M. Spurk (1998), INTCAL98 radiocarbon age calibration, 24,000-0 cal BP, *Radiocarbon*, *40*, 1041-1084.

Swart, P. K. (1991), Factors affecting the oxygen isotopic composition of the Black Sea. In: E. Izdar and J. W. Murray (Editors), *Black Sea Oceanography*. Kluwer, Dordrecht, Boston, London, pp. 75-88.

von Grafenstein, U., H. Erlenkeuser, A. Brauer, J. Jouzel and S. Johnsen (1999a), A Mid-European decadal isotope-climate record from 15,500 to 5000 Years B.P., *Science*, *284*, 1654-1657.

von Grafenstein, U., H. Erlenkeuser and P. Trimborn (1999b), Oxygen and carbon isotopes in modern fresh-water ostracod valves: assessing vital offsets and autecological affects of interest for palaeoclimate studies, *Palaeogeography, Palaeoclimatology, Palaeoecology*, *148*, 133-152.

Weninger, B. and O. Jöris, 2003. CALPAL version 2003, Cologne University, Germany. (software)

MANUSCRIPT 3

Abrupt changes during the deglacial and early Holocene in the Black Sea recorded with trace element (Sr, Mg, Ca), stable oxygen isotope and strontium isotope records

André Bahr[1*], Frank Lamy[2], Helge W. Arz[2], Candace Major[3] and Gerold Wefer[1]

[1]Universität Bremen, Fachbereich Geowissenschaften, Postfach 330440, 28334 Bremen, Germany

[2]GeoForschungsZentrum-Potsdam, Section 3.3, Telegrafenberg, 14473 Potsdam, Germany

[3]Woods Hole Oceanographic Institution, Geology and Geophysics, Woods Hole, MA 02543, USA

(to be submitted to *Geochemistry, Geophysics, Geosystems*)

Abstract

Stable oxygen isotopes, Mg/Ca, Sr/Ca and $^{87}Sr/^{86}Sr$ data obtained on ostracods from gravity cores located on the northwestern Black Sea slope were used to infer changes in the Black Sea hydrology and water chemistry for the period between 30 000 to 7 500 yr BP (calibrated radiocarbon years). The period prior to 14.5 kyr BP was characterised by stable conditions in all records with the exception of meltwater pulses reaching the Black Sea between 18 and 15.5 kyr BP which led to a temporally depletion of $\delta^{18}O$ and a sharp increase in $^{87}Sr/^{86}Sr$, caused by the hydrochemical properties of the meltwater source. While the Mg/Ca and Sr/Ca records remained rather unaffected by this meltwater inflow they show an abrupt rise with the onset of the Bølling/Allerød warm period. This rise was caused by authigenic calcite precipitation, which led to a sudden increase of the Sr/Ca and Mg/Ca ratios of the Black Sea water. The stable oxygen isotopes also start to increase around 15 kyr BP, although in a more gradual manner, due to isotopic enriched meteoric precipitation. While Sr/Ca remains constant during the following interval of the Younger Dryas cold period a decrease in the Mg/Ca ratio implies that the intermediate water masses of the Black Sea experienced a temporal cooling of 1-2°C during the Younger Dryas. The $^{87}Sr/^{86}Sr$ data had remained on the high level introduced by the meltwater inflow until the Younger Dryas, where it drops

towards values similar to those observed during the Last Glacial Maximum, what might point to a potential outflow to the Mediterranean Sea via the Sea of Marmara during this period. Differences in the trace element and oxygen isotope records obtained on cores from different water depths imply that there has been stratification in the Black Sea during the deglacial and Early Holocene. This stratification was finally replaced by a homogeneous water column during the inflow of Mediterranean water around 9.3 kyr BP, which is clearly detectable in the abrupt increasing Mg/Ca, Sr/Ca and $^{87}Sr/^{86}Sr$ values. The accompanying increase in the $\delta^{18}O$ record is less pronounced indicating that the inflow was relatively fast but not catastrophic.

1. Introduction

Today the Black Sea is the largest semi-enclosed basin of the world (V=537 000 km³) that is only connected with the global ocean through the ca. 36 m deep Bosphorus strait. This particular situation led to a complete disconnection with the open ocean during the last glacial period, when the global sea level was lower than the Bosphorus sill. As a consequence the Black Sea turned into a fresh or slightly brackish lake [*Mudie et al.*, 2002b] which reacted very sensitive to environmental changes with immediate impacts on the water chemistry, hydrology, and lake level of the Black Sea.

One of the major environmental variables is the freshwater budget of the Black Sea, which contributed e.g. to significant sea level oscillation since the glacial period (e.g., [*Ryan et al.*, 1997; 2003; *Aksu et al.*, 2002]). An example is the inflow of large amounts of meltwater from Scandinavian and/or Siberian ice sheets into the Black Sea between 18.5 and 15 kyr BP [*Ryan et al.*, 2003; *Mangerud et al.*, 2004] that resulted in an overflow of the Black Sea into the Sea of Marmara [*Kvasov*, 1979; *Smith et al.*, 2005] and a temporal freshening of the Black Sea [*Bahr et al.*, 2005] and the Sea of Marmara [*Mudie et al.*, 2003]. A further direct response to climatic changes is the precipitation of authigenic calcite during the Bølling/Allerød (B/A) and early Holocene [*Major et al.*, 2002; *Bahr et al.*, 2005] as a result of CO_2-assimilation through enhanced phytoplankton activity during favourable climatic conditions.

Due to the large volume of the Black Sea, variations in the isotopic composition of the water body are slow and mainly governed by the changes in the isotopic composition of meteoric precipitation and run-off [*Bahr et al.*, subm.]. Stable isotope records based on ostracod and bivalve shells from different water depths [*Bahr et al.*, subm.] and a bulk $\delta^{18}O$ record [*Major et al.*, 2002] suggest that the effect of temperature changes is rather restricted to the

uppermost water column. These data also suggest that the water column experienced periods with vertical stratification, but without developing anoxic conditions in the deeper basin.

The aim of this study is to scrutinize the substantial changes in the Black Sea in response to climatic and hydrologic changes since the Last Glacial Maximum (LGM) with a special focus on the past hydrochemical and temperature development. A further aspect is the timing and nature of the reconnection of the Black Sea with the Mediterranean Sea. For this purpose we investigated sediment cores from the northwestern Black Sea with a multiproxy-approach including XRF-scanning and Sr/Ca, Mg/Ca, $^{87}Sr/^{86}Sr$, and stable oxygen isotope ($\delta^{18}O$) measurements on ostracod shells.

2. Environmental setting and sampling material

At present the water balance of the Black Sea is positive. Freshwater sources (300 km^3yr^{-1} precipitation and 350 km^3yr^{-1} runoff), of which 190 km^3yr^{-1} is contributed by the Danube [*Panin and Jipa*, 2002]) alone, exceeds the losses by evaporation (350 $km^3 \cdot yr^{-1}$) [*Swart*, 1991]. The remaining components of the freshwater budget are compensated by the net flux through the Bosphorus [*Öszoy and Ünlüata*, 1997]. The high amount of freshwater flowing into the Black Sea is also responsible for its particular hydrographic situation. A stable pycnocline between 100 and 200 m water depth separates less saline near-surface water (18‰ salinity) from the more saline (22.5‰) deep water of Mediterranean origin. Due to this stable stratification, anoxic conditions prevail below a depth of ca. 150 m. The stable isotope composition of Black Sea waters reflect the present hydrology with values around -2.8‰ in the upper 50 m and -1.8‰ in depths >500 m [*Öszoy et al.*, 2002]. In areas with significant freshwater influence, like in our research area, $\delta^{18}O$ values are depleted (-10.5‰ near the Danube river mouth and -3‰ on the NW Black Sea shelf close to the coring sites [*Öszoy et al.*, 2002]).

The present-day values of Black Sea water for Sr/Ca (7.68 mmol/mol in 2000 m water depth [*Aloisi et al.*, 2004]) and Mg/Ca (4.55 mol/mol for the surface waters, 4.77 mol/mol in 2000 m water depth [*Manheim and Chan*, 1974]) approach typical marine ratios, but the freshwater influence on the upper water column is still expressed in the slightly reduced Mg/Ca ratio of surface water relative to the deep water. In areas of dominant freshwater input, like the Danube Delta, the Mg/Ca ratio can be as low as 0.612 mol/mol [*Manheim and Chan*, 1974]. The $^{87}Sr/^{86}Sr$ ratio of the Black Sea with 0.7093 ± 0.0007 [*Cox and Faure*, 1974] is also typical for marine environments.

This study is based on five gravity cores from the NW Black Sea, retrieved during RV Meteor cruise M51-4 [*Jørgensen*, 2003]. They are located on a depth transect ranging from the upper (465 m water depth) to the lower continental slope (1977 m) (Tab. 1, Fig. 1). The cores from the slope contain the classical sequence of the marine units I (finely laminated coccolith ooze) and II (sapropelic sediments) in the top ca. 45 cm, and the lacustrine unit III (homogeneous to (mostly) mm-scale laminated muddy clay) in the lower part of the cores [*Bahr et al.*, 2005].

Table 1
Location and length of the investigated gravity cores.

Core name	Latitude N	Longitude E	Water depth	Core length
GeoB 7604-2	42°56.2'	30°01.9'	1977 m	592 cm
GeoB 7607-2	43°09.7'	29°57.7'	1562 m	636 cm
GeoB 7608-1	43°29.2'	30°11.8'	1202 m	685 cm
GeoB 7609-1	43°32.8'	30°09.2'	941 m	655 cm
GeoB 7610-1	43°38.9'	30°04.1'	465 m	880 cm

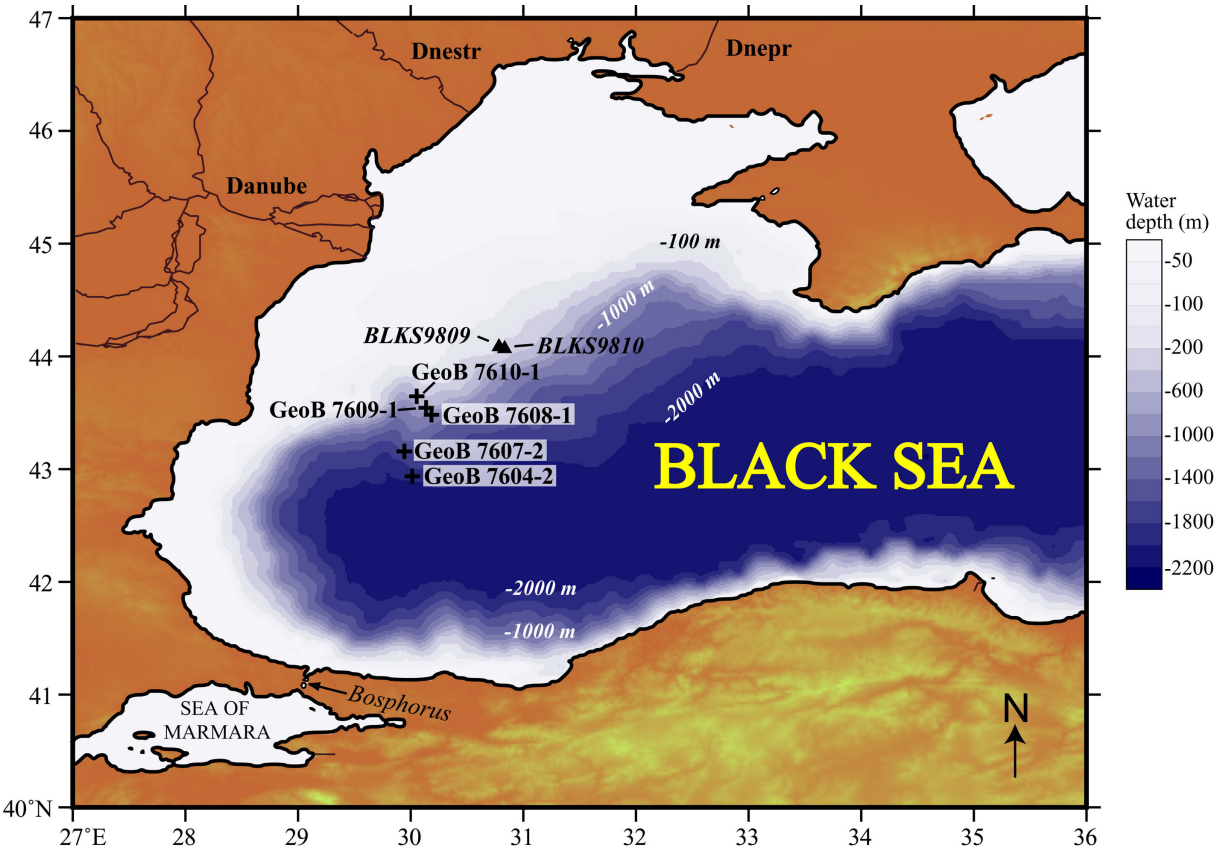

Fig. 1 Location of gravity cores retrieved during *RV Meteor* cruise M51-4 (crosses) and location of two cores presented in a previous paper [*Major et al.*, 2002] (triangles).

3. Methods

All cores listed in Tab. 1 were analysed in 1 cm resolution with a X-ray fluorescence scanner measuring the K, Ca, Ti, Mn, Fe, Cu and Sr contents at the University of Bremen [*Jansen et al.*, 1998; *Röhl and Abrams*, 2000] and for colour-reflectance with a Minolta CM-2002 hand-held spectrometer (for further details see *Bahr et al.* [2005]). Stable isotope analyses ($\delta^{18}O$ and $\delta^{13}C$) were performed on 5-8 shells of juvenile ostracods belonging to the genus *Candona* spp. (for further details see *Bahr et al.* [subm.]).

For trace element analysis (Mg/Ca and Sr/Ca) 3 to 10 ostracod valves of the species *Candona schweyeri* (adult) were picked from the 150 µm fraction. Each valve was cleaned individually in a faunal slide under the microscope with a fine brush and a few drops of deionised water. The cleaning procedure was repeated three times, after each cleaning the samples were immediately dried to avoid that the deionised water corrodes the carbonate. Valves were subsequently dissolved in 2% HNO_3 and measured with a Finnigan Element2 ICP-MS at the Woods Hole Oceanographic Institution (WHOI). The average analytical precision from replicates was 2.9% for Mg/Ca and 1.7% for Sr/Ca.

An age model was developed for core GeoB 7608-1 based on 6 AMS ^{14}C dates calibrated to calendar years BP (1950) [*Bahr et al.*, subm.] with the program CALPAL (Version 2003 [*Weninger and Jöris*, 2003]). For the present publication we refined the age model based on new dating obtained on a core from the southwestern Black Sea [*Lamy et al.*, in press]; for further detail see discussion in section 6.3. The age model of GeoB 7608-1 was transferred to the other cores from the slope transect through detailed correlations using XRF and colour data [*Bahr et al.*, 2005].

All data are available under the name of the corresponding author through the PANGAEA server (www.pangaea.de/PangaVista).

4. Factors influencing Sr/Ca and Mg/Ca in ostracod shells

Since the pioneering work in the early 1980s [*Chivas et al.*, 1983] many studies were performed to decipher the processes governing the uptake of trace elements (especially Sr and

Mg) into ostracod shells and to establish Mg/Ca and Sr/Ca records obtained on ostracod shells as powerful tools for reconstructing paleoenvironmental changes. Despite the steadily increasing heap of data from field and laboratory experiments, these studies brought different outcomes regarding the influence of parameters like the host water's Sr/Ca and Mg/Ca ratios, Mg and Sr concentrations, temperature, pH or salinity on the ostracod shell chemistry. *Chivas et al.* [1985, 1986a, 1986b] first determined the dependence of the Mg/Ca and Sr/Ca of the ostracode shell (in the following termed Mg/Ca_o and Sr/Ca_o) on the Mg/Ca and Sr/Ca ratio of the host waters (Mg/Ca_w and Sr/Ca_w). The uptake of Sr and Mg relative to Ca into the ostracod shell is controlled by the partition coefficient $D(M)_o$ (M stands for either Sr or Mg) that is defined as

$$D(M)_o=(M/Ca_o)/(M/Ca_w).$$

These authors also stated that $D(M)_o$ is the same for species belonging to the same genus and for closely related genera. This view was later contested claiming that the effect of Mg/Ca_w on Mg/Ca_o is minor and temperature is the controlling factor on Mg/Ca_o [*Palacios-Fest and Dettman*, 2001]. This point was also addressed by a study incorporating different species belonging to the genus *Candona* [*Wansard et al.*, 1998]. It showed an important influence of Mg/Ca_w on $D(Mg)_o$ which is constant above a Mg/Ca_w of ca. 1 mol/mol but increased exponentially below this threshold (Fig. 2).

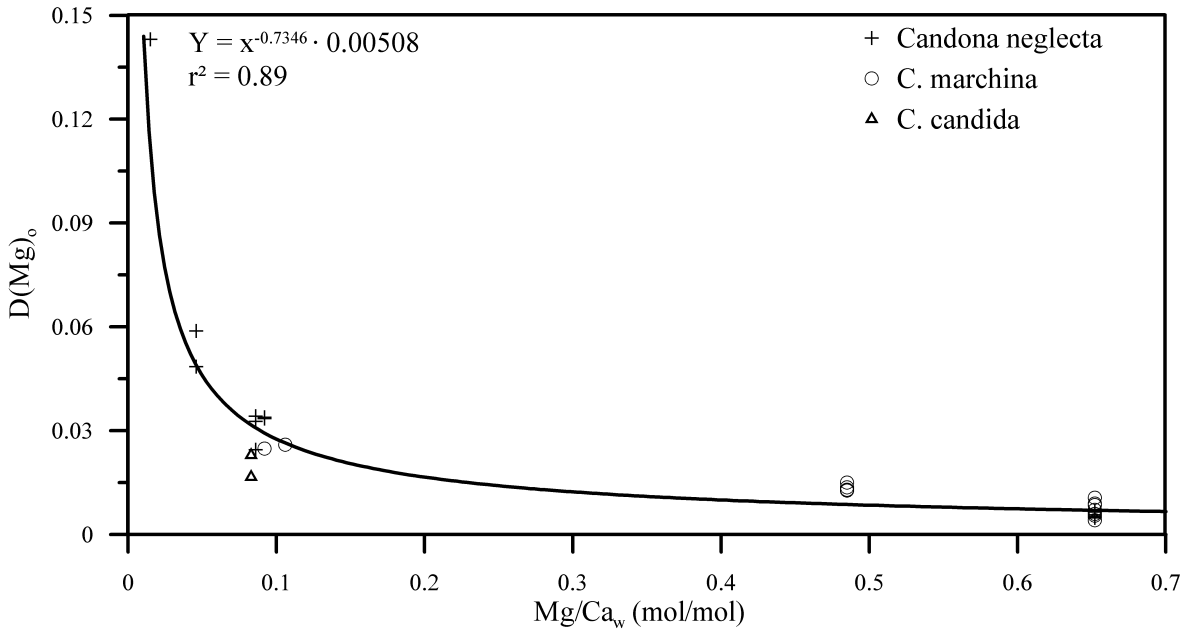

Fig. 2 Relation of the partition coefficient $D(Mg)_o$ of *Candona neglecta*, *C. marchina* and *C. candida* to the host water Mg/Ca_w (after [*Wansard et al.*, 1998]). The best fit (r^2=0.89) is represented by the function $D(Mg)_o = (Mg/Ca_w)^{-0.73} \cdot 0.0051$.

Although Mg/Ca_o is widely believed to be temperature dependent (with probable exceptions [*Wansard et al.*, 1999]), it has so far predominantly been used for temperature reconstructions in the marine realm (e.g., [*Dwyer et al.*, 1995; *Ingram*, 1998]). Reconstructions in mesohaline or freshwater conditions were performed in fewer cases [*Wansard*, 1996; *Wansard and Roca*, 1997; *Palacios-Fest et al.*, 2002; *Cronin et al.*, 2003]. *Engstrom and Nelson* [1991] did a temperature calibration for the species *Candona rawsoni* gaining the relation $T = (Mg/Ca_o - 0.004) / (Mg/Ca_w \cdot 0.0000968)$. Although later studies suggested that *C. rawsoni* might not belong to the genus *Candona*, one can assume that the temperature sensitivity lies in the range of that observed within other genera, i.e. a rise of 1 mmol/mol Mg/Ca equals a temperature increase of 1-2 °C [*Wansard*, 1996; *De Deckker et al.*, 1999b; *Müller*, 1999; *Palacios-Fest and Dettman*, 2001; *Cronin et al.*, 2003]. Temperature reconstructions on lakes are mainly hampered by the variability of Mg/Ca_w due to evaporation and the precipitation of different mineral phases while Mg/Ca_w in the ocean remains more or less constant on longer timescales. There were also suggestions that Sr/Ca_o is dependent on temperature [*De Deckker et al.*, 1999a; *Majoran et al.*, 1999; *Müller*, 1999]. *Müller* [1999] proposed that organisms building shells with a higher Sr/Ca_o ratio are generally showing a higher sensitivity of Sr/Ca_o towards temperature, while the temperature-dependence of Mg/Ca_o decreases simultaneously. This might help to explain the different sensibility of Sr/Ca_o from different species towards temperature.

Even though there are apparent uncertainties about the interspecific or even intraspecific variability of factors controlling the Mg and Sr uptake, it seems appropriate to apply the results obtained by *Wansard et al.* [1998] to our record, i.e. $D(Mg)_o$ is dependent on Mg/Ca_w and temperature, Sr/Ca_o only on Sr/Ca_w. This is reasonable, because in the aforementioned study, a broad spectrum of *Candona* species had been included and yielded consistent results [*Wansard et al.*, 1998]. Another important point is that the hydrological conditions in the ancient Black Sea (low salinity; low Mg/Ca_w and Sr/Ca_w) are similar to the environments investigated by *Wansard et al.* [1998].

5. Results

The glacial period until 18.5 kyr BP exhibits only low variability in all records. The first distinct change occurred between 18 and 15.5 ka where consecutive drops in $\delta^{18}O$ and an abrupt increase in $^{87}Sr/^{86}Sr$ are visible (Fig. 3). This period is marked by a series of reddish-

brown clay layers in the western Black Sea, characterised by higher concentration of terrigenous elements [*Bahr et al.*, 2005] and anomalous high illite and (to a lesser extent) kaolinite contents [*Major et al.*, 2002]. In contrast Sr/Ca and Mg/Ca are almost unaffected during this period, although Sr/Ca and Mg/Ca show an inverse correlation during this period and a tentative correlation of both elements to the $\delta^{18}O$ values might be indicated (Fig 4b). After 15.5 kyr BP $\delta^{18}O$ has a trend towards more enriched values, only interrupted by a relatively constant interval during the Younger Dryas. The overall $\delta^{18}O$-shift totals ca. +7.2‰ (from ca. -6.5‰ at 15.5 kyr BP to +0.7‰ at 8 kyr BP).

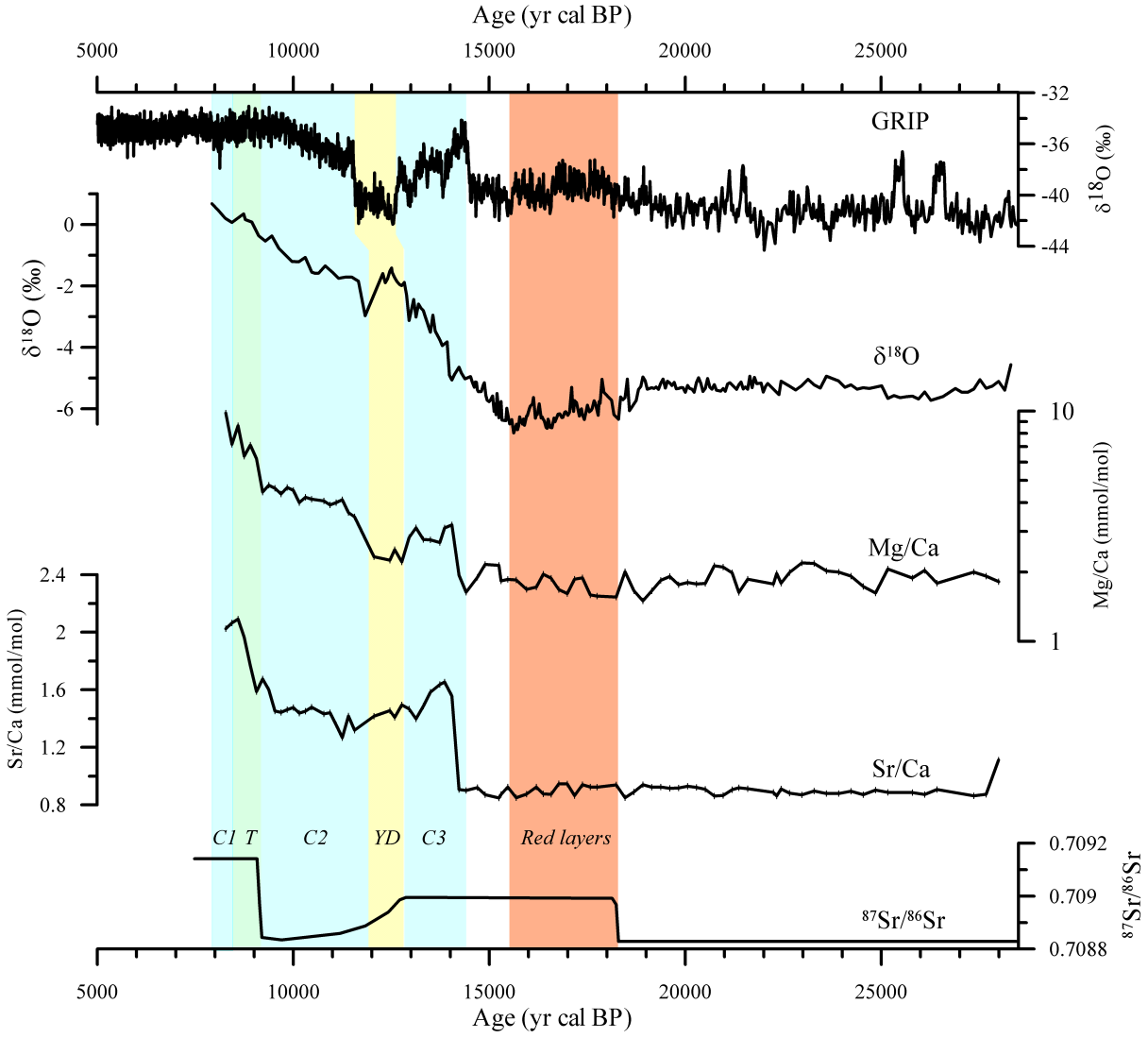

Fig. 3 Stable oxygen isotopes ($\delta^{18}O$), Mg/Ca, and Sr/Ca from core GeoB 7608-1, and $^{87}Sr/^{86}Sr$ from cores BLKS9809 and 9810 measured on ostracods [*Ryan et al.*, 2003] and their potential correlation to the GRIP ice core record. Note the logarithmic scale of the Mg/Ca record. Coloured bars indicate the occurrence of red clay layers (red), authigenic precipitated calcite (blue, "C1"-"C3"), clastic sedimentation during the Younger Dryas (yellow, "YD") and between ca. 9 and 8 kyr BP (green, "T").

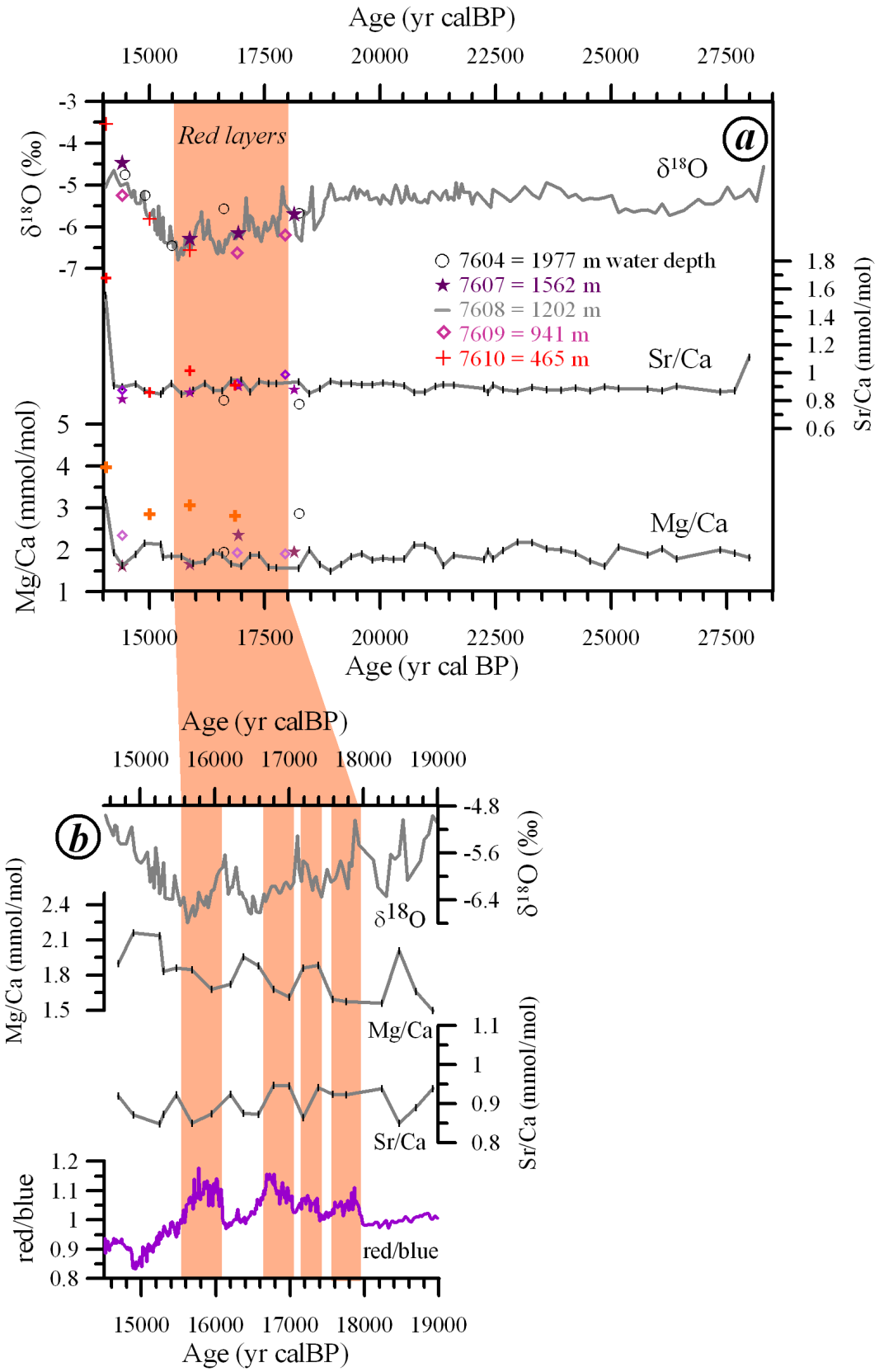

Fig. 4 (**a**) $\delta^{18}O$, Mg/Ca and Sr/Ca records from 14.5 to 28.5 kyr BP. The data from core GeoB 7608-1 (grey line) are compared to measurements on sediment cores from different water depths (GeoB 7604-2 (circles); 7607-2 (stars); 7609-1 (diamonds); 7610-1 (crosses)). (**b**) Focus on the period with red clay-layer deposition (marked as red bars during periods with high red/blue ratio).

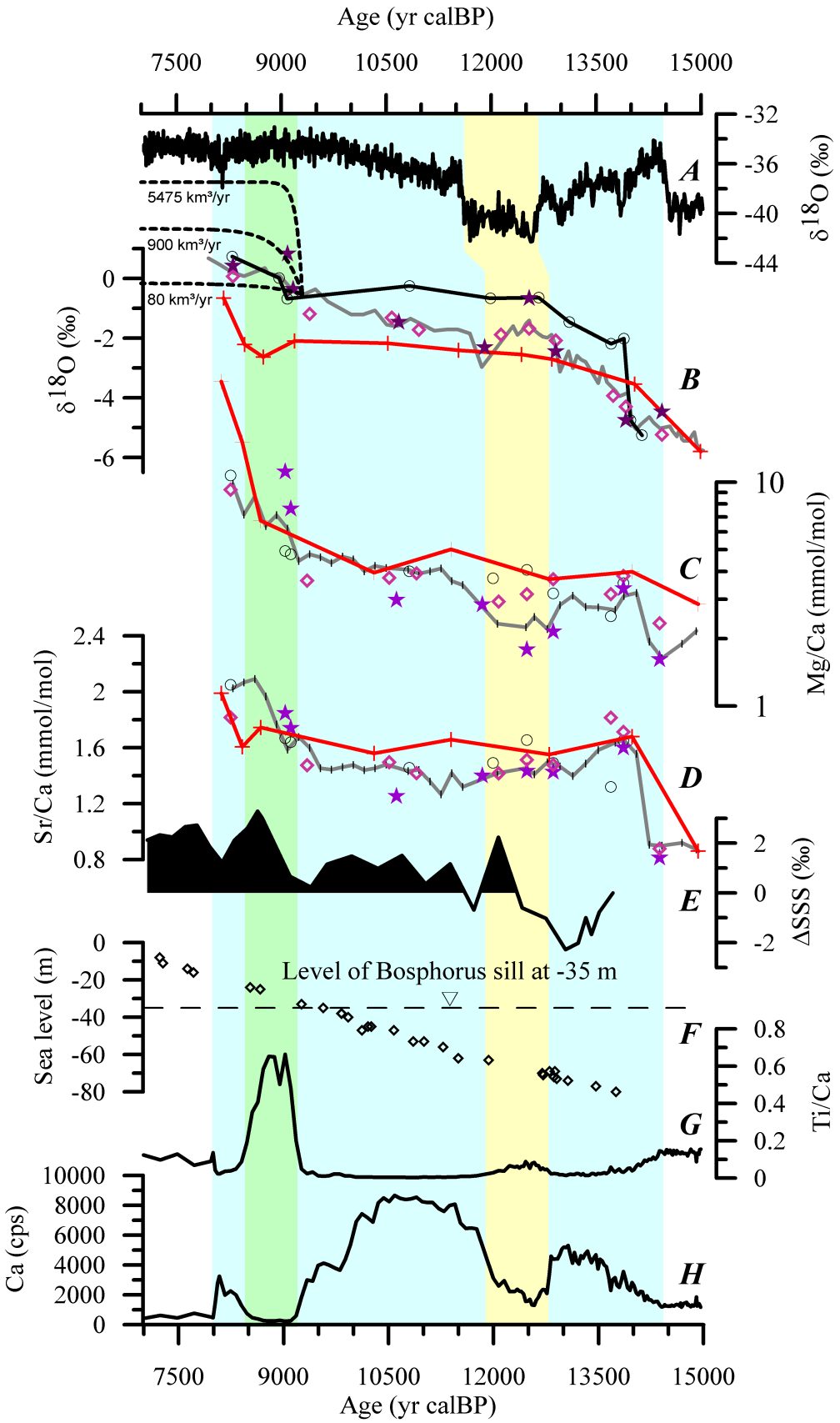

○ **7604 = 1977 m water depth**
★ **7607 = 1562 m**
7608 = 1202 m
◇ **7609 = 941 m**
\+ **7610 = 465 m**

Fig. 5 Comparison of geochemical data from the Black Sea [(**B**) ostracod-$\delta^{18}O$ records from GeoB 7608-1 (grey line), 7604-2 (circles), 7607-2 (stars), 7609-1 (diamonds) and 7610-1 (crosses); (**C**) Mg/Ca (logarithmic scale!) and (**D**) Sr/Ca from the same cores; (**G**) XRF-Ti/Ca ratio of GeoB 7608-1; (**H**) XRF-Ca record from GeoB 7608-1] with (**A**) the GRIP ice core record from Greenland; (**E**) a salinity record from the Sea of Marmara compared to modern [*Sperling et al.*, 2003]; (**F**) the global sea level record from Tahiti [*Bard et al.*, 1996]. Blue shading indicates periods with high authigenic calcite precipitation (high Ca-content), interrupted by two periods of dominant clastic sedimentation (yellow and green). Dashed lines in graph (B) indicate the hypothetical $\delta^{18}O$-evolution of Black Sea water for a maximum flux (5475 km³/yr), the present-day flux (in- and out-flow combined, 900 km³/yr) and a small inflow (80 km³/yr) of Mediterranean/Sea of Marmara water through the Bosphorus into the Black Sea.

Mg/Ca and Sr/Ca both increase drastically at 14.5 kyr BP (Mg/Ca from 1.6 to 3.2 mmol/mol; Sr/Ca from 0.9 to 1.6 mmol/mol) and later at ca. 9 kyr BP (Mg/Ca from 4.4 – 9.9 mmol/mol; Sr/Ca from 1.5 – 2.1 mmol/mol). The change in trace element composition at 14.5 kyr BP coincides with the precipitation of authigenic low-Mg calcite (marked with a blue bar in Fig. 3; Ca-peaks in Fig. 5), which lasts from 14.5 to 7.5 kyr BP, interrupted by two periods of dominant clastic deposition during the Younger Dryas (YD, yellow signature) and around 8.5 kyr BP (green signature). Although both trace element ratios seem to covary along the record at the first sight, they show some distinct differences, e.g. the low in Mg/Ca during the YD that is not mirrored in Sr/Ca, and the constant Sr/Ca level in the early Holocene during a slight but steady increase in Mg/Ca.

As shown in Fig. 4 and 5, most of the values taken from the cores along the slope transect are in the same range. Exceptions are the measurements taken from the shallow core GeoB 7610-1. The Mg/Ca values of core GeoB 7610-1 are constantly higher until 10.5 kyr BP, while Sr/Ca slightly increases between 12.5 and 10 kyr BP. Since 12.5 kyr BP, the $\delta^{18}O$ values of GeoB 7610-1 are getting lighter relative to the other sediment cores. A diverging trend is also visible in the $\delta^{18}O$ data from the deepest core GeoB 7604-2, which is heavier than equivalent measurements from the shallower cores between ca. 14.5 and at least 10 kyr BP.

$^{87}Sr/^{86}Sr$ keeps its high level until the onset of the YD where it returns to glacial values that last until 9 kyr BP; at that point a last abrupt shift to high values takes place (add precise values)

6. Interpretation and Discussion

Although $\delta^{18}O$ is a widely used parameter in paleo-studies, it bears high ambiguity in interpretations only based on this proxy, because it depends on numerous factors such as

ambient water temperature, evaporation, isotopic composition of run-off, and precipitation. With the additional use of Mg/Ca and Sr/Ca it is possible to further constrain the factors influencing $\delta^{18}O$, since Mg/Ca is temperature dependent and both Mg/Ca and Sr/Ca give insight into changes of the water chemistry. The reconnection of the Black Sea with the Mediterranean Sea via the Sea of Marmara is one of the main questions in the present paper. In this context, $^{87}Sr/^{86}Sr$ is also expected to give valuable results, because ocean water and fresh or slightly brackish lake water have distinctly different isotopic composition (see also *Ryan et al.* [2003]). Since the $\delta^{18}O$ and $^{87}Sr/^{86}Sr$ records have been the focus of other studies [*Major et al.*, 2002; *Ryan et al.*, 2003; *Bahr et al.*, subm.] we focus on the trace element record.

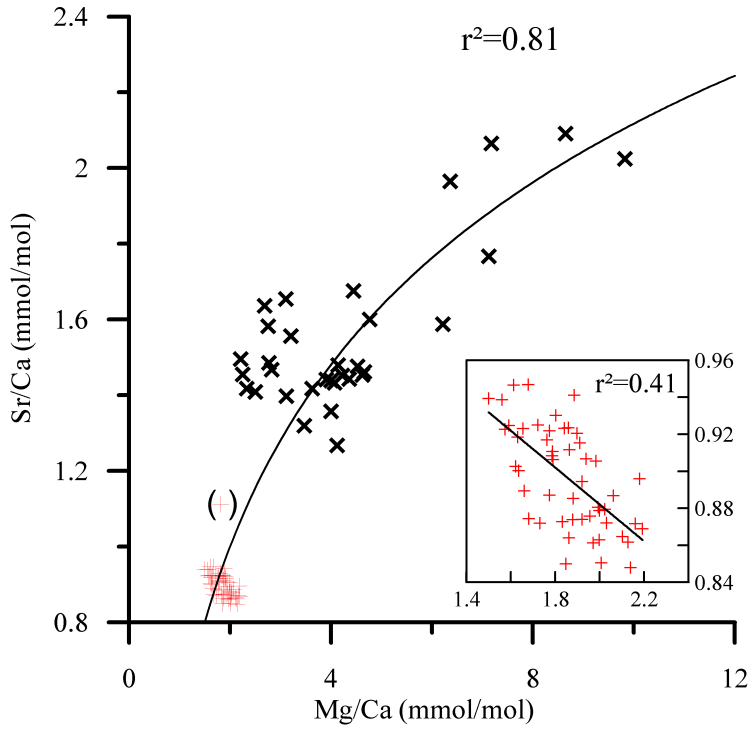

Fig. 6 Correlation of Mg/Ca and Sr/Ca measurements on ostracods from core GeoB 7608-1. The best fit (r^2=0.81) yields the logarithmic function Sr/Ca = 0.69 · ln(Mg/Ca) + 0.51. The small insert shows an augmentation of this anticorrelation for the period before 14.5 kyr BP, with a potential linear fit Sr/Ca = -0.100 · Mg/Ca + 1.081.

Mg/Ca and Sr/Ca values measured on sediment core GeoB 7608-1 are generally positively correlated (Fig. 6) and therefore suggest a common controlling factor. The best fit is logarithmic (r^2=0.81) due to the exponential behaviour of $D(Mg)_o$ at low Mg/Ca_w ratios [*Wansard et al.*, 1998] (Fig. 2). However, a closer inspection shows that the values obtained before 14.5 ka also exhibit a slight inverse correlation, although lying on the broad trend described by all values (Fig. 6). This indicates that the processes governing Sr/Ca and Mg/Ca

before and after 14.5 kyr BP might have been different. In the first section of the following discussion we will examine the glacial conditions until 14.5 kyr BP, the second section will be concerned with the late glacial to Holocene conditions, and finally we will focus on the events surrounding the inflow of Mediterranean waters around 9.2 kyr BP.

6.1 Glacial conditions

The rather low variability of all parameters during the glacial until 18 kyr BP implies stable conditions throughout this time (Fig. 4a). Generally low Sr/Ca, Mg/Ca, $\delta^{18}O$ and $^{87}Sr/^{86}Sr$ values indicate freshwater or slightly brackish conditions as also suggested by faunal investigations [*Mudie et al.*, 2002b].

The entrance of isotopically depleted glacial meltwater between 18.5 and 15 kyr BP causes a temporary drop of $\delta^{18}O$ [*Bahr et al.*, 2005]. High $^{87}Sr/^{86}Sr$ ratios during the same interval further suggests that an otherwise unimportant or inactive source region contributed to a considerable extent to the sediment and water input during this time. The location of this source might be found in the northern and northeastern drainage area of the Black Sea, where the Dnjepr, Dnjestr but also in the Caspian Sea – Manych Depression – Sea of Azov corridor acted as a spillway for the southward directed meltwater of the Scandinavian Ice Sheet [*Mangerud et al.*, 2004]. In contrast to $^{87}Sr/^{86}Sr$ both Mg/Ca and Sr/Ca only show a subtle influence (Fig. 4b) which indicates that the meltwater had Mg/Ca and Sr/Ca ratios similar to that of the glacial Black Sea. Although there is no significant correlation between trace element record and neither $\delta^{18}O$ nor red/blue ratio, the trace element ratios are somewhat inversely correlated during the glacial, and especially during the period of maximum meltwater inflow (Fig. 4b, 6). One potential reason could be that a slight warming (increased Mg/Ca_o) was accompanied by the input of slightly Sr/Ca-depleted meltwater (Fig. 4b). Compared to the full range of the climatic fluctuations one can expect that the amplitude of temperature variability in the deeper part of the Black Sea should be reduced. If we apply the temperature estimates discussed in section 2 to the Mg/Ca ratio, a variability of ca. 0.5 mmol/mol Mg/Ca during the meltwater inflow would equal ca. 0.5 to 1°C in the Black Sea at 1200 m depth. The higher values (ca. 1 mmol/mol) of Mg/Ca in GeoB 7610-1 from 465 m water depth would also indicate generally higher temperatures (1-2°C) at shallower water depths. This temperature divergence is however not clearly seen in the $\delta^{18}O$ record, which has a reduced sensitivity of -0.24‰ per 1°C warming [*von Grafenstein et al.*, 1999b].

6.2 Conditions after 14.5 ka

Both Sr/Ca and Mg/Ca show drastic changes after 14.5 kyr BP, at the onset of the Bølling/Allerød warm period (Fig. 3, 5). Since Sr/Ca and Mg/Ca are sensitive to changes in the water chemistry, it is suggestive to assume a relationship to the contemporaneous onset of authigenic calcite precipitation, mirrored e.g. in the Ca-record (Fig. 5). The uptake of Sr and Mg relative to Ca into the precipitated calcite (organic and inorganic) is controlled by the partition coefficient $D(M)_c$ that is defined similar to the partition coefficient that governs the uptake of Sr and Mg into the ostracod shell:

$$D(M)_c=(M/Ca_c)/(M/Ca_w)$$ [*Morse and Bender*, 1990]

where M is either Sr or Mg.

Numerous attempts to quantify $D(Sr)_c$ and $D(Mg)_c$ for anorganic calcite (e.g., [*Howson et al.*, 1987; *Morse and Bender*, 1990; *Burton and Walter*, 1991]) have shown that especially $D(Mg)_c$ is governed by a complex interaction of several parameters, including temperature, Mg/Ca_w, the Mg-concentration of the ambient water, PCO_2, and the calcite precipitation rate (e.g. [*Huang and Fairchild*, 2001]). For conditions that come close to the ancient Black Sea with low salinity and low to moderate alkalinity, the $D(Mg)_c$ for inorganic low-Mg calcite has been calculated to be in the range of 0.031 (for 25°C), 0.019 (15°C), and 0.012 (6.6°C) [*Huang and Fairchild*, 2001]. The same study gives $D(Sr)_c$ values between 0.057-0.078. As these values are below 1.0, precipitating calcite would therefore be depleted in Sr and Mg relative to Ca and the upper water column would remain enriched in Sr and Mg. An important question is however, if the Mg/Ca_o-increase at 14.5 kyr BP is caused exclusively by the described changes in the water chemistry, or if temperature changes add to the observed signal. The abrupt BA warming is well documented from other regions (e.g, central Europe [*Friedrich et al.*, 2001], Sea of Marmara [*Mudie et al.*, 2002a]), and it seems therefore likely that the shift in the Mg/Ca_o ratio also reflects a certain temperature change. Temperatures certainly play a role for the Mg/Ca_o decrease during the YD, because if changes in the water chemistry would be responsible only, Mg/Ca_o and Sr/Ca_o would parallel each other. This is apparently not the case (except for GeoB 7604-2, which is discussed later). A drop of 1 mmol/mol in Mg/Ca_o in GeoB 7608-1 equals a temperature decrease of 1-2°C at 1202 m water depth and explains the slightly increased $\delta^{18}O$ during the YD. If mainly governed by the change in the isotopic composition of the meteoric precipitation, the oxygen isotope data

would rather show a drop and not an increase, because precipitation-$\delta^{18}O$ almost reached LGM-level during the YD [*von Grafenstein et al.*, 1999a]. A slight temperature increase of the intermediate water column over the course of the early Holocene might as well help to explain the 1 mmol/mol increase of Mg/Ca in GeoB 7608-1 between 11.5 and 9.5 kyr BP, where Sr/Ca remains constant

A possible stratification of the Black Sea water column during this time interval has been already discussed based on the observation of diverging ostracod-$\delta^{18}O$ trends [*Bahr et al.*, subm.]. The overall increase in $\delta^{18}O$ since 15.5 kyr BP is, at least for the B/A, mainly caused by increased $\delta^{18}O$ in the atmospheric precipitation and run-off. Nevertheless, $\delta^{18}O$ values are found to be relatively enriched in the deep core GeoB 7604-2 (1977 m water depth) between 14.5 and 9.2 kyrs BP, indicating that the deep water is separated to a certain extent from the intermediate water body (465 – 1562 m; cores GeoB 7607-2, 7608-1, and 7609-1). There is, however, no significant difference in the Sr/Ca and Mg/Ca ratios for these depth levels. This is most likely due to the different factors influencing the $\delta^{18}O$ and trace element records. The diverging trend in $\delta^{18}O$ is probably controlled by the adjustment of the deepwater to increased $\delta^{18}O$ of atmospheric precipitation [*Bahr et al.*, subm.] that has no direct impact on the trace element record. An exception are Mg/Ca values from the deepest core GeoB 7604-2 that are higher than those in the intermediate cores during the YD, suggesting that the temperature drop during the YD did not affect the deep water.

It is important to note that the $^{87}Sr/^{86}Sr$ ratio decreases during the YD to values similar to those observed before the red clay layers. The drop in $^{87}Sr/^{86}Sr$ can be explained by an outflow of Black Sea water during the YD [*Ryan et al.*, 2003]. ^{87}Sr-depleted water would subsequently replace the ^{87}Sr-rich water, also implying that the Black Sea lake level was below the Bosphorus sill depth during the B/A warm phase.

6.3 Reconnection with the Mediterranean Sea

The deglacial rise of the global sea level together with the present sill depth of the Bosphorus (-35 m) suggests that the inflow of Mediterranean water started between 9.5 and 9 kyr BP (Fig. 5F). It was however argued that the Bosphorus sill might have been at least 7 m shallower before the breaching of the barrier [*Sperling et al.*, 2003], which would have postponed the inflow to about 8.7 kyr BP. The final increase of Sr/Ca_o in our record started at 9.3 kyr BP and is unquestionable related to the intrusion of Mediterranean water with a high

Sr/Ca_w ratio. This also fits to the abrupt $^{87}Sr/^{86}Sr$-increase. An additional point that supports the inflow of saline Mediterranean water at ca. 9 kyr BP are sea surface salinity (SSS) estimates from the Sea of Marmara [*Sperling et al.*, 2003]. This record shows a strong increase in SSS starting ~9 kyr BP (Fig. 5) that suggests an enhanced passing of high-salinity Mediterranean water through the Sea of Marmara during the flooding of the Black Sea. The largest part of the Mediterranean water was most likely influencing the location of the deeper cores first, since the final increase in Mg/Ca, Sr/Ca and $\delta^{18}O$ is delayed in the shallow core GeoB 7610-1.

A similar question as for the 14.5 kyr BP shift arises for the Sr/Ca and Mg/Ca increase after 9 kyr BP: is there a temperature-component in the Mg/Ca_o signal beside the introduction of Mg and Sr-enriched Mediterranean water? The introduction of warm Mediterranean water could have increased the temperature in the deep Black Sea during this time, probably accompanied by turbulent mixing that led to a subsequent homogenisation of the water column, as indicated by the similar values found for Mg/Ca, Sr/Ca and $\delta^{18}O$ in cores from different depth (Fig. 5). An exception is the youngest Mg/Ca measurement in 7610-1, which might be influenced by secondary processes related to the formation of carbonate crusts in the overlying sapropel. Any attempt to calculate the temperature-component in the final Mg/Ca_o increase is hindered by the exponential relation of $D(Mg)_o$ to Mg/Ca_w. Furthermore, it has to be taken into account, that the process of mixing of the two endmembers with different Mg/Ca_w and Sr/Ca_w ratios (Black Sea freshwater vs. Mediterranean marine water) is non-linear and the initial concentrations of Sr, Mg, and Ca in the water of the Black Sea are unknown (see e.g. [*Anadón et al.*, 2002]).

A simple calculation with an isotopic balance model based on the program HIBAL [*Benson and Paillet*, 2002], modified to fit the conditions of the Black Sea [*Bahr et al.*, subm.], was performed to calculate the hypothetical evolution of the $\delta^{18}O$ of the Black Sea water (Fig. 5) during the inflow of Mediterranean water. $\delta^{18}O$ measurements obtained on the planktic foraminifera *Turborotalita quinqueloba* from the Sea of Marmara at 9.5 kyr BP give an indication of the $\delta^{18}O$ of the inflowing water at that point of time. The values are around +1.2‰ [*Sperling et al.*, 2003], or ~3.32‰ for our record, if the vital offset of +2.2‰ for Candoninae [*von Grafenstein et al.*, 1999b] is taken into consideration. This yields an approximate $\delta^{18}O_{water}$ of +0.21‰ (calculated for 10°C water temperature) when using the formulas given in *von Grafenstein et al.* [2000]. For the Black Sea water a $\delta^{18}O$ value of -4.3‰ (for 8°C) was estimated from the ostrocod-$\delta^{18}O$ at 9.3 kyr BP. The three scenarios shown in Fig. 5 include a catastrophic inflow with the maximum possible flux thorough the

Bosphorus (5475 km³/yr [*Myers et al.*, 2003]), a more reduced inflow being equal to the present amount of water flowing in either directions through the Bosphorus (900 km³/yr [*Öszoy and Ünlüata*, 1997]), and a very low flux of 80 km³/yr. Although the boundary conditions of the calculations are debatable, $\delta^{18}O$ is not in steady state at the point at 9.3 kyr BP (indicated by steadily rising $\delta^{18}O$ values) and the simulation makes use of very simplifying assumptions (full mixing, constant inflow, steady water temperatures), it shows that a fast inflow would leave a clear signal in the $\delta^{18}O$ record (Fig. 5). On the other hand, a very low inflow would not change the $\delta^{18}O$ values considerably. Thus, the observed inflow seems to be of intermediate nature.

Although the start of the inflow of Mediterranean water can be assessed relatively well, the duration of the flooding (i.e. the adjustment of the levels of the Black Sea and Sea of Marmara) is less well constrained because of e.g. uncertainties related to potential changes in the reservoir ages. If the 1000 yrs age correction applied to the dated samples of core GeoB 7608-1 relates to aged Black Sea deep waters, this reservoir age should gradually approach the 470 yrs valid for the present marine Black Sea [*Jones and Gagnon*, 1994]. In the previously used stratigraphy of GeoB 7608-1 [*Bahr et al.*, 2005] the authors assumed an age of ca. 7500 yrs BP for the Unit II/Unit III boundary [*Jones and Gagnon*, 1994], a date based on AMS ^{14}C dating of organic material. However, new datings on a core from the southern Black Sea [*Lamy et al.*, in press], performed on planktonic larval shells of the bivalve *Mytilus galloprovinciales*, suggest that this boundary is ca. 8000 yrs old (Tab. 2). This is significantly older than the calibrated and with 1000 yrs corrected age of 7610 ± 40 yrs BP from core GeoB 7608-1 taken just below the Unit II/Unit III boundary at 34 cm. This discrepancy might be resolved if a lower age correction is applied to this date; 470 yrs as the smallest reasonable reservoir age would lead to a corrected age of 8080 ± 60 yrs BP, which is close to the 8000 yrs for the Unit II/III boundary of *Lamy et al.* [in press].

7. Conclusion

Sr/Ca, Mg/Ca, $\delta^{18}O$ and $^{87}Sr/^{86}Sr$ records obtained on ostracod valves reveal major changes in the Black Sea hydrochemistry from the Last Glacial Maximum to the early Holocene, driven by climatic and hydrological fluctuations. Prior to 18 kyr BP the records show little variability and thus constant environmental conditions. Between 18 and 15.5 kyr BP a series of meltwater pulses from the Scandinavian Ice Sheet led to a temporal depletion of the stable isotopic composition of the Black Sea water and to a significant, source-related increase in the

$^{87}Sr/^{86}Sr$ ratio. At 14.5 kyr BP major shifts in the water chemistry took place, related with the onset of the Bølling/Allerød warm period. While the $\delta^{18}O$ values are gradually increasing due to the influence of isotopic enriched atmospheric precipitation and run-off, the Sr/Ca and Mg/Ca ratios are abruptly shifting to higher values, caused by the precipitation of authigenic calcite during high phytoplankton productivity, and the associated increase in Mg and Sr concentrations in the water column. At 14.5 kyr BP a beginning stratification of the water column is visible in the $\delta^{18}O$ record, where data from the deepest core shows the formation of isotopic enriched deep water. During the Younger Dryas cold period low Mg/Ca values indicate a drop of 1-2°C in the deep water, accompanied by an interruption of the authigenic calcite precipitation. A potential outflow of the Black Sea during this time is implied by the decreasing $^{87}Sr/^{86}Sr$ values. The reconnection of the Black Sea with the Mediterranean Sea via the Sea of Marmara started at 9.3 kyr BP as marked in an increase in the former more or less stable Mg/Ca, Sr/Ca and $^{87}Sr/^{86}Sr$ ratios. The homogenisation of the water column, indicated by a merging of the isotopic and trace element records from different depths, suggest a relatively vigorous inflow of marine water. However, the lack of a significant shift in the $\delta^{18}O$ data implies that this inflow was not catastrophic.

Acknowledgements

We thank captain and crew of the RV Meteor for their support during the Meteor cruise M 51-4. We also gratefully acknowledge Scott Birdwhistell for running the ICP-MS at WHOI, Monika Segl (University Bremen) and her team for doing the stable isotope measurements, and U. Röhl (University Bremen) for support of the XRF measurements. A stay of A. B. at the WHOI was supported by the DAAD (ref. D/04/42992). This research was founded by the DFG grants no. LA 1273/2-1, LA 1273/2 and WE 992/47-3. RCOM No. XXXX.

References

Aksu, A. E., R. N. Hiscott, D. Yasar, F. I. Isler and S. Marsh (2002), Seismic stratigraphy of Late Quaternary deposits from the southwestern Black Sea shelf: evidence for non-catastrophic variations in sea-level during the last ~10000 yr, *Marine Geology*, *190*, 61-94.

Aloisi, G., M. Drews, K. Wallmann and G. Bohrmann (2004), Fluid expulsion from the Dvurechenskii mud volcano (Black Sea): Part I. Fluid sources and relevance to Li, B, Sr, I and dissolved inorganic nitrogen cycles, *Earth and Planetary Science Letters*, *225*(3-4), 347-363.

Anadón, P., E. Gliozzi and I. Mazzini (2002), Paleoenvironmental reconstruction of marginal marine environments from combined paleoecological and geochemical analyses on ostracods. In: Holmes, J. A. (Editor), *Ostracoda: Applications in Quaternary Research.* AGU, Washington, pp. 227-247.

Bahr, A., H. Arz, F. Lamy and G. Wefer (subm.) Late glacial to Holocene paleoenvironmental evolution of the Black Sea reconstructed with stable oxygen isotope records obtained on ostracod shells, *Earth and Planetary Science Letters*.

Bahr, A., F. Lamy, H. Arz, H. Kuhlmann and G. Wefer (2005), Late glacial to Holocene climate and sedimentation history in the NW Black Sea, *Marine Geology*, *214*, 309-322.

Bard, E., B. Hamelin, M. Arnold, L. Montaggioni, G. Cabioch, G. Faure and F. Rougerie (1996), Sea level record from Tahiti corals and the timing of deglacial meltwater discharge, *Nature*, *382*, 241-244.

Benson, L. and F. Paillet (2002), HIBAL: a hydrologic-isotopic-balance model for application to paleolake systems, *Quaternary Science Reviews*, *21*(12-13), 1521-1539.

Burton, E. A. and L. M. Walter (1991), The effects of PCO2 and temperature on magnesium incorporation in calcite in seawater and MgCl2-CaCl2 solutions, *Geochimica et Cosmochimica Acta*, *55*(3), 777-785.

Chivas, A. R., P. De Deckker and J. M. G. Shelley (1983), Magnesium, strontium and barium partitioning in nonmarine ostracod shells and their use in paleoenvironmental reconstructions - a preliminary study. In: Maddocks, R. F. (Editor), *Applications of Ostracoda*. Univ. Houston Geosci., Houston, pp. 238-249.

Chivas, A. R., P. De Deckker and J. M. G. Shelly (1985), Strontium content of ostracods indicates lacustrine palaeosalinity, *Nature*, *316*, 251.

Chivas, A. R., P. De Deckker and J. M. G. Shelley (1986a), Magnesium and strontium in non-marine ostracod shells as indicators of palaeosalinity and palaeotemperature, *Hydrobiologia*, *143*, 135-142.

Chivas, A. R., P. De Deckker and J. M. G. Shelly (1986b), Magnesium content of non-marine ostracod shells: a new palaeosalinometer and palaeothermometer, *Palaeogeography, Palaeoclimatology, Palaeoecology*, *54*, 43-61.

Cox, J. M. and G. Faure (1974), Isotope composition of strontium in carbonate phase of two cores from Black Sea. In: E.T. Degens and D. Ross (Editors), *The Black Sea - Geology, Chemistry and Biology.* AAPG, Tulsa, pp. 566-569.

Cronin, T. M., G. S. Dwyer, T. Kamiya, S. Schwede and D. A. Willard (2003), Medieval Warm Period, Little Ice Age and 20th century temperature variability from Chesapeake Bay, *Global and Planetary Change*, *36*(1-2), 17-29.

De Deckker, P., A. R. Chivas and J. M. G. Shelley (1999a), Uptake of Mg and Sr in the euryhaline ostracod Cyprideis determined from in vitro experiments, *Palaeogeography, Palaeoclimatology, Palaeoecology*, *148*, 105-116.

Dwyer, G. S., T. M. Cronin, A. R. Baker, M. E. Raymo, J. S. Buzas and T. Corrège (1995), North Atlantic deepwater temperature change during late Pliocene and late Quaternary climate cycles, *Science*, *270*, 1347-1351.

Engstrom, D. R. and S. Nelson (1991), Paleosalinity from trace metals in fossil ostracodes compared with observational records at Devils Lake, North Dakota, *Palaeogeography, Palaeoclimatology, Palaeoecology*, *83*, 295-312.

Friedrich, M., B. Kromer, K. F. Kaiser, M. Spurk, K. A. Hughen and S. J. Johnsen (2001), High-resolution climate signals in the Bolling-Allerod Interstadial (Greenland Interstadial 1) as reflected in European tree-ring chronologies compared to marine varves and ice-core records, *Quaternary Science Reviews*, *20*(11), 1223-1232.

Howson, M. R., A. D. Pethybridge and W. A. House (1987), Synthesis and distribution coefficient of low-magnesium calcites, *Chemical Geology*, *64*(1-2), 79-87.

Huang, Y. and I. J. Fairchild (2001), Partitioning of Sr2+ and Mg2+ into calcite under karst-analogue experimental conditions, *Geochimica et Cosmochimica Acta*, *65*(1), 47-62.

Ingram, C. (1998), Palaeoecology and geochemistry of shallow marine ostracoda from the Sand Hole formation, Inner Silver Pit, southern North Sea, *Quaternary Science Reviews*, *17*, 913-929.

Jansen, J. H. F., S. J. Van der Gaast, B. Koster and A. J. Vaars (1998), CORTEX, a shipboard XRF-scanner for element analyses in split sediment cores, *Marine Geology*, *151*, 143-153.

Jones, G. A. and A. R. Gagnon (1994), Radiocarbon chronology of Black Sea sediments, *Deep-Sea Research I*, *41*(3), 531-557.

Jørgensen, B. B. (2003), Cruise 51, Leg 4, Istanbul - Istanbul, *METEOR-Berichte*, 03-1, 1-57.

Kvasov, D. (1979), *The late-quaternary history of large lakes and inland seas of Eastern Europe*, Annales Academiae Scientiarum Fennicae 157, 71 pp.

Lamy, F., H. Arz, G. Bond, J. Pätzold and A. Bahr (in press), Multicentennial-scale hydrological changes in the Black Sea and northern Red Sea during the Holocene and the Arctic/North Atlantic Oscillation, *Paleoceanography*.

Major, C., W. Ryan, G. Lericolais and I. Hajdas (2002), Constraints on Black Sea outflow to the Sea of Marmara during the last glacial-interglacial transition, *Marine Geology*, *190*, 19-34.

Majoran, S., S. Agrenius and G. S. Dwyer (1999), The effect of temperature on the geochemical composition of the shells of the ostracod species Krithe praetexta praetexta, *GEOSOUND*, *35*, 93-113.

Mangerud, J., M. Jakobsson, H. Alexanderson, V. Astakhov, G. K. C. Clarke, M. Henriksen, C. Hjort, G. Krinner, J.-P. Lunkka and P. Moller (2004), Ice-dammed lakes and rerouting of the drainage of northern Eurasia during the Last Glaciation, *Quaternary Science Reviews*, *23*(11-13), 1313-1332.

Manheim, F. T. and K. M. Chan (1974), Interstitial waters of Black Sea sediments: new data and review, in *The Black Sea - Geology, Chemistry and Biology*, edited by Degens, E. T. and D. Ross, pp. 155-180, AAPG, Tulsa.

Morse, J. W. and M. Bender (1990), Partition coefficients in calcite: examination of factors influencing the validity of experimental results and their application to natural systems, *Chemical Geology*, *82*, 265-277.

Mudie, P. J., A. Rochon and A. E. Aksu (2002a), Pollen stratigraphy of Late Quaternary cores from Marmara Sea: land-sea correlation and paleoclimatic history, *Marine Geology*, *190*, 233-260.

Mudie, P. J., A. Rochon, A. E. Aksu and H. Gillespie (2002b), Dinoflagellate cysts, freshwater algae and fungal spores as salinity indicators in Late Quaternary cores from Marmara and Black seas, *Marine Geology*, *190*, 203-231.

Mudie, P. J., A. Rochon, A. E. Aksu and H. Gillespie (2003), Late glacial, Holocene and modern dinoflagellate cyst assemblages in the Aegean-Marmara-Black Sea corridor: statistical analysis and re-interpretation of the early Holocene Noah's Flood hypothesis, *Review of Paleobotany and Palynology*, *2563*, 1-25.

Müller, A. (1999), Mg/Ca- und Sr/Ca-Verhältnisse in biogenem Carbonat planktischer Foraminiferen und benthischer Ostracoden, PhD. thesis, Univ. Kiel, Kiel, Germany.

Myers, P. G., C. Wielki, S. B. Goldstein and E. J. Rohling (2003), Hydraulic calculations of postglacial connections between the Mediterranean and the Black Sea, *Marine Geology*, *201*, 253-267.

Öszoy, E. and Ü. Ünlüata (1997), Oceanography of the Black Sea: A review of some recent results, *Earth-Science Reviews*, *42*, 231-272.

Öszoy, E., D. Rank and I. Salihoglu (2002), Pycnocline and deep mixing in the Black Sea: stable isotope and transient tracer measurements, *Estuarine, Coastal and Shelf Science*, *54*(3), 621-629.

Palacios-Fest, M. R. and D. L. Dettman (2001), Temperature controls monthly variation in ostracod valve Mg/Ca: Cypridopsis vidua from a small lake in Sonora, Mexico, *Geochimica et Cosmochimica Acta*, *65*(15), 2499-2507.

Palacios-Fest, M., A. L. Carreno, J. R. Ortega-Ramirez and G. Alvarado-Valdéz (2002), A paleoenvironmental reconstruction of Laguna Babicore, Chihuahua, Mexico based on ostracod paleoecology and trace element shell chemistry, *Journal of Paleolimnology*, *27*, 185-206.

Panin, N. and D. Jipa (2002), Danube River sediment input and its interaction with the northwestern Black Sea, *Estuarine, Coastal and Shelf Science*, *54*, 551-562.

Röhl, U. and L. J. Abrams (2000), High-resolution, downhole, and nondestructive core measurements from site 999 and 1001 in the Caribbean Sea: application to the late Paleocene thermal maximum. In: Leckies, R. M., H. Sigurdsson, G. D. Acton and G. Draper (Editors), *Proc. ODP Sci. Res.*, College Station, TX, pp. 191-203.

Ryan, W. B. F., W. C. Pitman III, C. Major, K. Shimkus, V. Moskalenko, G. A. Jones, P. Dimitrov, N. Görür, M. Sakinc and H. Yüce (1997), An abrupt drowning of the Black Sea shelf, *Marine Geology*, *138*, 119-126.

Ryan, W. B. F., C. O. Major, G. Lericolais and S. L. Goldstein (2003), Catastrophic flooding of the Black Sea, *Annual Review of Earth and Planetary Science*, *31*, 525-554.

Smith, J. A., G. O. Seltzer, D. L. Farber, D. T. Rodbell and R. C. Finkel (2005), Early local Last Glacial Maximum in the tropical Andes, *Science*, *308*, 678-681.

Sperling, M., G. Schmiedel, C. Hemleben, K. C. Emeis, H. Erlenkeuser and P. M. Grootes (2003), Black Sea impact on the formation of eastern Mediterranean sapropel S1? Evidence from the Marmara Sea, *Palaeogeography, Palaeoclimatology, Palaeoecology*, *190*, 9-21.

Swart, P. K. (1991), Factors affecting the oxygen isotopic composition of the Black Sea. In: Izdar, E. and J. W. Murray (Editors), *Black Sea Oceanography*, Kluwer, Dordrecht, Boston, London, pp. 75-88.

von Grafenstein, U., H. Erlenkeuser, A. Brauer, J. Jouzel and S. Johnsen (1999a), A Mid-European decadal isotope-climate record from 15,500 to 5000 Years B.P., *Science*, *284*, 1654-1657.

von Grafenstein, U., H. Erlenkeuser and P. Trimborn (1999b), Oxygen and carbon isotopes in modern fresh-water ostracod valves: assessing vital offsets and autecological affects of interest for palaeoclimate studies, *Palaeogeography, Palaeoclimatology, Palaeoecology*, *148*, 133-152.

von Grafenstein, U., U. Eicher, H. Erlenkeuser, P. Ruch, J. Schwander and B. Ammann (2000), Isotope signature of the Younger Dryas and two minor oscillations at Gerzensee (Switzerland): palaeoclimatic and palaeolimnologic interpretation based on bulk and biogenic carbonates, *Palaeogeography, Palaeoclimatology, Palaeoecology*, *159*, 215-229.

Wansard, G. (1996), Quantification of paleotemperature changes during isotopic stage 2 in the La Draga continental sequence (NE Spain) based on the Mg/Ca ratio of freshwater ostracods, *Quaternary Science Reviews*, *15*(2-3), 237-245.

Wansard, G. and J. P. Roca (1997), Ètude expérimentale de l'incorporation du strontium et du magnesium dans le valves d'un ostracode d'eau douce, Heterocypris brevicaudata (Crustacea, Ostracoda), *Comptes Rendus de l'Académie des Sciences, 325,* 403-409.

Wansard, G., P. De Deckker and R. Julia (1998), Variability in ostracod partition coefficients D(Sr) and D(Mg): Implications for lacustrine palaeoenvironmental reconstructions, *Chemical Geology*, *146*(1-2), 39-54.

Wansard, G., J. P. Roca and F. Mezquita (1999), Experimental determination of strontium and magnesium partitioning in calcite of the freshwater ostracod Herpetocypris intermedia, *Archiv für Hydrobiologie*, *145*, 237-253.

Weninger, B. and O. Jöris (2003), *CALPAL version 2003* (software).

MANUSCRIPT 4

Multicentennial-scale hydrological changes in the Black Sea and northern Red Sea during the Holocene and the Arctic/North Atlantic Oscillation

Frank Lamy*[1], Helge W. Arz[1], Gérard C. Bond[2], André Bahr[3], and Jürgen Pätzold[3]

[1]GeoForschungsZentrum-Potsdam, Telegrafenberg, 14473 Potsdam, Germany.
[2]Lamont-Doherty Earth Observatory of Columbia University, 61 Route 9W/PO Box 1000, Palisades, NY 10964-8000, USA.
[3]Fachbereich Geowissenschaften, Universität Bremen, Klagenfurter Strasse, 28259 Bremen, Germany

(*Paleoceanography*, in press)

Abstract

Paleoenvironmental proxy data for ocean properties, eolian sediment input, and continental rainfall based on high resolution analyses of sediment cores from the southwestern Black Sea and the northernmost Gulf of Aqaba were used to infer hydroclimatic changes in northern Anatolia and the northern Red Sea region during the last ~7,500 years. Pronounced and coherent multicentennial variations in these records reveal patterns that strongly resemble modern temperature and rainfall anomalies related to the Arctic Oscillation/North Atlantic Oscillation (AO/NAO). These patterns suggest a prominent role of AO/NAO-like atmospheric variability during the Holocene beyond interannual to interdecadal timescales, most likely originating from solar output changes.

1. Introduction

It is now well accepted that the Arctic Oscillation/North Atlantic Oscillation (AO/NAO), the Northern Hemisphere's dominant mode of atmospheric variability at interannual to interdecadal timescales, exerts a strong influence on mid- and high-latitude continental climate [*Hurrell*, 1995; *Thompson and Wallace*, 2001]. These changes are particularly evident around the North Atlantic but also considerably affect climates of remote regions, such as

Turkey and the Middle East [*Cullen and deMenocal*, 2000; *Turkes and Erlat*, 2003; *Felis et al.*, 2004]. In order to improve our understanding of natural AO/NAO variations at multicentennial timescales in relation to the potential impact of human activities, it is crucial to investigate the long-term behaviour of this atmospheric mode during the present warm climate stage, the Holocene. AO/NAO reconstructions based on instrumental, historical, and different climate proxy data from e.g. tree-rings and ice-cores only reach back to the past millennium and give insight into interannual to interdecadal-scale variability [*Cullen et al.*, 2001; *Cook et al.*, 2002; *Luterbacher et al.*, 2002]. On longer time-scales, only a few sedimentological and geochemical proxy records have been interpreted in relation to AO/NAO changes. *Keigwin and Pickart* [1999] provided, for example, evidence of anti-phase SST changes north and south of the Gulf Stream during the last 2000 years that are similar to SST anomalies related to the modern AO/NAO. *Noren et al.* [2002] showed that variations in New England storminess may reflect millennial-scale changes in the preferred phase of the AO during the Holocene. A comparison of drift-ice variations with temperature changes in Europe, Greenland, and the subtropical North Atlantic suggests, on the other hand, basin-wide uniform changes on multicentennial to millennial timescales distinct from the modern AO/NAO anomaly pattern [*Bond et al.*, 2001].

Two sensitive regions where modern AO/NAO changes at interannual to interdecadal timescales result in large hydrological impacts and which are also suitable for long-term climate reconstructions are Turkey and the Middle East (Fig. 1) [*Cullen and deMenocal*, 2000; *Turkes and Erlat*, 2003; *Felis et al.*, 2004]. Here, we present a comparison of paleoenvironmental proxy data for ocean properties, eolian sediment input, and continental rainfall based on high resolution analyses of sediment cores from the southwestern Black Sea and the northernmost Gulf of Aqaba. These proxy records of hydroclimatic changes in northern Anatolia and the northern Red Sea region show multicentennial scale variations during the last ~7,500 years that strongly resemble modern AO/NAO-related temperature and rainfall anomalies, suggesting a prominent role of the AO/NAO during the Holocene not only at interannual to interdecadal timescales.

2. Study Areas

2.1 Black Sea

We focus on two sediment cores from the Anatolian continental slope in the southwestern Black Sea, GeoB 7622-2 (41°32.1'N, 31°10.1'E, 1305 m water depth) and GeoB 7625-2 (41°26.7'N, 31°04.0'E, 1242 m water depth) (Fig. 1). The two coring sites are located ~65 and ~50 km northeast of the Sakarya River mouth on topographically elevated ridges on the continental slope away from the pathways of turbidity currents (Fig. 2) and are thus particularly suitable for reconstructing past variations in the terrigenous input from rivers. The Sakarya River is the longest Anatolian river and drains parts of the central Anatolian plain and the Pontide Mountains along the Black Sea [*Algan et al.*, 1999] where interannual to decadal-scale rainfall changes in this Mediterranean-type winter-rain climate region are strongly coupled to AO/NAO [*Turkes and Erlat*, 2003].

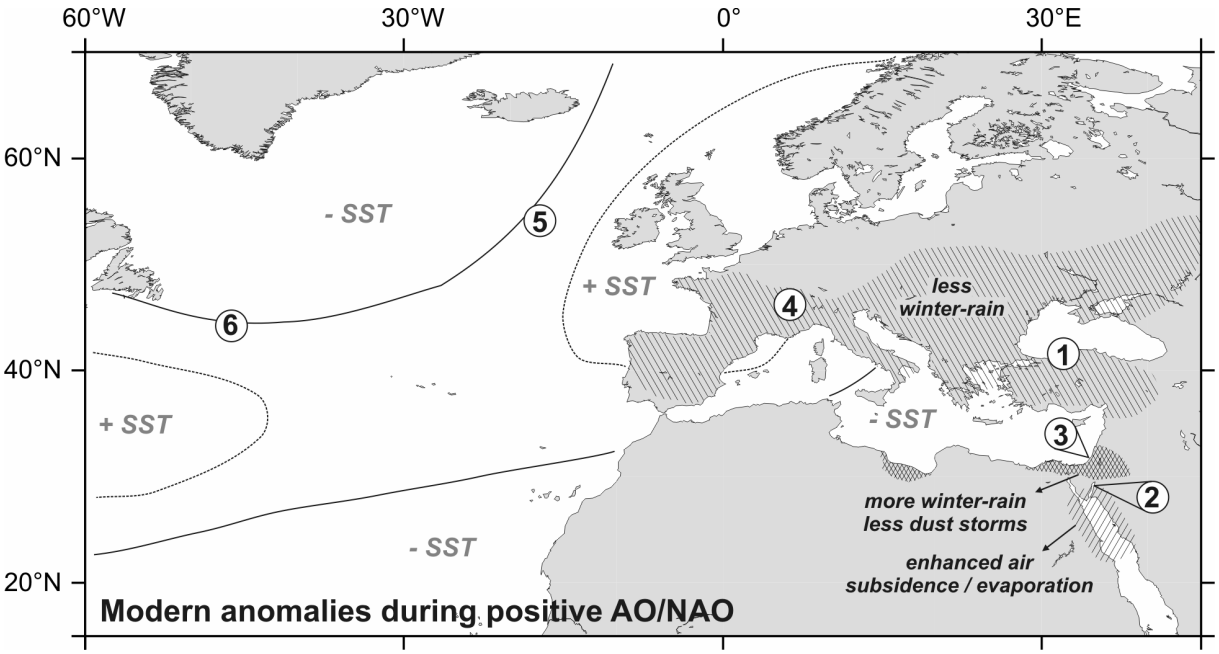

Fig. 1 Map showing location of sites discussed in the text and the modern regional impact of positive AO/NAO anomalies (North Atlantic [*Visbeck et al.*, 2003]; Turkey [*Cullen and deMenocal*, 2000; *Turkes and Erlat*, 2003]; Northern Red Sea/southern Israel [*Cullen and deMenocal*, 2000; *Eshel et al.*, 2000; *Rimbu et al.*, 2001; *Zangvil et al.*, 2003]. [1]Cores GeoB 7622-2 and GeoB 7625-2 (this study), [2]core GeoB 5804-4 (this study), [3]cores GA-112/GA-110 off southern Israel [*Schilman et al.*, 2001], [4]lake level reconstructions from the French/Swiss Jura mountains [*Magny*, 2004], [5,6]North Atlantic sediment cores used for stacked drift ice record [*Bond et al.*, 2001].

Late glacial to Holocene sediments of the Black Sea are classically subdivided into three lithological units [*Ross and Degens*, 1974; *Hay et al.*, 1991]. The most recent one is Unit I which is characterised by finely laminated coccolith ooze of late Holocene age. Unit II basically covers the middle Holocene and consists of likewise finely laminated sapropelic sediments. Both units were deposited under marine conditions (anoxic in the basin). Unit III sediments are lacustrine clays with occasional cm-scale laminations representing the glacial to early Holocene freshwater lake stage of the Black Sea. A recent view of the general late glacial to Holocene history of the Black Sea can be found in *Bahr et al.* [2005] and *Ryan et al.* [2003].

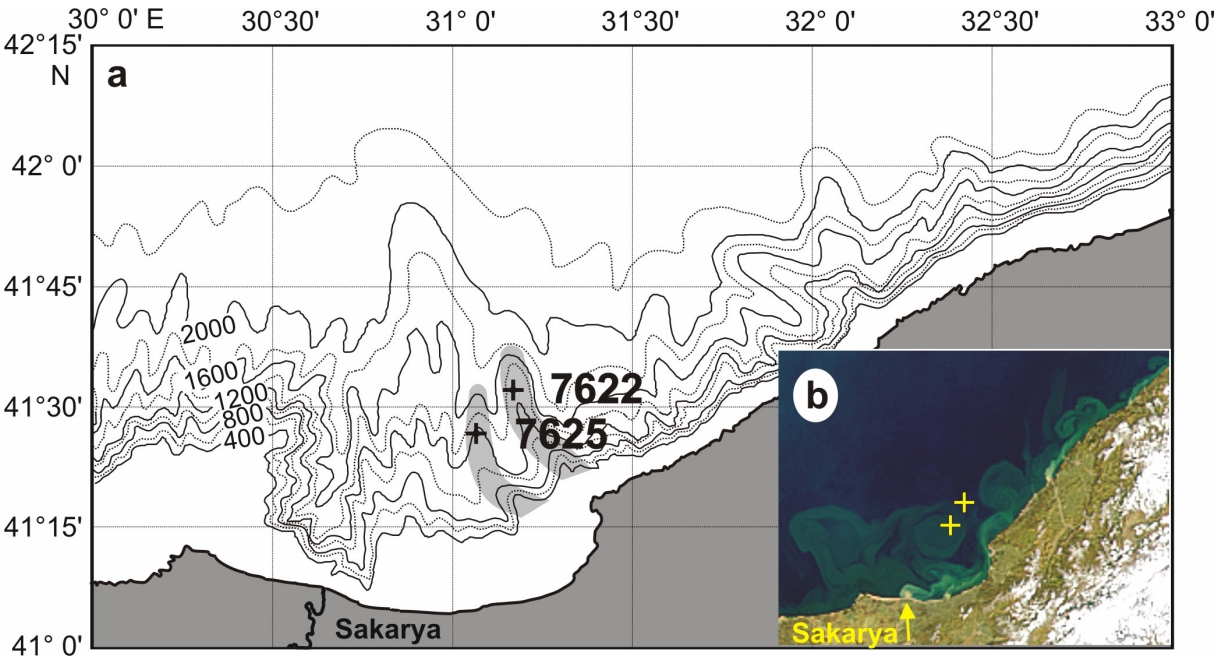

Fig. 2 Regional setting of the Black Sea. **(a)** Detailed bathymetric map of the study area showing the location of cores GeoB 7622-2 and 7625-2 collected during R/V METEOR cruise 51-4 [*Jørgensen*, 2003]. Both sites are located on topographic ridges (gray shading) and should therefore not be influenced by resedimentation processes such as turbidity currents. A further argument for the fluvial origin of the clay layers is the observation of very similar clay layer frequency records at both sites (Fig. 4) that are located on different topographic ridges. (**b**) Satellite image of the Sakarya River mouth with location of the sediment cores showing that both sites receive large amounts of suspended sediment originating from the river (source: http://visibleearth.nasa.gov/).

2.2 Northern Red Sea

Our study here is based on sediment core GeoB 5804-4 (29°30.1'N, 34°57.4'E; 464 m water depth) retrieved from the northernmost Gulf of Aqaba (Fig. 3a). The coring site is located on an elevated ridge separated by two north-south oriented channel structures [*Ehrhardt et al.*,

2005], and should therefore not be influenced by resedimentation processes such as turbidity currents. Sediments are oxic and predominately siliciclastic with biogenic carbonate contents ranging around 30wt-% and low organic carbon contents (ca. 0.35wt-% on average). Sediments delivered from the Wadi Mubarak (marked as cone in Fig. 3b) are mainly displaced towards the southward extending Elat Deep (> 800 m water depth) and sediment cores from this area show frequent intercalations of distinct sandy turbidites [*Pätzold et al.*, 1999].

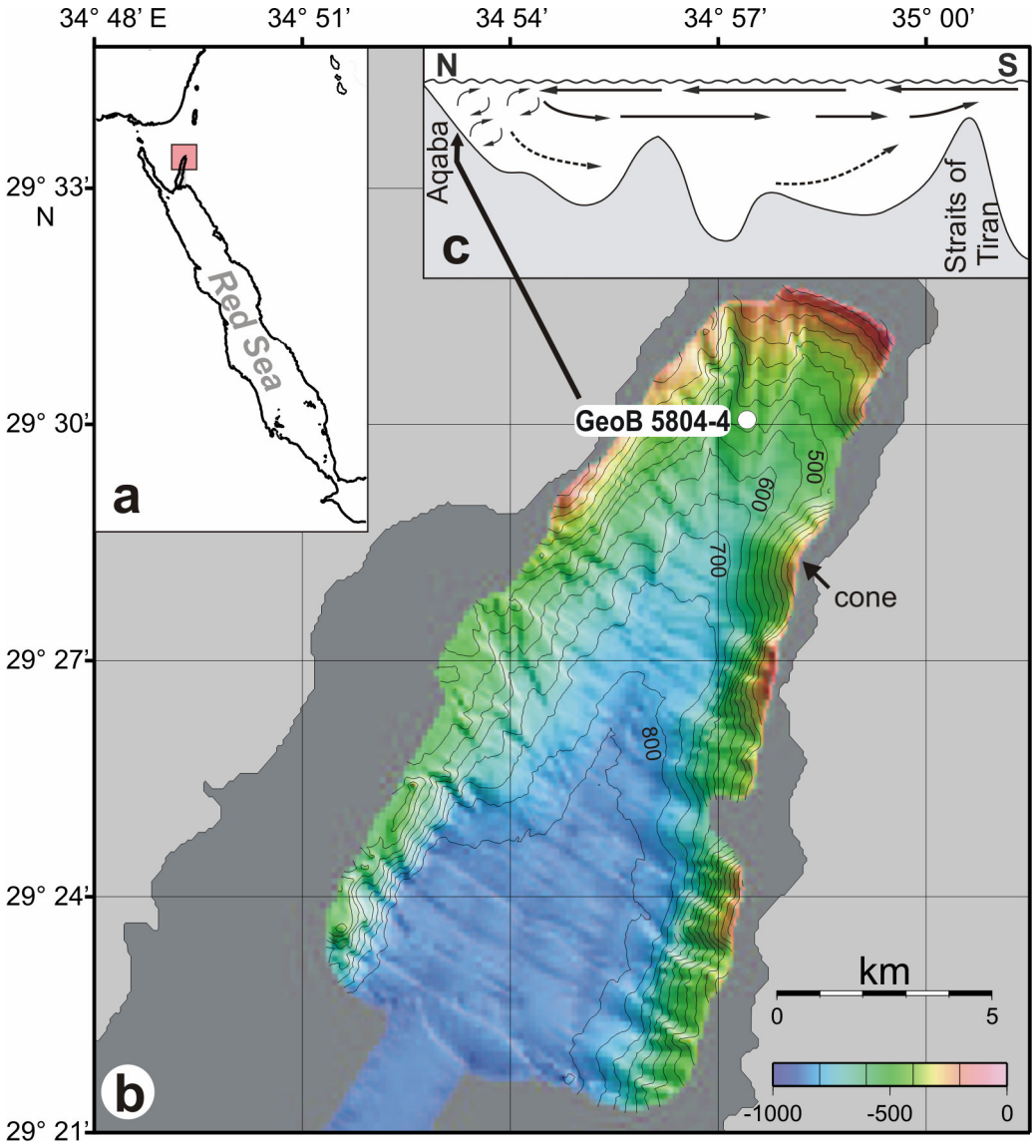

Fig. 3 Regional setting of the Gulf of Aqaba. (**a**) Location of the northern Gulf of Aqaba as the northeastern extension of the Red Sea. (**b**) Detailed bathymetric map of the study area [*Ehrhardt et al.*, 2005] showing the location of core GeoB 5804-4 collected during R/V METEOR cruise 44-3 [*Pätzold et al.*, 1999]. (**c**) Schematic illustration of the predominantly thermohaline driven circulation within the Gulf of Aqaba (after *Eshel and Naik* [1997]).

The Gulf of Aqaba is located at the extreme north of the northern Red Sea thermohaline overturning cell [*Eshel and Naik*, 1997] where water mass stratification and deep water formation are particularly sensitive to temperature and aridity changes [*Eshel et al.*, 2000]. Fig. 3c shows a schematic illustration of the predominantly thermohaline driven circulation within the Gulf of Aqaba. Due to an upper warm layer inflow from the Red Sea over a shallow sill (Straits of Tiran), the overall vertical stratification in the Gulf is unusually weak resulting in relatively warm, homogenous deep waters, which are formed in the northernmost Gulf of Aqaba during the cold winter months. Small interannual anomalies in surface water temperatures and densities result in episodic extreme deep convective mixing events (>850 m water depth) [*Genin et al.*, 1995; *Felis et al.*, 1998]. Presently, evaporation (~200 cm/year) exceeds precipitation that is restricted to rare winter rain (10 to 25 mm/year) originating from the southeastern Mediterranean Sea.

Coral records that cover the past 250 years suggest a strong AO/NAO control on temperature and aridity variability on interannual and interdecadal time scales in the northern Red Sea region [*Eshel et al.*, 2000; *Rimbu et al.*, 2001]. Studies on fossil corals show that this high sensitivity to AO/NAO appears to be characteristic for both the late Holocene and the Eemian interglacial [*Felis et al.*, 2004].

3. Methods

3.1 Stratigraphy

Age models for the Black Sea cores GeoB 7622-2 and GeoB 7625-2 were obtained by ^{14}C-accelerator mass spectrometry (AMS) dating and recognition of a distinctive ash layer (Tab. 1). The two classical Black Sea Units I and II [*Ross and Degens*, 1974, *Hay et al.*, 1991] can be clearly distinguished, e.g. based on gray scale data (Fig. 4a, see also section 4.1). However, compared to the classical Black Sea sequences, both cores reveal unusual high sedimentation-rates due to the nearshore position close to the mouth of the Sakarya River resulting in enhanced terrigenous sediment input and the intercalation of homogenous clay layers (see section 4.1 for further details).

Sediments of Units I and II are generally laminated. Based on sediment trap studies [*Hay et al.*, 1990] and sedimentological analyses of laminated sequences from the Black Sea abyssal

plains [*Hay et al.*, 1991], the laminae most likely represent annual varves. However, the trap studies suggest that the coccolithophoride blooms do not occur every year and a recent sedimentological study suggests that individual laminae may additionally be postdepositionally destroyed by large fecal pellets that form after exceptional productivity events [*Pilskaln and Pike*, 2001].

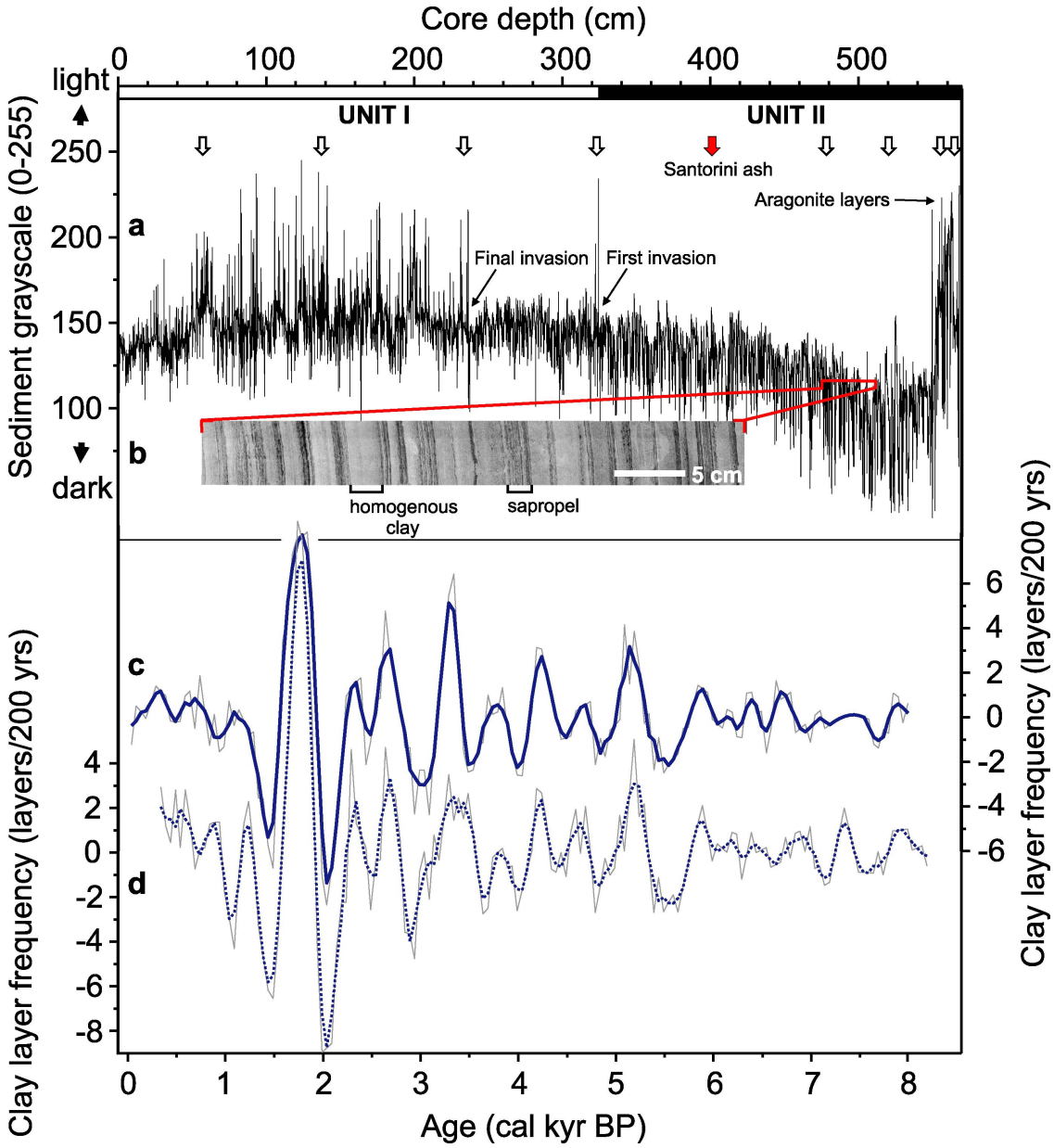

Fig. 4 Black Sea records. (**a**) Gray scale record from core GeoB 7622-2 for visualisation of Black Sea unit division (after *Hay et al.* [1991]) and indication of marker horizons. Arrows indicate ^{14}C-AMS datings (Tab. 1). (**b**) Detail of Unit II sediments in core GeoB 7622-2 showing the intercalation of homogenous clay layers with finely laminated sapropelitic intervals. (**c**) Clay layer frequency record from core GeoB 7622-2 (and multicorer core GeoB 7622-2) showing pronounced multi-centennial scale variability (detrended data; thick line is three-point moving average). **(d)** Clay layer frequency record from core GeoB 7625-2 displays a very similar pattern (r=0.83) (detrended data; thick line is three-point moving average).

Table 1 Details on age control points used to construct the age models of the individual cores.

Age model of GeoB 7622-2 (7622-3) Black Sea

Core depth (cm)	Lab.-ID	^{14}C AMS age(yr B.P.) (Remarks)	±Err (yr)	Calibrated age (cal. yr B.P.)
MUC surface	surface of multicorer GeoB 7622-3			modern age
57(54-60)	KIA 25671*	1170	±35	655
137(134-140)	KIA 25749*	2095	±30	1580
233.5(230-237)	KIA 25672*	2385	±35	1920
323(320-326)	KIA 25751*	3080	±35	2760
400.0	Santorini ash			3595§
478(476-480)	KIA 25674*	4605	±55	4785
520	KIA 19273#	5715	±25	5430$
555(553-557)	KIA 25675*	6590	±70	7005
564.5(563-566)	KIA 25753*	7625	±55	7995

* monospecific carbonate samples of juvenile bivalve shells (*Mytilus galloprovincialis)* # organic matter;
$ corrected and calibrated after *Jones and Gagnon* [1994]; § age after *Hammer et al.* [1987],

Age model of GeoB 7625-2, Black Sea

Core depth (cm)	Remarks	Calibrated age (cal. yr B.P.)
0	age assigned from correlation with GeoB 7622-2, 13.5 cm	247
46	age from correlation with GeoB 7622 ^{14}C date at 57 cm	655
158	age from correlation with GeoB 7622 ^{14}C date at 137 cm	1580
293	age from correlation with GeoB 7622 ^{14}C date at 233.5 cm	1920
388	age from correlation with GeoB 7622 ^{14}C date at 323 cm	2760
466.2	Santorini ash	3595§
537.5	age from correlation with GeoB 7622 ^{14}C date at 478 cm	4785
578	age from correlation with GeoB 7622 ^{14}C date at 520 cm	5430
614	age from correlation with GeoB 7622 ^{14}C date at 555 cm	7005
624	age from correlation with GeoB 7622 ^{14}C date at 564.5 cm	7995

§ age after *Hammer et al.* [1987]

Age model of GeoB 5804-4, Gulf of Aqaba, northern Red Sea

Lab.-ID	Core depth (cm)	Foraminifera species	^{14}C AMS age (yr B.P.)	±Err (yr)	Calibrated age (cal. yr B.P.)
KIA8615	0	*G. sacculifer*	440	25	Post AD 1950
KIA8614	50	*G. sacculifer*	1900	25	1272
KIA8613	100	*G. ruber* (white)	2700	35	2158
KIA8611	150	*G. sacculifer*	4110	50	3897
KIA8610	200	*G. sacculifer*	5095	35	5270
KIA8609	250	*G. sacculifer*	6210	40	6435
KIA8607	300	*G. sacculifer*	6595	45	6882
KIA8606	329	*G. sacculifer*	6940	60	7274

Thus a more detailed age model for the Holocene Black Sea sediments must primarily rely on ^{14}C dating that has however historically been hampered by the lack of suitable carbonate material for ^{14}C dating. As a result, ^{14}C dating of the Black Sea sequence in the basin has in the past been based almost entirely on bulk carbonate and organic carbon [e.g., *Jones and Gagnon*, 1994], both of which are very sensitive to terrestrial contamination. Careful analyses of our cores from the Turkish continental margin has revealed the presence of datable carbonate shells that are free of contamination problems. In most parts of the record, we found small (ca. 200 µm) and very well preserved shells that represent the larval stage of the mollusc *Mytilus galloprovincialis*. During this juvenile stage, *Mytilus galloprovincialis* is planktonic and therefore represents the age of the surface waters. We find the shells in comparatively high concentrations (we picked ca. 2000 individual shells per dating sample) due to the near-shore location of our sediment cores (Fig. 2) where the *Mytilus* larvae are more abundant [*Aral*, 1999]. Therefore, they could not be dated in previous studies that concentrated on the deep basin sediments.

We further recognized an ash layer that has been previously found in sediments of the Black Sea and originates from the Minoan eruption of Santorini [*Guichard et al.*, 1993]. These age control points are complemented by an additional ^{14}C-AMS date on organic matter (core GeoB 7622-2) that we obtained from the older part of Unit II. This sample was taken from the richest organic carbon interval that should be influenced by continental detrital carbon input in a similar way as the basin sediments. We therefore performed the detrital carbon correction applied to the basin sediments [*Jones and Gagnon*, 1994]. Additional ^{14}C ages obtained on core GeoB 7622-2 were substantially too old due to enhanced terrestrial carbon input to the continental slope in comparison to the basin. ^{14}C ages were corrected with a regional deviation from the global reservoir effect (ΔR) of ~70 years (according to the Marine Reservoir Correction Database; http://depts.washington.edu/qil/marine/) and converted to calendar years with the Calib 4.3 software (http://depts.washington.edu/qil/). We applied modern reservoir ages because the age Black Sea surface waters should be largely controlled by the inflow of Mediterranean surface waters that do not show significant reservoir age changes during the Holocene [*Siani et al.*, 2001]. Considering the extraordinarily stable vertical stratification of the Black Sea, we assume that mixing with potentially older deep waters should not significantly affect the reservoir ages.

Between individual dated levels we used a linear interpolation. All ages were measured on core GeoB 7622 and could be exactly transferred to core GeoB 7625 by careful visual inspection of the lamination pattern. Finally, we assumed a modern age for the surface of multicore GeoB 7622-3 that could be appended to the top of the two sediment cores, indicating that 20 cm and 33.5 cm of sediment are missing in core GeoB 7622-2 and GeoB 7625-2, respectively.

The age model for Gulf of Aqaba core GeoB 5804-4 is based on eight ^{14}C AMS dates, conversion to calendar years with the Calib 4.3 software, and linear interpolation between these dates (Tab. 1). We considered a regional deviation from the global reservoir effect (ΔR) of ~180 years based on recent dating of living corals in the northern Red Sea [*Felis et al.*, 2004]. With a sampling interval of 1 cm (for oxygen isotopes below 250 cm core depth 2 cm), the average time resolution of the presented records is between 20 and 30 years.

3.2 Clay layer frequencies

As further discussed in section 4.1, the records from the southwestern Black Sea are characterised by frequent intercalation of homogenous clay layers (Fig. 4b). Visual counting of these clay layers was performed on split sediment cores and x-ray radiographs by counting every clay layer greater than 0.3 cm in thickness resulting in ~270 and ~310 layers in core GeoB 7622-2 and GeoB 7625-2, respectively, implying a recurrence time of ~25 years. The record was extended to the present by appending the clay layers in multicorer core GeoB 7622-3. Clay layer frequencies were calculated for 200 year time windows shifted in 50 year steps along the record. The resulting frequency curve was detrended by subtracting a 1000-year moving average.

3.3 Stable oxygen isotopes

Stable oxygen isotope measurements on core GeoB 5804-4 have been performed on shells of the planktic foraminifer *Globigerinoides ruber* (white) and the benthic foraminifer *Cibicidoides mabahethi* employing an automatic carbonate preparation system (Kiel device) attached to a Finnigan MAT 251 mass spectrometer. To avoid size-dependent effects on the $\delta^{18}O$ values and to reduce potential intrasample noise, 50 specimens of 350 to 400 µm diameter (measured along the longest axis) of *G. ruber* (white) were hand-picked and

homogenized before measurement. The ratio of $^{18}O/^{16}O$ is given in ‰ relative to the VPDB standard. Analytical standard deviation is about ±0.07‰ PDB (Isotope Lab, Bremen University).

3.4 Sand accumulation rates

Sand accumulation rates were calculated from terrigenous sand contents (>63 µm) data that were obtained by wet sieving of the carbonate and organic-matter-free sediment samples of core GeoB 5804-4. The major part (~80 %) of the sand fraction is <150 µm (fine to very fine sand).

3.5 Spectral analyses

Spectral analyses were performed with the AnalySeries software package [*Paillard et al.*, 1996]. Spectra were calculated following the classical and very robust Blackman-Tukey method. The algorithm computes first the autocovariance of the data, applies a Tukey window, and finally Fourier transforms the covariance functions to compute the power spectrum. We applied a 50 yr sampling interval, 73 lags, and 0.00041 bandwidth. Prior to spectral analyses, we removed potential millennial-scale variability by detrending the records in order to further enhance the dominant multicentennial-scale changes in the records.

4. Results and Discussion

4.1 Proxy records from the southwestern Black Sea and northern Red Sea

The analysed sedimentary sequence from the southwestern Black Sea was deposited during the most recent anoxic phase of the Black Sea covering the marine Black Sea Units I and II [*Hay et al.*, 1991] and is laminated throughout. The gray scale record shown in Fig. 4a visualises major characteristics of Units I and II known from the abyssal sediments. Close to the base of the sapropel Unit II, light colours reflect the occurrence of anorganically precipitated aragonite layers found throughout the Black Sea [e.g., *Hay et al.*, 1991]. Within Unit II, excursions towards low gray scale values reflect intervals with dominating sapropelic layers. The first invasion of the coccolithophoride *E. huxleyi* into the Black Sea marks the base of Unit I, when the salinity of the Black Sea exceeded for the first time the tolerance

level of this species [e.g., *Hay et al.*, 1991], and is shown in the gray scale record by the occurrence of light laminae. The same applies for the final invasion of *E. huxleyi* after a short interval of reduced salinities [*Hay et al.*, 1991].

Regional sedimentation-rates on the southwestern Black Sea continental slope are an order of magnitude higher than on the abyssal plains due to enhanced terrigenous sediment input. This enhanced sediment input is manifested in frequent intercalations of homogeneous clay layers that interrupt finely laminated intervals of predominating sapropelic sediments (Unit II) and coccolith ooze (Unit I) (Fig. 4b). The homogenous clay layers most likely represent suspension fallout events from the Sakarya River plume related to increased winter-rain in its western Anatolian drainage basin (see modern sediment plume in Fig. 2b). In order to infer centennial-scale rainfall changes, we counted the homogenous clay layers that were visually distinguishable. Subtracting the counted clay layers from the sequence, still leaves enhanced sedimentation-rates at our sites suggesting that we do not cover the fluvial sediment input completely. The major record of multicentennial-scale changes should however be well captured by our layer counting.

The resulting frequency records show distinct variations on multicentennial time-scales that are very well correlated between the two cores (Fig. 4c and 4d). The fact that the cores are located on different topographic ridges (Fig. 2a) strengthens our assumption that we record regional fluvial sediment input originating from the Sakarya River and thus long-term Anatolian rainfall changes. Modern AO/NAO related rainfall anomalies in this region are negative (positive) during phases of more positive (negative) AO/NAO [*Turkes and Erlat*, 2003], and would therefore be associated with intervals of lower (higher) clay layer frequencies.

In order to reconstruct regional changes in hydroclimatic conditions in the northern Red Sea area, we use two different types of proxy data. Our primary data are stable oxygen isotope records based on surface dwelling (*Globigerinoides ruber* (white)) and epibenthic foraminifera (*Cibicidoides mabahethi*) (Fig. 5a and 5b). The difference between the stable oxygen isotope composition of the planktic ($\delta^{18}O_{pl}$) and epibenthic species records past changes in the vertical $\delta^{18}O$ gradient ($\Delta\delta^{18}O$) providing an indicator for the stratification of the water column in the northern Gulf of Aqaba (Fig. 5c). The undetrended $\Delta\delta^{18}O$ record shows a major shift from ~7 to ~6.25 kyr B.P. that relates to the end of the early Holocene

humid period in the region [*Arz et al.*, 2003a]. During this period, fresh-water input substantially decreased salinity and thus the $\delta^{18}O$ of surface waters in the northern Red Sea [*Arz et al.*, 2003a]. Besides this large long-term shift, a number of smaller-scale variations suggest substantial multicentennial-scale perturbations (Fig. 6c). At the latest with the end of the humid period at ~6.25 kyr B.P., the direct effect of fresh-water input on $\delta^{18}O$ becomes negligible and it is reasonable to assume that, since then, $\delta^{18}O$ variations are primarily a responds to changes in temperature and evaporation.

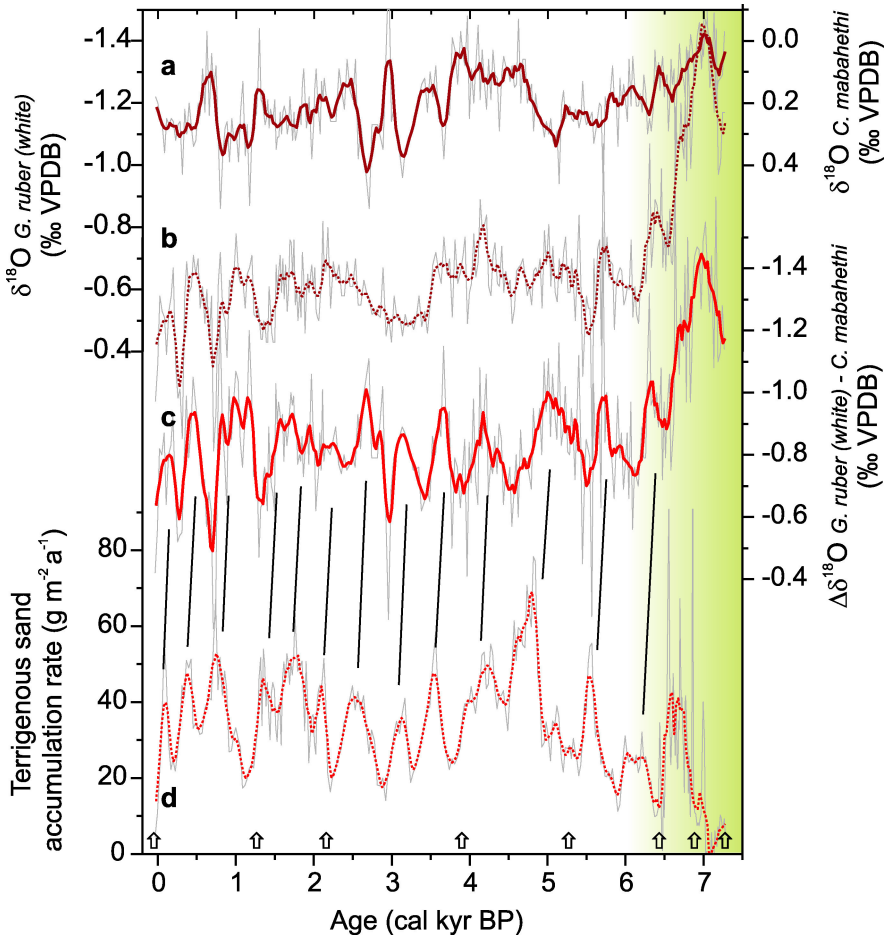

Fig. 5 Original (undetrended) paleoenvironmental data from the northern Red Sea (core GeoB 5804-1). (**a**) Stable oxygen isotope ($\delta^{18}O$) record of the epibenthic foraminifera *Cibicidoides mabahethi* (thick line is five-point moving average). (**b**) $\delta^{18}O$ record of the planktic foraminifera (*Globigerinoides ruber* (white) (thick line is five-point moving average). (**c**) Stable oxygen isotope difference ($\Delta\delta^{18}O$) between planktic (*Globigerinoides ruber* (white)) and epibenthic foraminifera (*Cibicidoides mabahethi*) as a proxy for changes in water column stratification (thick line is five-point moving average). (**d**) Terrigenous sand accumulation record (thick line is five-point moving average). Black lines show systematic lag (maximum correlation between sand accumulation and isotopes at a lag of 125 years) of the multicentennial changes in the sand record compared to the very similar variations in $\Delta\delta^{18}O$. Arrows indicate ^{14}C datings (Tab. 1). Shading marks the early Holocene humid period in the region (after *Arz et al.* [2003]).

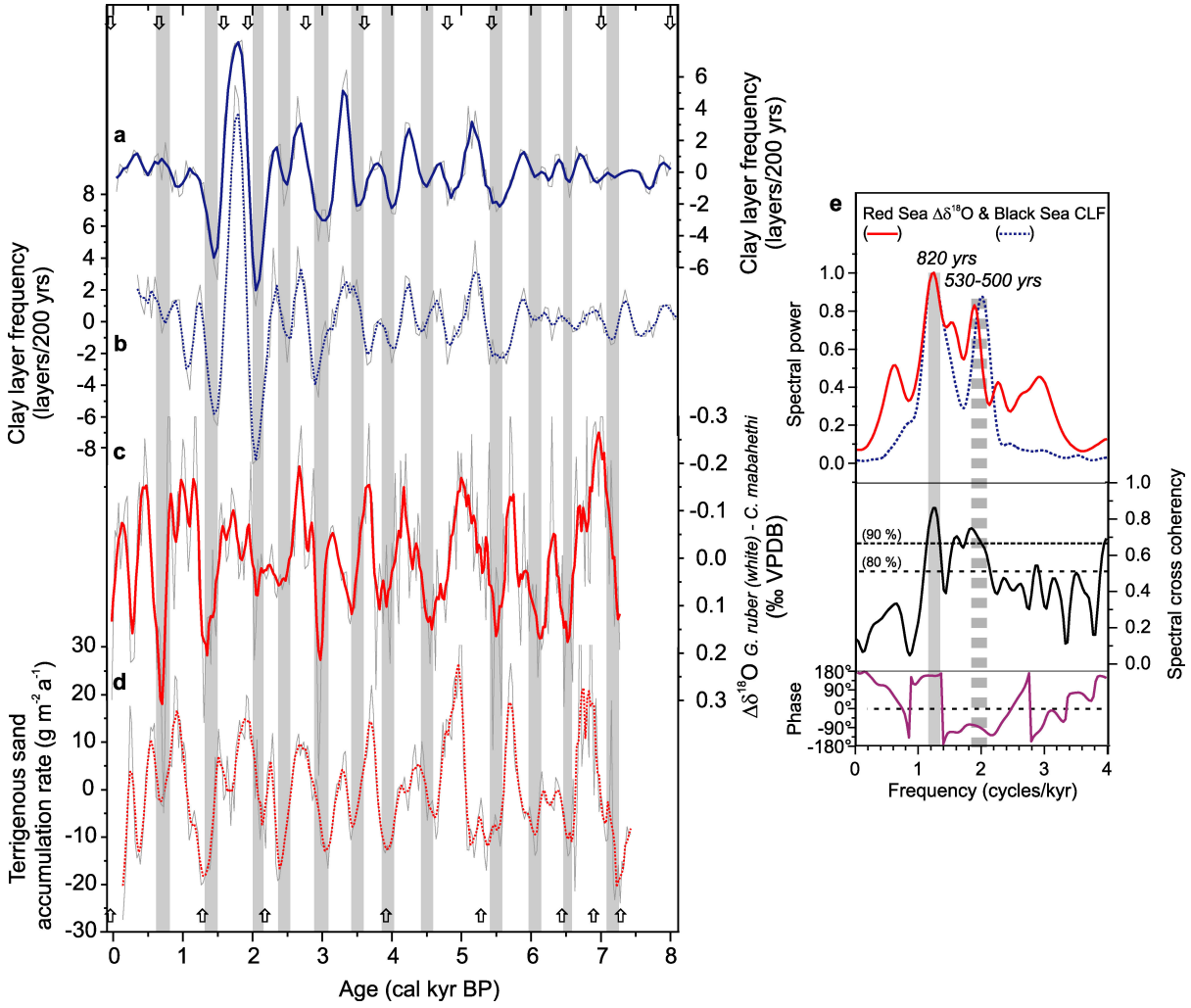

Fig. 6 Proxy records from the southwestern Black Sea and the northernmost Red Sea. **(a)** Clay layer frequency record from core GeoB 7622-2 as shown in Fig. 4. Arrows indicate ^{14}C-AMS datings. (**b**) Clay layer frequency record from core GeoB 7625-2 as shown in Fig. 4. (**c**) Stable oxygen isotope difference ($\Delta\delta^{18}O$) between planktic (*Globigerinoides ruber* (white)) and epibenthic foraminifera (*Cibicidoides mabahethi*) as a proxy for changes in water column stratification (Core GeoB 5804-4, detrended data, original data are shown in Fig. 5; thick line is five-point moving average). (**d**) Terrigenous sand accumulation rate as a proxy for dust input to the northern Gulf of Aqaba (Core GeoB 5804-4, detrended data-set shifted by 125 years; original data are shown in Fig. 4; thick line is five-point moving average). Arrows indicate ^{14}C-AMS datings. Gray bars indicate proposed graphic correlation between the records. (**e**) Spectral analyses. Clay layer frequency (CLF) record (GeoB 7622; red line) and Red Sea $\Delta\delta^{18}O$ record (blue line) with cross spectral coherency between both records at the 80% and 90% confidence levels, and phasing. Labels indicate major coherent periods in the data sets. ~180° phasing of the ~800 years cycles suggests hydroclimatic changes in both regions similar to those presently observed during AO/NAO extremes.

A coral-based $\delta^{18}O$ record from the northern Red Sea [*Eshel et al.*, 2000] has been used as a direct proxy for surface water density changes and related deep water mass formation during the past decades. That study suggests that northern Red Sea deep water formation is strongly

coupled to large-scale atmospheric processes in the Eastern Mediterranean region involving a subsiding air flow from the Eastern Mediterranean towards the northern Red Sea region. These large-scale atmospheric processes appear to be closely coupled to AO/NAO. During positive AO/NAO, an anomalously high pressure system covers large parts of the Mediterranean resulting in northerly winds in the eastern part that drive the advection of dry and cold air. This enhances the surface water densities in the northern Red Sea and weakens the water column stratification [*Eshel and Farrell*, 2000; *Eshel et al.*, 2000; *Felis et al.*, 2000; *Rimbu et al.*, 2001]. We assume that direct impacts of changes in the tropical monsoon system can only be minor because of the predominating control of extratropical atmospheric circulation changes on the northern Red Sea over a wide range of time-scales during the Holocene [*Arz et al.*, 2003a; *Felis et al.*, 2004], last glacial [*Arz et al.*, 2003b], and previous interglacial [*Felis et al.*, 2004].

Our second, independent data-set from the Red Sea is the terrigenous sand accumulation record as an indicator of changes in the eolian input from the surrounding desert areas (Fig. 5d). After removing the long-term trend, which is mainly related to the transition from the Holocene humid period to the present arid conditions (Fig. 5d), the high resolution record shows repeated periods of reduced and enhanced sand accumulation reoccurring on multicentennial timescales (Fig. 6d) that are remarkably similar to the changes in water stratification recorded in our $\Delta\delta^{18}O$ record (Fig. 6c). However, the multicentennial changes in the sand record appear to systematically lag the very similar variations in $\Delta\delta^{18}O$ (maximum correlation between sand accumulation and isotopes at a lag of 125 years; Fig. 5d). It is unlikely that eolian sediment input and water column stratification show a different response time as both processes are controlled by atmospheric processes. Therfore, the lag is most likely induced by differential mixing processes through bioturbation as observed in several studies [e.g., *Brown et al.*, 2001]. Such processes generally produce younger apparent ages for finer-grained material (in our case the predominantly fine to very fine-grained sand; <150 μm) than for coarser-grained particles (in our case foraminifera; 350 to 400 μm).

Lower sand accumulation occurred during periods of weaker water column stratification, which today are associated with intervals of more positive AO/NAO. A potential mechanism would be reduced aridity during such periods. Regional rainfall in southernmost Israel (close to the Gulf of Aqaba) indeed tends to increase during positive AO/NAO intervals as for example during the period 1975-1995 [*Zangvil et al.*, 2003]. Likewise on longer time-scales,

surface water reconstructions on planktic foraminifera off southern Israel [*Schilman et al.*, 2001] (Fig. 1) covering the last ca. 3,500 years, suggest repeated intervals of more humid (and/or warmer) conditions that roughly correlate to our intervals of lower sand accumulation and weaker water column stratification. However, considering the hyper-arid conditions of the region, aridity changes can not be the only reason for changes in eolian supply. Also conceivable is a relation to the frequency and intensity of dust storms. The majority of dust storms in Israel are associated with southwesterly winds during intervals of strong low pressure systems in the Eastern Mediterranean (Cyprus Low) [*Pye*, 1987] as presently occurring during negative AO/NAO phases [*Hurrell*, 1995; *Zangvil et al.*, 2003].

4.2 Long-term changes in AO/NAO?

Taken together, our independent proxy records from the Black Sea and Red Sea show similar multicentennial variability over the past ~7,500 years (Fig. 6). Spectral analyses of the Black Sea clay layer frequencies and the Red Sea $\Delta\delta^{18}O$ record show prominent multicentennial cycles at ~800 and ~500 years, both of which reveal significant cross coherency (Fig. 6e). The phasing of the dominant cycle at ~800 years is clearly anti-phased in both records (~180°), whereas the ~500 years cycle reveals a phasing of ~-100°. The deviation from a strict anti-phasing is probably induced by dating limitations due to small errors in ^{14}C-dating, reservoir age corrections, and interpolation between the dating points. The latter likewise applies to the graphic correlation between the records that shows a general anti-phased pattern but reveals some remaining ambiguities (Fig. 6a-6d). In addition, the multicentennial changes in our Black Sea and Red Sea records show a different amplitude evolution. While the amplitudes in the Red Sea records (Fig. 6c and 6d) do not vary significantly, there are large fluctuations in the amplitudes of the clay layer frequency records from the Black Sea (Fig. 6a and 6b), particularly the low amplitudes in the early part of the record and the large swing between ca. 1.5 and 2 kyr B.P. The low amplitudes are likely related to substantially decreased sedimentation-rates that decrease the resolution of the record and deteriorate the visual distinction of individual clay layers. The low sedimentation rates could be the expression of dryer conditions during the early part of the record that would correspond to the early Holocene humid period in the Red Sea [*Arz et al.*, 2003] and may suggest an “anti-phasing” likewise on longer than multicentennial timescales [*Rimbu et al.*, 2003]. The large amplitude change in the late Holocene probably reflects a very humid interval in Anatolia. The Red Sea records shown in this paper do not show a particular event during this interval but preliminary

planktic foraminifera census counts in the whole northern Red Sea suggest anomalous surface water conditions during this interval.

The anti-phasing between the records shown in both the spectral analyses results and the graphic correlation (Fig. 6) suggests a multicentennial pattern similar to modern AO/NAO-related environmental changes on interannual to interdecadal timescales in both regions: Intervals of reduced (enhanced) clay layer frequency and thus less (more) Anatolian rainfall recorded in our Black Sea cores (Fig. 6a and 6b) were accompanied by increased (decreased) surface water densities, substantially reduced (enhanced) water stratification (Fig. 6c), and less (more) intense dust transport in the northern Red Sea region (Fig. 6d) implying more frequent or more persistent positive (negative) AO/NAO conditions (Fig. 1).

Holocene climate fluctuations on different time-scales have been linked to decadal to multicentennial-scale variations in solar activity [*Bond et al.*, 2001; *Fleitmann et al.*, 2003]. Comparing our records to the tree-ring based residual $\Delta^{14}C$ record as a proxy for solar variability [*Stuiver et al.*, 1998] shows that similar multicentennial cycles are present in the records. Spectral analyses of the $\Delta^{14}C$ record reveal dominant peaks at ~720/920, ~530, and ~350 years that are close to the ~800 and ~500 years cycles found in our Black Sea and Red Sea records (Fig. 7) (a cycle of ~350 years appears to be present only in the Red Sea $\Delta\delta^{18}O$ record). The graphic correlation suggests that intervals of more negative AO/NAO (higher clay layer frequencies) relate, within dating uncertainties, to reduced solar activity (Fig. 8a and 8b). This relationship is consistent with a modelling study on the AO/NAO pattern during the Maunder solar output minimum [*Shindell et al.*, 2001]. Further support comes from well-dated lake level records in the French/Swiss Jura mountains (Fig. 1) that were originally interpreted to represent latitudinal displacements of the Atlantic westerly jet linked to solar variability [*Magny*, 2004]. However, such displacements presently also occur in relation to AO/NAO [*Hurrell*, 1995] implying that higher lake levels (Fig. 8c) may represent more negative AO/NAO phases. In addition, several studies from the Mediterranean Sea have described a number of cold spells reoccurring on millennial time-scales during the Holocene [e.g., *Cacho et al.*, 2001; *Rohling et al.*, 2002; *Sbaffi et al.*, 2004]. Though the individual records are of lower time resolution and thus mainly capture millennial-scale variability, we note that in particular the Aegean records of *Rohling et al.* [2002] could be interpreted in terms of atmospheric forcing involving AO/NAO as well (polar/continental air outbreaks and associated SST cooling in the Aegean Sea occur more frequently during positive AO/NAO [*Rimbu et al.*, 2003]).

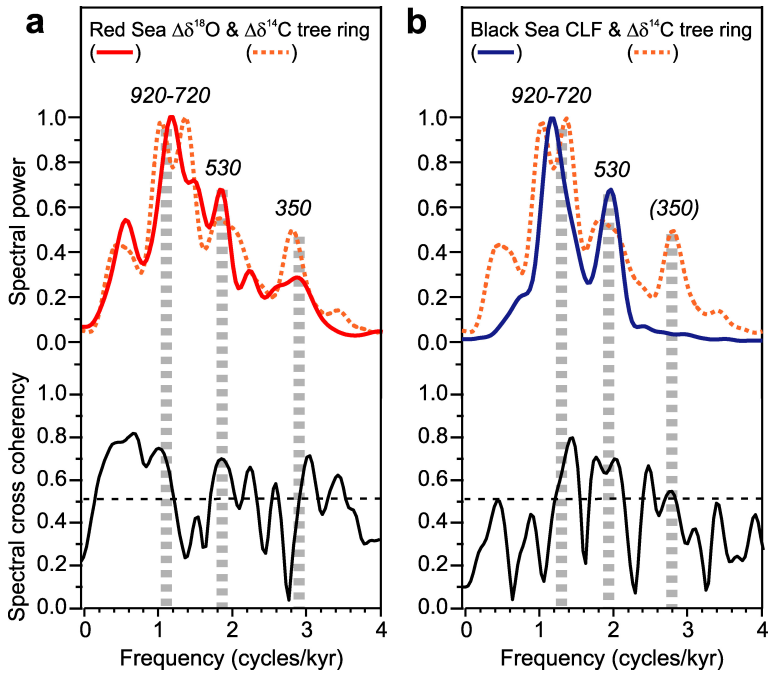

Fig. 7 Comparison of (**a**) Red Sea $\Delta\delta^{18}O$ record and (**b**) Black Sea clay layer frequency (CLF) to the tree-ring based residual $\Delta^{14}C$ record as a proxy for solar variability [*Stuiver et al.*, 1998] to show similar multicentennial-scale variability. Blackman-Tukey spectra of the detrended records as shown in Fig. 6 and cross spectral coherency at the 80% confidence level. Labels indicate major coherent periods in the data sets.

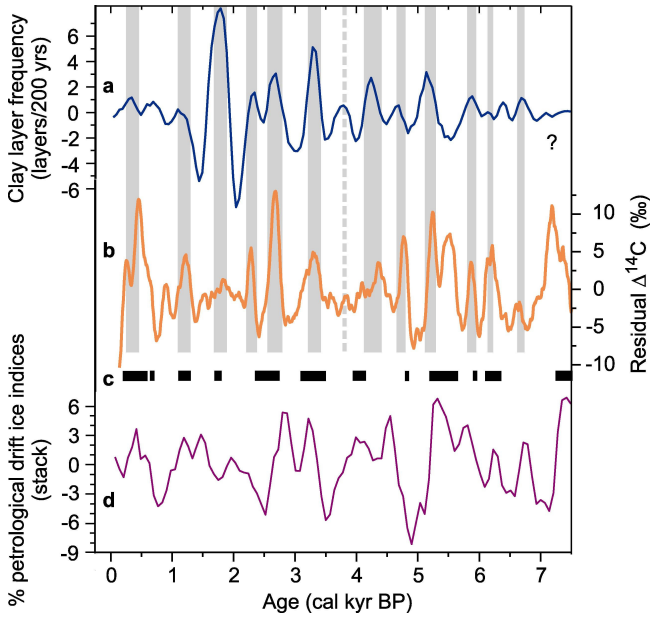

Fig. 8 Comparison of the Black Sea record to the solar variability and other relevant records. **(a)** Clay layer frequency record; southwestern Black Sea (core GeoB 7622 as shown in Fig. 6); more (less) frequent clay layers are interpreted to represent negative (positive) AO/NAO phases. (**b**) Residual $\Delta^{14}C$ record as a proxy for solar variability (positive $\Delta^{14}C$ represents reduced solar output; detrended decadal data-set smoothed with a 13-point moving average) [*Stuiver et al.*, 1998]. **(c)** Lake level highstands in the French/Swiss Jura mountains interpreted to represent a southward displacement of the Atlantic westerly jet [*Magny*, 2004] as presently occurring during negative AO/NAO phases. **(d)** Stacked drift ice record from the North Atlantic [*Bond et al.*, 2001]. Less (more) drift ice represents warmer (cooler) sea surface temperatures (negative AO/NAO; see text for discussion).

Our findings, on the other hand, appear to be in conflict with the previous conclusions derived from North Atlantic drift ice-records [*Bond et al.*, 2001] (Fig. 8d). At least during the late Holocene, increased drift ice associated with cooler surface water temperatures south of Greenland occurred during basin-wide cold phases recorded in Europe, Greenland, and the subtropical North Atlantic [*Bond et al.*, 2001], a pattern that is clearly distinct from the modern AO/NAO temperature anomalies in that region [*Visbeck et al.*, 2003] (Fig. 1). However, it has been recently suggested that the North Atlantic temperature response to AO/NAO may be substantially different on multidecadal or longer time-scales [*Visbeck et al.*, 2003]. Due to a larger involvement of ocean circulation changes, including changes in the large-scale North Atlantic thermohaline circulation, a basin-wide temperature response to prolonged AO/NAO forcing is conceivable [*Visbeck et al.*, 2003] and would result in North Atlantic cooling during long-term negative AO/NAO intervals, a response consistent with the proxy records (Fig. 8).

5. Conclusions

Paleoenvironmental proxy data for hydroclimatic changes in northern Anatolia and the northern Red Sea region show multicentennial-scale variations during the last ~7,500 years that strongly resemble modern AO/NAO-related temperature and rainfall anomalies. Taken together, the available data suggest a prominent role of AO/NAO-like atmospheric variability during the Holocene beyond interannual to interdecadal timescales. The multicentennial variability appears to be similar to changes observed in proxy records for solar output changes.

In remote, more continental regions, our records show large scale atmospheric circulation changes and resulting hydroclimatic shifts with spatial patterns similar to the modern AO/NAO, most likely forced ultimately by solar output changes. In contrast, changes in the North Atlantic are distinct from the modern AO/NAO temperature anomalies in that region. The exact physical mechanism that transfers small solar irradiance changes either to symmetric responses in the North Atlantic circulation or to atmospheric circulation changes involving an AO/NAO-like pattern, remains unclear. Further research is needed to better understand the oceanic response and associated feedbacks of the Northern Hemisphere atmospheric circulation. Such findings are a major prerequisite to obtaining more reliable forecasts of the behaviour of the AO/NAO on longer time-scales, as particularly the impact of

(natural) centennial-scale climate variability on future climate projections could be more substantial than previously thought [*Moberg et al.*, 2005].

Acknowledgements

We thank M. Segl and B. Meyer-Schack, University of Bremen for carrying out the stable isotope measurements. T. Felis and G. Haug contributed with helpful comments on earlier versions of the manuscript that, in addition, greatly benefited from the constructive reviews of P. deMenocal and G. Schmiedl. Financial support was made available through the Deutsche Forschungsgemeinschaft (LA 1273/2-1, LA 1273/2-2, and WE 992/47-3).

References:

Algan, O., C. Gazioglu, N. Cagatay, Z. Yücel, and B. Gönencgil (1999), Sediment and water influxes into the Black Sea by Anatolian Rivers, *Zeitschrift für Geomorphologie, 43,* 61-79.

Aral, O. (1999), Growth of The Mediterranean Mussel (Mytilus galloprovincialis Lam., 1819) on Ropers in The Black Sea, Turkey, *Turkish Journal of Veterinary and Animal Sciences*, *23*, 183-189.

Arz, H. W., F. Lamy, J. Pätzold, P. J. Müller, and M. Prins (2003a), Mediterranean moisture source for an early-Holocene humid period in the northern Red Sea, *Science*, *300*, 118-122.

Arz, H. W., J. Pätzold, P. J. Müller, and M. O. Moammar (2003b), Influence of Northern Hemisphere climate and global sea level rise on the restricted Red Sea marine environment during termination I, *Paleoceanography*, *18*, doi:10.1029/2002PA000864.

Bond, G., B. Kromer, J. Beer, R. Muscheler, M. N. Evans, W. Showers, S. Hoffmann, R. Lotti-Bond, I. Hajdas, and G. Bonani (2001), Persistent solar influence on north Atlantic climate during the Holocene, *Science*, *294*, 2130-2136.

Brown, L., G. T. Cook, A. B. MacKenzie, and J. Thomson (2001), Radiocarbon age profiles and size dependency of mixing in Northeast Atlantic sediments, *Radiocarbon*, *43*, 929-937.

Cacho, I., J. O. Grimalt, M. Canals, L. Sbaffi, N. J. Schackleton, J. Schofeld, and R. Zahn (2001), Variability of the Western Mediterranean sea surface temperature during the last 25,000 years and its connection with the Northern Hemisphere climatic changes, *Paleoceanography*, *16*, 40-52.

Cook, E. R., R.D D'Arrigo, and M. E. Mann (2002), A well-verified, multiproxy reconstruction of the winter North Atlantic Oscillation index since A.D. 1400, *Journal of Climate*, *15*, 1754-1764.

Cullen, H. M., and P. B. deMenocal (2000), North Atlantic influence on Tigris-Euphrates streamflow, *International Journal of Climatology*, *20*, 853-863.

Cullen, H. M., R.D D'Arrigo, E. R. Cook, and M. E. Mann (2001), Multiproxy reconstructions of the North Atlantic oscillation, *Paleoceanography*, *16*, 27-39.

Ehrhardt, A., C. Hübscher, Z. Ben-Avraham, and D. Gajewski (2005), Seismic study of pull-apart-induced sedimentation and deformation in the Northern Gulf of Aqaba (Elat), *Tectonophysics, 396*, 59-79.

Eshel, G., and N. H. Naik (1997), Climatological coastal jet collision, intermediate water formation, and the general circulation of the Red Sea, *J. Phys. Oceanogr.*, *27*(7), 1233–1257.

Eshel, G., and B. F. Farrell (2000), Mechanisms of eastern Mediterranean rainfall variability, *Journal of the Atmospheric Sciences*, *57*, 3219-3232.

Eshel, G., D. P. Schrag, and B. F. Farrell (2000), Troposphere-planetary boundary layer interactions and the evolution of ocean surface density: Lessons from Red Sea corals, *Journal of Climate*, *13*, 339-351.

Felis, T., J. Pätzold, Y. Loya, and G. Wefer (1998), Vertical water mass mixing and plankton blooms recorded in skeletal stable carbon isotopes of a Red Sea coral, *Journal of Geophysical Research C: Oceans*, *103*, 30731-30740.

Felis, T., J. Pätzold, Y. Loya, M. Fine, A. H. Nawar, and G. Wefer (2000), A coral oxygen isotope record from the northern Red Sea documenting NAO, ENSO, and North Pacific teleconnections on Middle East climate variability since the year 1750, *Paleoceanography*, *15*, 679-694.

Felis, T., G. Lohmann, H. Kuhnert, S. J. Lorenz, D. Scholz, J. Pätzold, S. A. Al-Rousan, and S. M. Al-Moghrabi (2004), Increased seasonality in Middle East temperatures during the last interglacial period, *Nature*, *429*, 164-168.

Fleitmann, D., S. J. Burns, M. Mudelsee, U. Neff, J. Kramers, A. Mangini, and A. Matter (2003), Holocene forcing of the Indian Monsoon recorded in a stalagmite from Southern Oman, *Science*, *300*, 1737-1739.

Genin, A., B. Lazar, and S. Brenner (1995), Vertical mixing and coral death in the Red Sea following the eruption of Mount Pinatubo, *Nature*, *377*, 507-510.

Guichard, F., S. Carey, M. A. Arthur, H. Sigurdsson, and M. Arnold (1993), Tephra from the Minoan eruption of Santorini in sediments of the Black Sea, *Nature, 363*, 610-612.

Hammer, C. U., H. B. Clausen, W. L. Friedrich, and H. Tauber (1987), The Minoan eruption of Santorini in Greece dated to 1645 BC?, *Nature, 328*, 517-519.

Hay, B. J., S. Honjo, S. Kempe, V. A. Ittekkot, E. T. Degens, T. Konuk, and E. Izdar (1990), Interannual variability in particle flux in the southwestern Black Sea, *Deep-Sea Research*, *37*, 911-928.

Hay, B. J., M. A. Arthur, W. E. Dean, E. D. Neff, and S. Honjo (1991), Sediment deposition in the Late Holocene abyssal Black Sea with climatic and chronological implications, *Deep-Sea Research*, *38*; Suppl. 2, S1211-S1235.

Hurrell, J. W. (1995), Decadal trends in the North Atlantic oscillation: regional temperatures and precipitation, *Science, 269,* 676-679.

Jones, G. A., and A. R. Gagnon (1994), Radiocarbon chronology of Black Sea sediments, *Deep-Sea Research*, *41*, 531-557.

Jørgensen, B. B. (2003), METEOR-Berichte, Cruise 51, Leg 4, Istanbul – Istanbul, *METEOR-Berichte 03-1*, *57*.

Keigwin, L. D., and R. S. Pickart (1999), Slope water current over the Laurentian Fan on interannual to millennial time scales, *Science, 286*, 520-523.

Luterbacher, J., C. Schmutz, D. Gyalistras, E. Xoplaki, and H. Wanner (2002), Extending North Atlantic Oscillation reconstructions back to 1500, *Atmospheric Science Letters*, doi:10.1006/asle.2001.0044.

Magny, M. (2004), Holocene climate variability as reflected by mid-European lake-level fluctuations and its probable impact on prehistoric human settlements, *Quaternary International*, *113*, 65-79.

Moberg, A., D. M. Sonechkin, K. Holmgren, N. M. Datsenko, and W. Karlen (2005), Highly variable Northern Hemisphere temperatures reconstructed from low- and high-resolution proxy data, *Nature*, *433*, 613-617.

Noren, A. J., P. R. Bierman, E. J. Steig, A. Lini, and J. Southon (2002), Millennial-scale storminess variability in the northeastern United States during the Holocene epoch, *Nature*, *419*, 821-824.

Paillard, D., L. Labeyrie, and P. Yiou (1996), Macintosh program performs time-series analysis, *EOS Transactions American Geophysical Union*, *77*, 379.

Pätzold, J., and cruise participants (1999). *Report and preliminary results of Meteor Cruise M 44/3, Aqaba (Jordan) - Safaga (Egypt) - Duba (Saudi Arabia) - Suez (Egypt) - Haifa (Israel), March 12 - March 26 - April 2 - April 4, 1999*, 135 pp., Department of Geosciences, University Bremen, Bremen.

Pilskaln, C. H. and J. Pike (2001), Formation of Holocene sedimentary laminae in the Black Sea and the role of the benthic flocculent layer, *Paleoceanography*, *16*, 1-19.

Pye, K. (1987), *Aeolian dust and dust deposits*, 334 pp., Academic Press Inc., London.

Rimbu, N., G. Lohmann, T. Felis, and J. Pätzold (2001), Arctic oscillation signature in a Red Sea coral, *Geophysical Research Letters*, *28*, 2959-2962.

Rimbu, N., G. Lohmann, J. H. Kim, H. W. Arz, and R. Schneider (2003), Arctic/North Atlantic Oscillation signature in Holocene sea surface temperature trends as obtained from alkenone data, *Geophysical Research Letters*, *30*, doi:10.1029/2002GL016570.

Rohling, E. J., P. A. Mayewski, R. H. Abu Zied, J. S. L. Casford, and A. Hayes (2002), Holocene atmosphere-ocean interactions: Records from Greenland and the Aegean Sea, *Climate Dynamics*, *18*, 587-594.

Ross, D. and E. T. Degens, (1974), Recent Sediments of Black Sea. In: E. T. Degens and D. Ross (Editors), *The Black Sea - Geology, Chemistry and Biology*. AAPG, Tulsa, pp. 183-199.

Ryan, W. B. F., C. O. Major, G. Lericolais and S. L. Goldstein (2003), Catastrophic flooding of the Black Sea, *Annu. Rev. Earth Planet. Sci.*, *31*, 525-554.

Sbaffi, L., F. C. Wezel, G. Curzi, and U. Zoppi (2004), Millennial- to centennial-scale palaeoclimatic variations during Termination I and the Holocene in the central Mediterranean Sea, *Global and Planetary Change*, *40*, 201-217.

Schilman, B., M. Bar Matthews, A. Almogi Labin, and B. Luz (2001), Global climate instability reflected by Eastern Mediterranean marine records during the late Holocene, *Palaeogeography, Palaeoclimatology, Palaeoecology*, *176*, 157-176.

Shindell, D. T., G. A. Schmidt, M. E. Mann, D. Rind, and A. Waple (2001), Solar forcing of regional climate change during the Maunder Minimum, *Science*, *294*, 2149-2152.

Siani, G., M. Paterne, E. Michel, R. Sulpizio, A. Sbrana, M. Arnold, and G. Haddad (2001), Mediterranean sea surface radiocarbon reservoir age changes since the last glacial maximum, *Science*, *294*, 1917-1920.

Stuiver, M., P. J. Reimer, E. Bard, J. W. Beck, G. S. Burr, K. A. Hughen, B. Kromer, G. McCormac, J. van der Plicht, and M. Spurk (1998), INTCAL98 radiocarbon age calibration, 24,000-0 cal BP, *Radiocarbon*, *40*, 1041-1083.

Thompson, D. W. J., and J. M. Wallace (2001), Regional climate impacts of the Northern Hemisphere annular mode, *Science*, *292*, 85-89.

Turkes, M., and E. Erlat (2003), Precipitation changes and variability in Turkey linked to the North Atlantic Oscillation during the period 1930-2000, *International Journal of Climatology*, *23*, 1771-1796.

Visbeck, M., E. P. Chassignet, R. G. Curry, T. L. Delworth, R. R. Dickson, and G. Krahmann (2003), The ocean´s response to North Atlantic Oscillation variability. In: Hurrell, J. W., Y. Kushnir, G. Ottersen and M. Visbeck (Editors), *The North Atlantic Oscillation - climatic significance and environmental impact*. American Geophysical Union, Washington, DC, pp. 113-145.

Zangvil, A., S. Karas, and A. Sasson (2003), Connection between Eastern Mediterranean seasonal mean 500 HPA height and sea-level pressure patterns and the spatial rainfall distribution over Israel, *International Journal of Climatology, 23*, 1567-1576.

MANUSCRIPT 5

A preliminary study on alkenones from the western Black Sea – is there a potential for SST reconstructions?

André Bahr[1], Helge W. Arz[2], Frank Lamy[2]

[1]Universität Bremen, Fachbereich Geowissenschaften, Postfach 330440, 28334 Bremen, Germany

[2]GeoForschungsZentrum-Potsdam, Section 3.3, Telegrafenberg, 14473 Potsdam, Germany

unpublished

Abstract

Temperatures based on the alkenone-method were calculated for 11 core tops from the western Black Sea, located at various water depths on the shelf, continental slope and in the deep basin. The calculated temperatures are consistently lower than the observed annual mean sea surface temperatures, indicating that the temperature calibration generally used for samples from the open ocean is not valid for material from the Black Sea. Other factors like preferential degradation of more unsaturated alkenones under anoxic conditions and the contribution of a different population of alkenone-producing organisms to the signal are discussed.

1. Introduction

Alkenones are long-chain, unsaturated methyl and ethyl-ketones widely used for reconstructions of past sea-surface temperatures (SST). They were first discovered in sediments from the Walvis Ridge and the Black Sea [*Boon et al.*, 1978; *de Leeuw et al.*, 1980] and are characteristic compounds found in haptophyte microalgae, namely (but not exclusively) in Emiliania huxleyi, an abundant coccolithophorid algae belonging to the Prymnesiophyceae [*Volkman et al.*, 1980]. The potential of alkenones for paleotemperature reconstructions derives from the fact that the concentration of diunsaturated ketones ($C_{37:2}$)

increases relative to the concentration of more unsaturated isomers ($C_{37:3}$ and $C_{37:4}$) with rising temperatures. This relation was first found in laboratory cultures [*Marlowe,* 1984; *Brassel et al.*, 1986] and later verified in independent experiments and field studies including measurements on particulate organic matter POM (e.g., [*Prahl and Wakeham*, 1987; *Prahl et al.*, 1988; *Sikes et al.,* 1991]). It is common to express the ratio of di-, tri- and tetraunsaturated C_{37} alkenons ($C_{37:2}$, $C_{37:3}$ and $C_{37:4}$) as the alkenone unsaturation index U_{37}^{K} [*Brassel et al.*, 1986],

$$U_{37}^{K} = \frac{[C_{37:2}] - [C_{37:4}]}{[C_{37:2}] + [C_{37:3}] + [C_{37:4}]}$$

which can be simplified to

$$U_{37}^{K'} = \frac{[C_{37:2}]}{[C_{37:2}] + [C_{37:3}]}$$

if tetraunsaturated components are absent. The relationship between unsaturation index and temperature was first calculated using U_{37}^{K} with $U_{37}^{K} = 0.033T + 0.043$ [*Prahl and Wakeham*, 1987] but later revised to $U_{37}^{K'} = 0.034T + 0.039$ [*Prahl et al.*, 1988]. The latter equation was later confirmed by core top measurements [*Müller et al.*, 1998].

It is tempting to apply the alkenone method to samples from the late Holocene of the Black Sea because the uppermost lithostratigraphic section, Unit I, is a laminated coccolith ooze dominated by the remains of *Emiliania huxleyi* [*Arthur et al.*, 1994]. The first invasion of *E. huxleyi* into the Black Sea was dated to 2700 yrs calBP [*Jones and Gagnon*, 1994] with a short interruption by a transition sapropel; the final invasion of *E. huxleyi* started then at ca. 1635 yrs calBP [*Jones and Gagnon*, 1994]. So far two detailed studies of alkenones from the Black Sea have been published [*Freeman and Wakeham*, 1992; *Xu et al.*, 2001], both of them raising serious doubts if temperature reconstructions are possible with alkenones from the Black Sea (for more detail, see results and discussion section). For this preliminary study we chose core top samples from the western Black Sea to investigate if alkenones are suited for paleotemperature reconstructions in this basin.

2. Material and Methods

2.1 Sediment samples

A total of 11 samples were obtained from multicores retrieved during RV Meteor cruise M 51-4 in December 2001 (Tab. 1).

The multicores were sliced in 1 cm pieces and freezed at -20 °C. Later the samples were freeze-dried and ground in an agate mortar. Generally the uppermost 2 cm were analysed, in some cases the samples are from the 2-3 cm depth interval. Since below ca. 160 m water depth anoxic conditions prevail, all multicores from below that depth lack bioturbation. The time span covered in the uppermost 2-3 cm is approximately 300-400 years.

Table 1

Multi-corer (MUC)	Lat. N	Long. E	Water depth (m)	Sampled interval	$[C_{37:2}]$ (µg/g)	$[C_{37:3}]$ (µg/g)	$[C_{37:4}]$ (µg/g)	U^{K}_{37}	$U^{K'}_{37}$	T* (°C)
7613-1	43°43.7'	29°50.3'	84	0-2 cm	3.25	3.33	0.188	0.452	0.494	13.38
7614-1	43°42.8'	29°54.4'	91	0-2 cm	5.53	6.12	0.393	0.427	0.475	12.85
7615-1	43°41.1'	30°01.9'	148	0-2 cm	3.96	4.63	0.328	0.407	0.461	12.41
7616-2	43°41.0'	30°02.5'	168	2-3 cm	510.4	440.2	1.222	0.535	0.537	14.64
7617-2	43°38.9'	30°04.1'	468	2-3 cm	32.82	42.37	4.079	0.363	0.436	11.69
7618-2	43°32.8'	30°09.2'	943	2-3 cm	19.27	33.56	3.899	0.271	0.365	9.58
7619-1	43°29.2'	30°11.8'	1246	2-3 cm	58.13	53.39	2.934	0.482	0.521	14.18
7606-2	43°00.9'	29°59.5'	1809	0-2 cm	69.34	64.08	2.955	0.487	0.520	14.10
7604-1	42°56.2'	30°01.9'	1988	0-2 cm	44.47	49.57	4.093	0.411	0.473	12.76
7605-4	42°43.7'	30°14.7'	2165	0-2 cm	17.28	14.95	0.757	0.501	0.536	14.6
7622-2	41°32.1'	31°10.0'	1305	2-3 cm	10.05	9.08	0.415	0.493	0.525	14.30

T* was calculated with $U^{K'}_{37}$ [*Prahl et al.*, 1988]

2.2 Methodology

To determine the alkenone unsaturation index $U^{K'}_{37}$, an amount of 0.2 to 1.5 g (Tab. 1) of freeze-dried and homogenized sediment was used. After adding an internal standard (squalane, $C_{30}H_{62}$, and 2-nonadecanone, $C_{19}H_{38}O$), mixtures of methanol and methylene chloride with subsequently decreasing polarity (MeOH, MeOH/CH_2Cl_2 1:1, CH_2Cl_2) were used to extract the alkenones under ultrasonification (UP 200H sonic disruptor probe, Hielscher GmbH, 200W, 105 µm amplitude, 0.5 s pulse). The extracts were centrifuged and combined, then desalted with de-ionized water, dried with Na_2SO_4 and evaporated to dryness. The residue was dissolved in CH_2Cl_2. Interferences with co-eluting C_{36}-fatty acid methyl esters were avoided by saponification using 0.1 N KOH in methanol (90/10 CH_3OH/H_2O) at 80°C for 2 hours followed by partitioning of the neutral fraction containing the alkenones into hexane. Finally the extracts were concentrated under N_2 and taken up in 25 µl MeOH/CH_2Cl_2 (1:1).

For analyzing the extracts a HP 5890 serie II Plus gas chromatograph equipped with a 60 m x 0.32 mm fused silica column using split/splitless injection and flame ionization detection was used. The carrier gas was helium with a constant pressure of 150 psd. After injection at 50°C

the oven temperature was heated to 250°C at a rate of 25°C/min, then to 290°C with 1°C/min, held for 26 min and finally heated to 310°C at a rate of 30°C/min; the final temperature was maintained for 10 min. The quantification of the alkenones was performed using HPGC ChemStation as analytical software. The SST values derived from the calibration of *Prahl et al.* [1988] ($U_{37}^{K'}$ = 0 0.034T + 0.039) have an analytical precision of ±0.5°C.

3. Results and discussion

The calculated temperatures using $U_{37}^{K'}$ show broad variations between 9.6 and 14.6°C and are, with the exception of the measurement taken from the core top at 168 m water depth, considerably higher than temperatures yielded with the equation based on U_{37}^{K} (Fig. 1A).

Striking are the big differences in the alkenone content, ranging between 3.3 and 510 µg/g for the di- and triunsaturated component (Fig. 1, Tab. 1). While values of up to 50 µg/g have been previously reported for Black Sea sediments [*Xu et al.*, 2001], a value of 510 µg/g seems dubious but remeasuring yielded a comparable result of 471.4 µg/g for $C_{37:2}$ and 426.1 µg/g for $C_{37:3}$. When comparing the concentrations of the isomers $C_{37:2}$ and $C_{37:3}$ with the calculated temperatures (Fig. 1C) and the concentration of $C_{37:4}$ (Fig. 1D), a split of the samples into two groups, one with high and another with low concentrations of $C_{37:2}$ and $C_{37:3}$ is apparent. This appears to be primarily related to the preservation potential of organic matter at the respective location, because samples with high concentrations are generally found at water depths below 160 m, in the anoxic part of the water column, while those with lower alkenone content are situated in the oxic upper part of the water column, where the degradation of organic material should be much faster. The amount of clastic material diluting the alkenone concentration at the respective core position might also play a role, because the two cores from anoxic waters with relatively low alkenone contents, MUC 7605-4 and 7622-2, receive high amounts of clastic material from turbidites (MUC 7605-4) and riverine material from the Sakarya River (MUC 7622-2) [*Jørgensen*, 2003]. That the alkenone concentration is dependent on factors like geographical position and local oceanography and not only on water depth is evident from Fig. 1B, where no clear depth dependence of alkenone concentrations could be observed, although the concentration of alkenones as a whole seems to have a maximum in the cores between 1500 and 2000 m water depth, taken aside the abnormal concentration found in the core from 168 m depth (Fig. 1B). However, there is no difference in the calculated temperature ranges between the samples with high and

low alkenone content (Fig. 1C), implying that, at least in this case, the alkenone concentration does not play an important role for the performed temperature calculations.

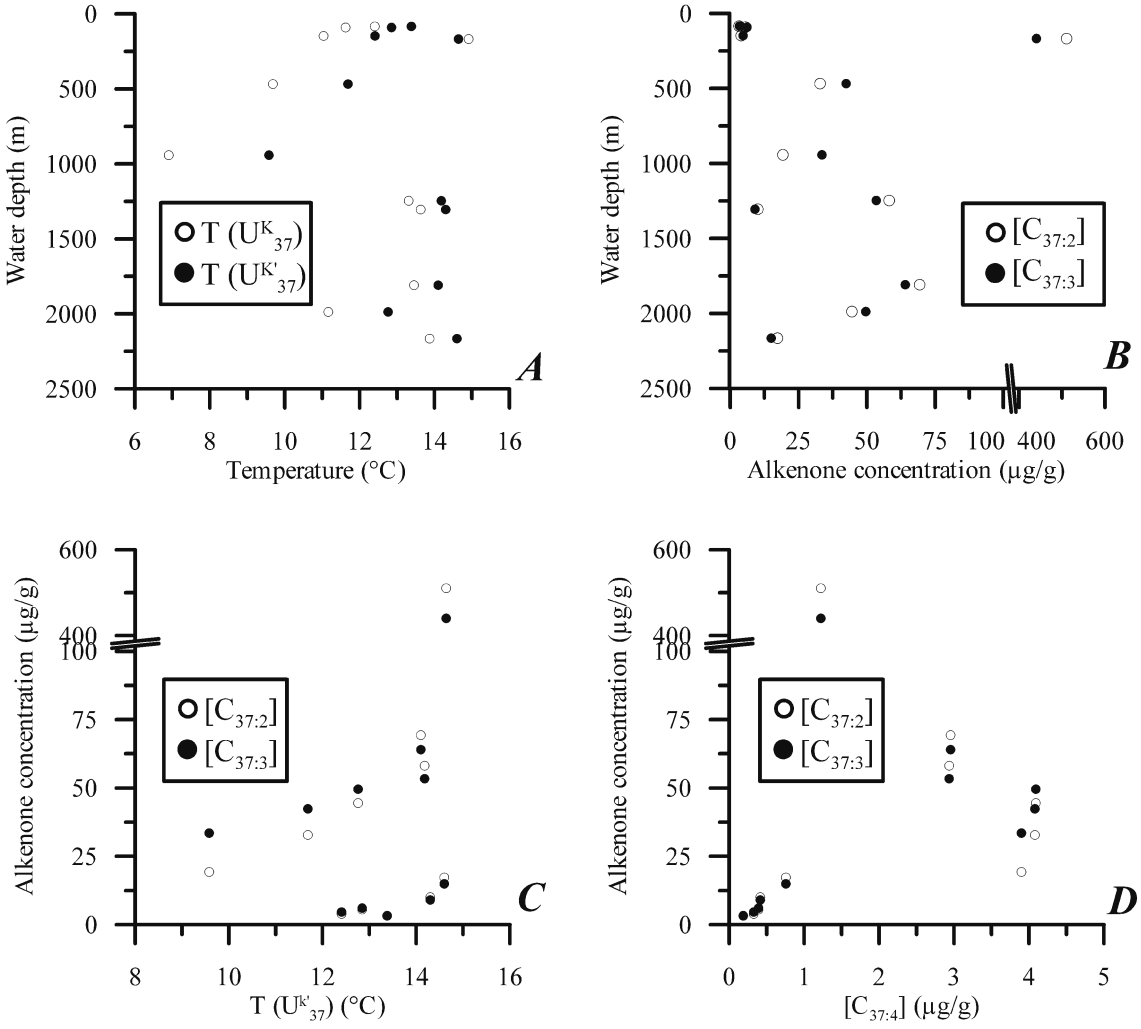

Fig. 1 (**A**) Alkenone-derived temperatures based on the indices U^{K}_{37} and $U^{K'}_{37}$ versus water depth of the sampled multicorer; (**B**) concentrations of di- and triunsaturated alkenones relative to the water depth; (**C**) temperatures calculated with $U^{K'}_{37}$ compared with the concentration of the di- and triunsaturated components, and (**D**) concentration of tetraunsaturated alkenones plotted against the concentration of di- and triunsaturated alkenones.

One would expect that alkenone-derived temperatures resemble the spatial distribution of the instrumental SSTs in the Black Sea. The annual mean SST of the western Black Sea show a general north-south gradient with temperatures around 14.0°C in the north and 15.6°C towards the Bosphorus entrance in the south (Fig. 2). This trend is not convincingly reflected in the temperature reconstructions, although a slight trend to higher temperatures towards the south might be visible. The calculated temperatures are also constantly below the annual mean SST.

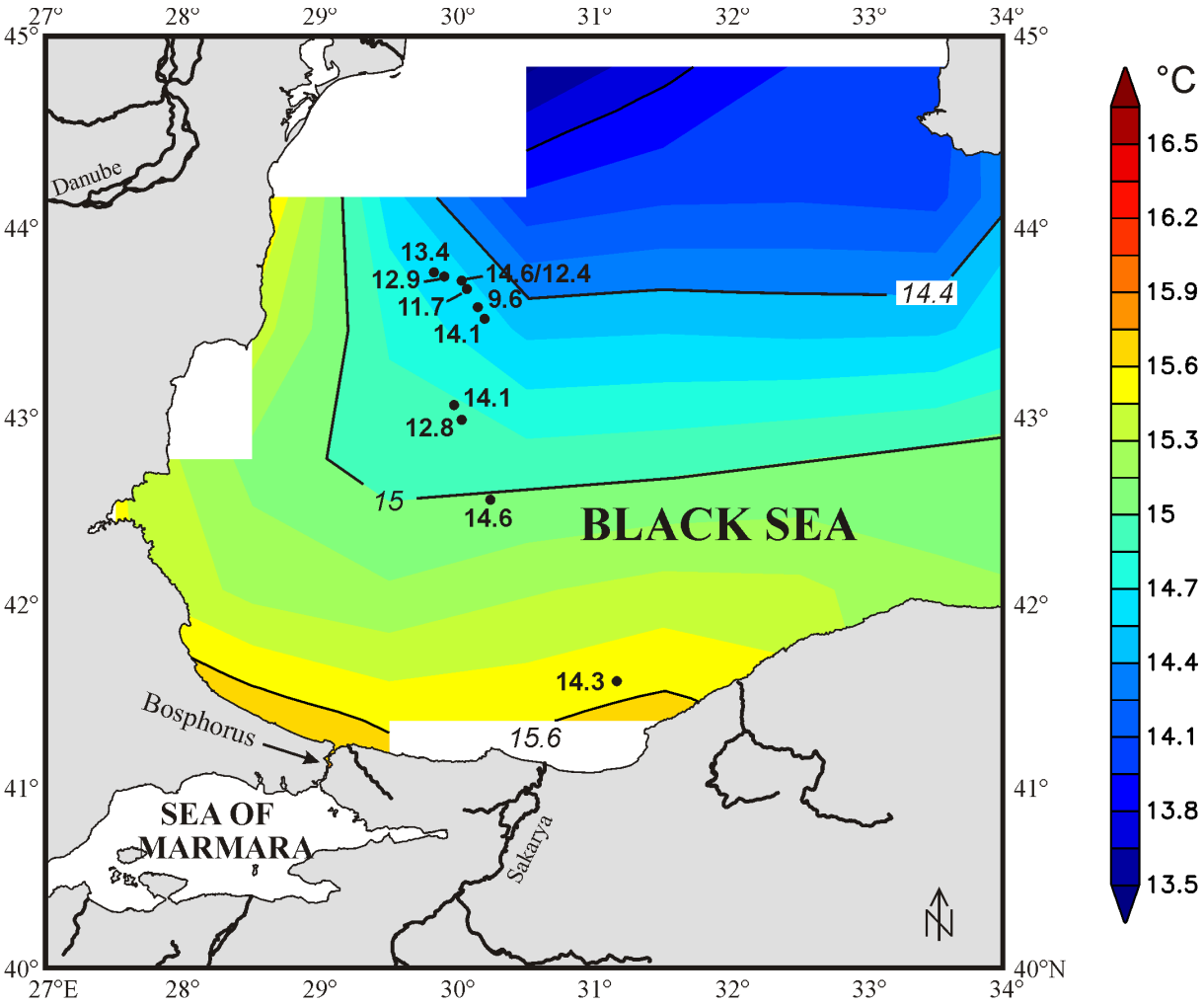

Fig. 2 Annual mean SST (in °C) in the western Black Sea measured between 1962 and 2002 (COADS 1-degree Enhanced data from NOAA-CIRES). The black dots and the assigned numbers indicate the position of the cores used in this study and the calculated temperatures (see also Tab. 1).

Two previous studies performed on water samples, sediment traps [*Freeman and Wakeham*, 1992; *Xu et al.*, 2001] and sediment samples [*Freeman and Wakeham*, 1992; *Xu et al.*, 2001] have already shown that alkenone-based temperature reconstructions in the Black Sea might be problematic, at least with the calibration by *Prahl et al.* [1988]. The present results could not erase these doubts, but on the other hand they do not differ totally from the expected temperature range. One explanation for the generally too low calculated temperatures and the observed ones might be the strong seasonality of the coccolithophoride blooms that add a bias towards the preferred growing time (May – July [*Cokacar et al.*, 2004]). Conversely, the SST in late spring and early summer is higher than the annual mean SST, thus if the calculated temperature reflects the primary growth period one would expect above-average temperature recorded in the alkenones. *Emiliania huxleyi* occasionally also blooms during winter, and

May – July blooms could be weak or absent in some years [*Cokacar et al.*, 2004], thus a low temperature component could be added occasionally to the integrated signal, but on the time span of 300 or 400 years covered by the core top samples, this should not play a significant role. Sediment trap and water samples also showed the same effect of underestimating SST, even if the tetraunsaturated component is incorporated into the calculation [*Freeman and Wakeham*, 1992; *Xu et al.*, 2001]. These authors also found that the calculated temperature increased with depth from 6°C at the surface to around 13-14°C below 300 m. This might imply that the more unsaturated components are more easily degraded in the water column than the diunsaturated alkenones or (the preferred option) that the alkenones are a combination of different sources. These sources might be different populations of the same species growing during different times in diverging depths and/or other alkenone-producing organisms than *Emiliania huxleyi* [*Xu et al.*, 2001]. The preferential degrading of more unsaturated alkenones in the water column could not be confirmed with the comparison of alkenone concentrations and water depth presented in Fig. 1, therefore the explanation by different contributors to the alkenone signal seems to be preferable.

It is worth noting that the calculated temperatures for the cores in shallow water depths (84, 91, 148 m, Tab. 1) are higher than those observed in the sediment trap and water samples from the same depths (ca. 9-11°C) [*Freeman and Wakeham*, 1992]. Here, early diagenetic processes in the sediment might play a role; it was for example suggested, that the presence of inorganic sulphur might slowly increase the $U^{K'}_{37}$ of alkenones stored in the sediment, and that the same might occur during a particle's residence time in the anoxic water column [*Sinninghe Damsté et al.*, 1989; *Freeman and Wakeham*, 1992]. However, following other studies, the role of diagenesis on the alkenone unsaturation index seems to be of minor importance [*Brassel et al.*, 1986; *Xu et al.*, 2001]. This view is also strengthened by a comparison of alkenone-derived temperatures from anoxic brine deposits from the northwestern Red Sea [*Arz et al.,* in press] with alkenone-temperatures from adjacent oxic sediments [*Arz et al.,* 2003] which yielded comparable results. Finally, it must also be taken into consideration that the cores are located in a geographically wide-spread area with diverse current regimes and dissimilar magnitudes of terrestrial input. It is also more likely to have contamination by reworked organic matter in areas with high riverine input. Reworking of old material in areas with high current velocity as on the northwestern Black Sea shelf should also play a role.

4. Conclusions and outlook

In accordance to previous studies, the analysis of core top samples in the western Black Sea raises serious doubts if temperature reconstructions based on alkenones might be possible in the Black Sea. The factors that could make the temperature calibrations valid for the global ocean inapplicable in the Black Sea might include early diagenetic alteration, contribution of reworked material, and probably most important, contribution of alkenones from different source organisms and/or populations. Changes in the seasonality of coccolithophoride blooms might also have an impact on the temperature signal.
Further research on the behaviour of the different alkenones during early diagenesis under the anoxic conditions prevailing in the Black Sea should be performed to decipher to which degree the ratio of di-, tri- and tetraunsaturated alkenones changes with time. Useful would also be a long-time sediment trap survey to shed more light on the seasonal to interannual variations of the coccolithophoride blooms and alkenone production, as well as the variability of the depth-distribution of alkenones in the water column. This could help understanding the manifold factors influencing the alkenone distribution in the Black Sea sediments. At the moment an alkenone-based paleothermometer applicable for the Black Sea requires a deeper understanding of the underlying mechanisms of alkenone production and preservation in the Black Sea.

Another possibility for temperature reconstructions in the marine sediments of the Black Sea might be the application of the TEX_{86} (TetraEther indeX of tetraethers consisting of 86 carbon atoms) paleothermometer [*Schouten et al.*, 2002]. This method is based on the composition of membrane lipids derived from Crenarchaeota, an ubiquitous component of marine plankton, also very common in the Black Sea [*Schouten et al.*, 2002]. Although relatively new, this technique has been successfully applied e.g., for reconstructing Cretaceous temperatures in the Arctic Ocean [*Jenkyns et al.*, 2004] and it might be useful to test it in the Black Sea.
This research could be accompanied by stable oxygen isotope measurements obtained on shells of planktonic juvenile stages of the bivalve *Mytilus galloprovinciales* which were found in great abundance in the marine sediments the southwestern Black Sea. A combination of $\delta^{18}O$ measurements and temperature reconstructions on e.g. TEX_{86} or perhaps alkenones would also deliver information about the salinity development of the Black Sea during the Holocene.

Aknowledgements

We thank captain and crew of the RV Meteor for their efficient support during Meteor cruise M 51-4. We also thank Ralph Kreutz for the introduction into the alkenone-method and running the gas chromatograph. This research was founded by the DFG grants no. LA 1273/2-1, LA 1273/2-2, and WE 992/47-3. No. RCOMXXXX.

References

Arthur, M. A., W. A. Dean, E. D. Neff, B. J. Hay, J. King and G. Jones (1994), Varve calibrated records of carbonate and organic carbon accumulation over the last 2000 years in the Black Sea, *Global Biogeochemical Cycles*, *8*(3), 195-217.

Arz, H. W., F. Lamy and J. Pätzold (in press), A pronounced dry event recorded around 4.2 kyr in brine sediments from the Northern Red Sea, *Quaternary Research*.

Arz, H. W., F. Lamy, J. Pätzold, P. J. Müller and M. Prins (2003), Mediterranean moisture source for an early-Holocene humid period in the northern Red Sea, *Science*, *300*, 118-121.

Boon, J. J., F. W. v. d. Meer, P. J. W. Schuyl, J. W. de Leeuw, P. A. Schenck and A. L. Burlingame, 1978. Organic geochemical analyses of core samples from Site 362, Walvis Ridge. DSDP Leg 40, Initial reports of the Deep Sea Drilling Project. US Government Printing Office, Washington D.C., pp. 627-637.

Brassel, S. C., G. Eglinton, I. T. Marlowe, U. Pflaumann and J. M. Sarnthein (1986), Molecular stratigraphy: A new tool for climatic assessment, *Nature*, *320*, 129-133.

Cokacar, T., T. Oguz and N. Kubilay (2004), Satellite-detected early summer coccolithophore blooms and their interannual variability in the Black Sea, *Deep-Sea Research I*, *51*, 1017-1031.

de Leeuw, J. W., F. W. v. d. Meer, W. I. C. Rijpstra and P. A. Schenck, 1980. On the occurence and structural identification of long chain unsaturated ketons and hydrocarbons in sediments. In: A. G. Douglas and J. R. Maxwell (Editors), Advances in Organic Geochemistry 1979. Pergamon Press, New York, pp. 211-217.

Freeman, K. H. and S. G. Wakeham (1992), Variations in the distributions and isotopic compositions of alkenons in Black Sea particles and sediments, *Organic Geochemistry*, *19*(1-3), 277-285.

Jenkyns, H. C., A. Forster, S. Schouten and J. S. Sinninghe Damste (2004), High temperatures in the Late Cretaceous Arctic Ocean, *Nature*, *432*(7019), 888-892.

Jones, G. A. and A. R. Gagnon (1994), Radiocarbon chronology of Black Sea sediments, *Deep-Sea Research I*, *41*(3), 531-557.

Jørgensen, B. B. (2003), *METEOR-Berichte 03-1, 57*, *METEOR-Berichte, Cruise 51, Leg 4, Istanbul - Istanbul*.

Marlowe, I. T., 1984. Lipids as palaeoclimatic indicators. PhD thesis Thesis, University of Bristol, Bristol, UK.

Müller, P. J., G. Kirst, G. Ruhland, I. von Storch and A. Rosell-Melé (1998), Calibration of the alkenone paleotemperature index Uk37' based on core-tops from the eastern South Atlantic and the global ocean (60°N-60°S), *Geochimica et Cosmochimica Acta*, *62*(10), 1757-1772.

Prahl, F. G. and S. G. Wakeham (1987), Calibration of unsaturation patterns in long-chain ketone compositions for palaeotemperature assessment, *Nature*, *330*, 367-369.

Prahl, F. G., L. A. Muehlhausen and D. L. Zahnle (1988), Further evaluation of long-chain alkenones as indicators of paleoceanographic conditions, *Geochimica et Cosmochimica Acta*, *52*, 2303-2310.

Schouten, S., E. C. Hopmans, E. Schefuß and J. S. Sinninghe Damste (2002), Distributional variations in marine crenarchaeotal membrane lipids: a new tool for reconstructing ancient sea water temperatures?, *Earth Planet. Sci. Lett.*, *204*, 265-274.

Sikes, E. L., J. W. Farrington and L. D. Keigwin (1991), Use of the alkenone unsaturation ratio UK37 to determine past sea surface temperatures: core-top SST calibrations and methodology considerations, *Earth and Planetary Science Letters*, *104*, 36-47.

Sinninghe Damsté, J. S., W. I. C. Rijpstra, A. C. Kock-van Dalen, J. W. de Leeuw and P. A. Schenck (1989), Quenching of labile functionalised lipids by inorganic sulphur species: evidence for the formation of sedimentary organic sulphur compounds at the early stages of diagenesis, *Geochimica et Cosmochimica Acta*, *53*, 1343-1355.

Volkman, J. K., G. Eglinton, E. D. S. Corner and T. E. V. Forsberg (1980), long-chain alkenes and alkenones in the marine coccolithophorid Emiliania huxleyi, *Phytochemistry*, *19*, 2619-2622.

Xu, L., C. M. Reddy, J. W. Farrington, G. S. Frysinger, R. B. Gaines, C. G. Johnson, R. K. Nelson and T. I. Eglinton (2001), Identification of a novel alkenone in Black Sea sediments, *Organic Geochemistry*, *32*(5), 633-645.

CONCLUSIONS AND OUTLOOK

1. Conclusions

Addressing the main research objectives described in chapter 1.1, this thesis' most important findings can be summarised as follows:

About the hydrologic evolution of the Black Sea in the course of the major late glacial to Holocene climatic oscillations:

- The Black Sea underwent significant changes in its water chemistry during its lacustrine stage. Trace element records show that authigenic calcite precipitation during warm phases (Bølling/Allerød and Early Holocene) led to an abrupt increase of the Mg/Ca and Sr/Ca ratios in the water column. The stable oxygen isotope chemistry of the Black Sea also exhibits distinct variations, most prominently a continuous $\delta^{18}O$ increase since 15 kyr BP, mainly related to heavier $\delta^{18}O$ in atmospheric precipitation since the onset of the Bølling warm period and to the inflow of marine water around 9.3 kyr BP.
- The inflow of isotopically depleted meltwater from the northern drainage area between 18 and 15.5 kyr BP is clearly depicted in the stable oxygen isotopes. Negative excursions in the $\delta^{18}O$ record closely follow periods of maximum meltwater input that led to the deposition of characteristic red clay layers. The effect on Mg/Ca and Sr/Ca is only minor.
- The Black Sea has been a homogenous water body throughout the glacial period. Since the onset of the Bølling/Allerød warm period deepwater formation started because of either increased evaporation and thus production of saline, dense surface water, or because of cold water sinking to the bottom of the basin during winter. Deepwater formation was persistent until the reconnection with the Mediterranean Sea started, but, unlike today, oxic conditions constantly prevailed at the bottom waters.
- The inflow of Mediterranean water has started around 9.3 kyr BP. This is most clearly visible in the Sr/Ca and Mg/Ca records that show a dramatic increase since 9.3 kyr BP. The available data do not definitively allow to state about the nature of the reconnection with the Mediterranean Sea via the Sea of Marmara (slow or catastrophic?), although a homogenisation of the measured parameters from different water depths indicates that it might have happened fairly vigorous.

Short-term climatic variability in the records:

- It was possible to detect interannual to multicentennial-scale climatic variations in our records. These are related to variations in the discharge of major rivers (Danube and Sakarya) and can be used for further paleoclimatic investigations.
- The data shows the influence of the North Atlantic Oscillation (NAO) and other climatic modes that are related to the Arctic/North Atlantic climate regime on different time scales and time intervals. The respective records cover multicentennial-scale discharge variations of the Sakarya River, located in western Antolia, during the past ca. 7500 years; an interannual to decadal-scale record of run-off fluctuations of the Danube during the Younger Dryas/Allerød transition, and multicentennial-scale fluctuations in the meltwater input between 18 and 15.5 kyr BP.
- The records suggest that the climate of the Atlantic region and particularly the NAO are persistent factors that govern the climate of the western Black Sea and its surrounding areas on long time scales and under considerably different climatic regimes

2. Outlook

One of the main problems facing paleoenvironmental reconstructions on lacustrine Black Sea sediments is constructing a robust age model. This is caused by unknown reservoir corrections and the scarcity of material appropriate for radiocarbon dating. To further constrain the stratigraphic framework independent age markers are needed, as for example the 22 kyr Santorini ash layer recently found in a core from the SW Black Sea (O. Kwiecien, unpublished data). Ideally, such tephra age markers are combined with radiocarbon dates obtained on components deposited *in situ* (e.g. large bivalve shells in living position, ostracods). To avoid contamination by reworked material, dating of large bivalve shells seems to represent one of the best solutions. This is, however, only possible in sediment cores from shallower water depths (below ca. 350 m).

The complex history of the late Pleistocene Black Sea with a proposed deepwater formation and periods of meltwater input furthermore implies that even with further age constraints the assessment of reservoir ages will remain a challenging task. As true for the lacustrine sediments, the current stratigraphy of the marine sapropel and coccolith ooze is also not finally resolved. The comparison between varve counting and radiocarbon dating of organic material yields big differences, because radiocarbon ages are around 20-30% older than

suggested by varve counts [*Jones and Gagnon*, 1994]. The sediment cores from the SW Black Sea contain high amounts of bivalve shells belonging to the planktonic larval stage of *Mytilus galloprovencialis*. By using these shells for extensive dating we expect to achieve more robust stratigraphic frameworks than with radiocarbon dates on organic material, that are prone to contamination by reworked terrestrial material.

One of the questions that still have to remain open is the time the marine inundation of the Black Sea needed, i.e. whether it was a catastrophic event ("Noah's Flood") or a slow process. Although the data clearly depict the inflow of marine water into the Black Sea basin, the number of radiocarbon dates during the respective interval between ca. 9.5 and 8 ka, i.e. from the start of the final increase of Mg/Ca and Sr/Ca to the onset of anoxia, is too sparse to give further insight into the dynamics of the reconnection. To circumvent the paucity of datable material in the studied cores two possibilities might be considered. One is the sampling of shallow cores containing macroscopic mollusc shells that would give enough material for a radiocarbon analysis (as done in this thesis for the shelf core GeoB 7616-4). The other possibility is to sample with other coring devices or to sample multiple cores at one position in order to increase the amount of datable material. One has, however, to consider that the dating of bivalve shells in shallow cores would potentially postdate the saltwater-intrusion, if the saltwater is directly sinking into the deep Black Sea.

Another important aspect for further research should be the period of meltwater inflow into the Black Sea between 18 and 15.5 kyr BP. Here more information about the dynamics of the Scandinavian Ice Sheet might be obtained by studying the contemporaneous red clay layers and the incorporated mm-scale laminations in high resolution, as it is currently done at the GFZ Potsdam with thin-sections and µ-XRF scanning. To further constrain the drainage corridor of the meltwater pulses, it would be ideal to core the Sea of Azov – Manych – Caspian Sea (Volga Delta) passage and probe ancient terraces of Dnepr or Dnestr to find out if mineralogical and geochemical signatures found in the red clays of the Black Sea can be traced to these drainage areas. It would also be intriguing to see, if the inflow of meltwater from the Siberian and/or Scandinavian ice sheets occurred in similar ways during earlier periods of the last glacial and previous glacials, perhaps coupled to Heinrich-Events or Dansgaard/Oeschger-cylces. For this purpose longer sedimentary records such as envisaged by the IODP drilling in the southern Black Sea would be highly valuable.

The paleoclimatic studies presented in this thesis have demonstrated the suitability of the Black Sea for paleoenvironmental investigations. While the reconstruction of run-off variations of major rivers was successful, the reconstruction of past temperatures is still

problematic because the temperature-sensitivity of $\delta^{18}O$ and Mg/Ca is surpassed by changes in the water chemistry and other factors obscuring the temperature signal. In order to reconstruct paleotemperatures, the alkenone method was also tested but generated ambiguous results. It might still be possible to use this method for the last 2700 years in the Black Sea (with regular blooms of *Emiliania huxleyi*), but further knowledge about the degradation of alkenones in the water column and during early diagenesis under the special conditions in the anoxic Black Sea is required. In addition to previous sediment trap investigations [*Hay et al.*, 1990], long-term studies of the interannual variability of the coccolithophoride blooms would be important for understanding which temperatures exactly are recorded in the alkenone composition and how variable the seasonality of the annual plankton blooms is. An alternative to alkenones could be the application of the TEX_{86} paleothermometer. In combination with $\delta^{18}O$ data currently obtained on larval shells of the planktonic bivalve *Mytilus galloprovincialis* in sediment cores off western Anatolia the paleotemperatures could give valuable information about the hydrographic evolution of the Black Sea during the last 7500 years.

Reference

Hay, B. J., S. Honjo, S. Kempe, V. Ittekkot, E. T. Degens, T. Konuk and E. Izdar (1990), Interannual variability in particle flux in the southwestern Black Sea, *Deep-Sea Research A*, *37*(6), 911-928.

Danksagung

Mein Dank gilt zunächst Herrn Prof. Dr. Gerold Wefer für die Vergabe und Betreuung dieser Doktorarbeit und Herrn Prof. Dr. Gerhard Bohrmann für die Bereitschaft, die Arbeit des Zweitgutachters zu übernehmen. An dieser Stelle sollen auch die zahlreichen Möglichkeiten zur wissenschaftlichen Weiterbildung in Form von Graduiertenkursen und Workshops erwähnt werden, die eine hervorragende Ausbildung von Nachwuchswissenschaftlern in Bremen möglich machen.

Ein großer Dank geht auch nach Potsdam, an Helge Arz und Frank Lamy. Sie waren maßgeblich für die Initiierung des Projektes und dessen Durchführung verantwortlich, und haben in vielerlei Art und Weise zum Gelingen dieser Arbeit beigetragen. Dies bezieht sich auf die immerwährender Diskussionsbereitschaft und viele gute (wissenschaftlichen) Ideen, aber auch auf praktische Hilfe wie die Einführung in Labortechniken. Mein Dank gilt auch Olga Kwiecien für lange Diskussionen um die Mysterien des Schwarzen Meeres. Viele hilfreiche Ratschläge und Ideen kamen ebenfalls von Holger Kuhlmann, Thomas Felis und Henning Kuhnert, danke dafür! Für die Unterstützung bei Laborarbeiten bzw. der Durchführung von Messungen möchte ich mich auch bedanken bei Monika Segl, Ralph Kreutz, Jan-Berend Stuut, Christoph Vogt, Alex Wülbers und Scott Birdwhistell (WHOI).

Mein Dank geht ebenfalls an Candace Major, Woods Hole, die meinen Aufenthalt am WHOI möglich gemacht hat und sich aufopferungsvoll um alle Eventualitäten gekümmert hat. In diesem Zusammenhang möchte ich mich bei Enno Schefuss für die zeitweise Überlassung seiner Wohnung danken, und bei Jens Holtvoeth und Dan Shoemaker für die nette Gesellschaft während des neuenglischen Winters.

In guter Erinnerung behalten werde ich auch die (Post-)Doktorandenschar an der Uni Bremen, besonders erwähnt seien hier meine beiden Bürokollegen Jérôme und Uli, sowie die üblichen Bremer Verdächtigen (Snjez, Söhnke, Ismene, Jens, Iris).

So, und ganz besonders möchte ich mich für die moralische, finanzielle und sonstige Unterstützung meiner Eltern bedanken, ohne die das Unternehmen „Doktorarbeit“ kaum möglich gewesen wäre.

Das dieser Arbeit zugrunde liegende Projekt wurde durch die DFG gefördert; der Aufenthalt in Woods Hole wurde mit Hilfe eines Kurzzeitstipendiums des DAAD finanziert.